DELFT UNIVERSITY OF TECHNOLOGY

MSc Thesis

CIEM0500

2024-2025

Swelling caused by excavation pit in soft soil conditions (Analytical and Numerical Study)

Mahmoud Ghanem

5861985

To obtain the degree of Master of Science in Civil Engineering
at the Delft University of Technology

Supervisor:	Dr. Mandy Korff,	TU Delft, Geotechnical Engineering (Chair)
Thesis committee:	Dr. Mark Voorendt,	TU Delft, Hydraulic Engineering
	Ing. Michel de Koning,	CRUX Engineering BV
	Ing. Korneel de Jong,	CRUX Engineering BV

TU Delft

CRUX

Abstract

This thesis presents a comprehensive investigation into excavation-induced swelling in soft clay soils, with a specific focus on the influence of embedded structural elements and pile installation effects. The motivation for this research stems from the conservative nature of traditional analytical methods, which tend to overestimate swelling due to their simplifying assumptions—highlighting the need for a simple yet more advanced modeling approach that captures soil-structure interaction more realistically. The research integrates both analytical and numerical methods to assess vertical deformation and swelling pressure under varying geotechnical configurations. The analytical approach employs the Koppejan method, a classical consolidation-based method, to estimate heave resulting from dissipation of excess pore water pressure during the last phase of consolidation. Implemented in Excel, the analytical model assumes idealized elastic soil behavior and uniform unloading. This method serves as a baseline for identifying trends and quantifying the level of conservatism in traditional estimates.

The numerical simulations are carried out using PLAXIS 2D, applying the Hardening Soil model to realistically capture the nonlinear behavior of soft clay. Various scenarios are modelled, including the presence or absence of floor slabs, embedded piles, and volumetric expansion resulting from pile installation. Volumetric expansion is introduced via prescribed initial strains, mimicking the stress redistribution caused by displacement-type pile installation. Five structured cases are developed to isolate and analyse the effects of pile stiffness, spacing (centre-to-centre distances of 2 m and 2.5 m), floor rigidity, and interaction effects.

Results demonstrate that analytical methods consistently overestimate both swelling displacements and floor swelling pressures by up to 70% in some configurations due to their inability to account for soil-structure interaction and stress redistribution. Numerical findings highlight that embedded piles, particularly when closely spaced and combined with stiff floor systems, significantly reduce the magnitude of swelling and associated pressures. Additionally, pile installation effects play a vital role in stress buildup, altering pore pressure dissipation and influencing upward soil movement.

This dual-framework approach offers critical insight into the mechanisms driving swelling in excavation contexts and provides practical guidance for improving predictive accuracy in design. The outcomes underscore the necessity of incorporating installation effects and realistic structural modeling in modern geotechnical practice.

Acknowledgments

I would like to express my sincere gratitude to my supervisor, Dr. Mandy Korff, for her continuous support, guidance, and valuable feedback throughout my thesis at TU Delft. Her expertise and encouragement were instrumental in shaping this research and pushing it forward.

I would also like to thank Dr. Mark Voorendt, committee member at TU Delft, for his insightful comments and constructive suggestions, which helped me improve the quality and clarity of this work.

A special word of thanks goes to Michel de Koning and Korneel de Jong from CRUX Engineering for their technical input, professional support, and for giving me the opportunity to gain practical experience alongside my academic research. Their knowledge and collaboration greatly enriched the applied aspect of this thesis.

I am also grateful to my fellow students and friends for their motivation and support throughout this journey. Lastly, I would like to thank my family for their constant encouragement, patience, and belief in me during every step of my studies.

Nomenclature

Symbols

σ'	Effective stress
σ	Normal stress
u	Pore water pressure
K	Hydraulic conductivity
OCR	Over-consolidation ratio
ε_v:	Vertical strain
s_v:	Vertical displacement
d :	Thickness
C_p:	Primary compression constant
C_s:	Secondary compression constant
A_p:	Primary swelling constant
A_s:	Secondary swelling constant
$U(t)$:	Degree of consolidation
$\sigma'_{v,0}$:	Initial vertical effective stress
$\sigma'_{v,1}$:	Vertical effective stress
t:	Time
η :	The geometry factor
γ_{unsat}:	Unsaturated unit weight
γ_{sat}:	Saturated unit weight
φ':	Effective cohesion
Cv_{swell}:	Coefficient of swelling

Table of Contents

1 Introduction

Excavation pits have been a fundamental component of construction for many years, driven by the growing demand for underground structures such as parking garages, tunnels, and other underground facilities. These underground solutions have become increasingly popular as they allow for efficient land use, minimizing the spatial demands of surface structures and preserving valuable above-ground space for other purposes such as green areas, public spaces, or additional infrastructure. Such considerations have become particularly important in densely populated areas where efficient land use is critical.

One of the key geotechnical challenges associated with deep excavations is the phenomenon of swelling, the upward movement of soil at the base of the excavation caused by stress relief following soil removal. This behavior is especially pronounced in cohesive soils like clay, where unloading leads to volumetric expansion and under_pressure generation. Swelling can have significant implications on structural stability and serviceability, particularly for floor slabs and foundation elements resting on or embedded in the underlying soil. If not properly accounted for, it may result in uplift pressures, deformation, cracking, or even failure of structural components.

1.1 Research Context

Excavation in soft soils poses major geotechnical challenges due to the stress redistribution and delayed pore pressure dissipation that follow soil removal. One of the most significant effects observed in deep excavations is swelling—an upward deformation of the excavation base caused by the release of overburden pressure. This phenomenon is particularly pronounced in low-permeability clays, where unloading reduces the vertical effective stress faster than pore pressure can dissipate, leading to (under_pressure), which gradually dissipates over time, often resulting in measurable heave(Terzaghi & Peck, 1967).

Swelling can lead to serviceability problems such as cracking in slabs, uplift of foundation elements, and instability of the base in deep pits (Powrie, 2014). Its magnitude depends on several factors, including soil stiffness, permeability, excavation depth, and construction sequence (Wood , 1990 ;Ou, 2006). Additionally, the interaction between swelling and structural components like piles or floor slabs can amplify or mitigate the ground response, complicating the prediction process. Additionally, the interaction between swelling and structural components like piles or floor slabs can amplify or mitigate the ground response, complicating the prediction process.

Conventional estimation of swelling often relies on analytical solutions derived from elasticity theory or one-dimensional consolidation models (Terzaghi, 1943 ;Fox, 1948). While useful for preliminary design, these approaches tend to be conservative and may oversimplify critical aspects such as nonlinear stress-strain behavior, three-dimensional effects, and partial drainage conditions (Ng & Wang, 2001). As a result, they often overpredict swelling magnitudes or fail to capture the localized interaction between soil layers and structures.

To address these limitations, recent research emphasizes the use of numerical methods, particularly finite element consolidation analyses, which can simulate time-dependent behavior under realistic construction sequences (Zienkiewicz et al., 1980 ;Desai & Zaman, 1984).

Numerical modelling enables more accurate representation of pore pressure development, stress redistribution, and the influence of structural elements such as piles, offering a more refined assessment of swelling behavior (Brinkgreve et al., 2016).

With the growing demand for underground infrastructure in soft ground environments, particularly in urban settings, improving the reliability of swelling predictions is essential for both design safety and economic efficiency. This research aims to bridge the gap between conservative analytical methods and advanced numerical tools by evaluating swelling in excavation pits through both approaches, with a focus on understanding the role of pile geometry, spacing, and soil-pile interaction in the overall response.

1.2 Research Objectives

The primary objective of this thesis is to develop a simple, accurate, and practical numerical modeling approach to predict soil swelling induced by unloading in excavation pits, particularly in soft clays. This goal stems from the limitations of traditionally conservative analytical methods, which tend to overestimate swelling pressures and do not fully capture soil-structure interaction or time-dependent behavior.

To address this, the study first applies an analytical method based on the SBRCur Design Guideline for Swelling to establish a reference scenario. This is then complemented by a numerical modeling approach using PLAXIS and the Hardening Soil model, which provides a more advanced representation of soil behavior under unloading conditions.

A key focus of this research is to evaluate how well the numerical approach replicates the time-dependent swelling response of soft clays and to investigate its applicability in design. In addition, the study examines the uplift behavior of pile foundations using Embedded Beam elements, allowing for a more realistic simulation of pile-soil interaction under swelling conditions.

The numerical analysis covers a range of excavation configurations, including:

- Swelling in an excavation pit without piles or a floor slab.
- Swelling in an excavation pit with only piles.
- Swelling in an excavation pit with both piles and a floor slab.

Through these scenarios, the study aims to improve the reliability of swelling predictions and inform more efficient and cost-effective design practices for foundation systems in soft ground.

Accordingly, this research seeks to answer the following main question:

- What simple numerical modeling approach can be used to predict soil swelling during unloading (e.g., in an excavation pit) as a more realistic alternative to traditional analytical methods?

Sub-questions guiding this investigation include:

- How do variations in excavation pit configurations (e.g., width, depth, presence of floors or embedded piles) influence swelling behavior, particularly in clay soils?
- What influence does the pile installation process have on the soil's swelling behavior?

1.3 Research Methodology

To systematically evaluate the swelling behavior of soft clays under excavation-induced unloading, this study adopts a structured, multi-phase methodology integrating both analytical and numerical approaches. The purpose of this combined framework is to leverage the simplicity and conservative nature of analytical methods while utilizing the greater detail and realism offered by numerical simulations. Each approach serves a distinct role: the analytical method offers a benchmark for conservative estimation, whereas the numerical analysis captures complex interactions such as stress redistribution, pore pressure dissipation, and volumetric expansion from pile installation.

The methodology is divided into a sequence of well-defined steps, each corresponding to a specific modeling phase and described in the following chapters:

Step1: Analytical method (chapter 3.2)

The study begins by applying the Koppejan method, a classical one-dimensional consolidation theory, to estimate vertical swelling due to unloading. This analytical formulation, implemented via Excel, assumes uniform stress release and linear elastic behavior, and serves as a baseline for comparison with more advanced models.

Step 2: Numerical modelling using Plaxis 2D (chapter 6)

A series of 2D numerical models were developed in PLAXIS using the Hardening Soil model to simulate more realistic geotechnical responses. These are divided into five distinct cases:

- Case 1 : Infinite model without structural element (chapter 6.1)

  This model represents an excavation pit in a simplified, infinite configuration to validate the numerical results against the analytical solution under comparable soil conditions and loading.

- Case 2 : 2D Finite Model with Sheet Pile and Strut (Chapter 6.2)

  A finite excavation setup incorporating retaining structures (sheet pile and strut) is introduced. Parametric studies assess how variations in excavation geometry and soil properties influence swelling behavior.

- Case 3: 2D Finite model with sheet pile-strut-Embedded pile system with and without volumetric expansion (Chapter 6.3)

  This phase investigates the effect of pile installation using the volumetric expansion method. Two pile spacing configurations (c.t.c = 2.0 m and 2.5 m) and multiple pile widths are examined to study horizontal stress build-up and its correlation with vertical swelling.

- Case 4: 2D Model Without Piles (Sheet Pile–Strut–Floor System) (Chapter 6.4)

  The impact of floor slab stiffness on swelling and swelling pressure is studied. Different floor stiffness values (E1, E2 = 2E1, E3 = 2E2) are considered, and the numerical results are compared with analytical predictions.

- Case 5 : 2D Model-Full Structural System – Sheet Pile, Strut, Floor, and Embedded Piles (Chapter 6.5).

  This final step includes the full excavation support system and focuses on the interaction between excess pore pressure generation, consolidation, and pile-soil interaction. The influence of pile width and spacing on swelling mechanisms is closely examined.

Where relevant, numerical results—including swelling magnitude and swelling pressure—were compared against those from the analytical method to assess model reliability and to highlight the limitations of simplified analytical approaches under complex boundary conditions.

2 Literature Review

2.1 Characteristics of Soft Soils and Their Relation to Swelling

Excavating soft soil significantly alters the in-situ stress conditions and pore pressure equilibrium, often leading to delayed ground responses such as swelling or heave. Soft soils are typically fine-grained, saturated, and exhibit time-dependent behavior. Their mechanical response under unloading conditions is governed by a complex interplay of mineralogy, water content, permeability, and stress history (Atkinson & Bransby, 1978). These properties become particularly critical in the context of deep excavations, where stress release can trigger swelling—an upward soil displacement that affects the performance of pile foundations, floor slabs, and surrounding structures.

Soft soils generally consist of solid particles (minerals), water, and air, making them a three-phase material system. The behavior of these soils is governed by the movement and interaction of the phases, particularly under changing load conditions. In saturated clays, where pore spaces are largely filled with water, any external stress change, such as unloading due to excavation, leads to the development of underwater pressure. This pressure, at least in the short term, supports a significant portion of the applied stress, preventing immediate volume change (Wood, 1990) . The soil's response depends on how fast the excess pore pressure dissipates, which defines whether the condition is undrained (short term) or drained (long term).

Swelling typically occurs during the drained phase, when under pore water pressure have dissipated and effective stress recovers. However, unlike primary consolidation under loading, swelling during unloading tends to be faster—due to stress relief initiating immediate volume expansion—but results in a smaller total strain. This is because the soil's structure has already undergone prior compression and is less deformable upon rebound. This behavior is well captured by the unloading stress path, which moves the stress point leftward in the effective stress space, typically reducing the mean effective stress p' while maintaining or decreasing the deviatoric stress q. As a result, swelling paths tend to follow a recompression line with higher stiffness and less volumetric strain compared to loading paths.

The effective stress principle, first introduced by Terzaghi, remains central to the understanding of soft soil behavior. It states that the stress actually carried by the soil skeleton is the difference between the total stress and pore water pressure as state in equation 2.1:

$$\sigma' = \sigma - u \tag{2.1}$$

Where σ' is the effective stress, σ is the total stress, and u is the pore water pressure. This principle highlights why swelling is predominantly a long-term process: only after pore water pressures adjust can the soil skeleton undergo significant strain (Mitchell & Soga, 2005). During this transition, the structure of soft soils plays a major role.

Another critical parameter is the Over-consolidation Ratio (OCR), which represents the ratio of the soil's preconsolidation pressure to its current vertical stress. Soils with high OCR values are more likely to exhibit swelling upon unloading, as they have been previously compressed and store elastic rebound energy. Upon excavation, this rebound can cause the soil to expand vertically, especially when the stress drops below the preconsolidation level (Leroueil & Hight,

2003). This is why excavation in overconsolidated clays often results in base heave, which can impact stability and lead to excessive deformation of foundation elements.

The time-dependent nature of swelling is often analysed through consolidation theory, particularly one-dimensional formulations based on Terzaghi's work. These models describe how water flow and soil skeleton stress evolve over time, and they serve as the basis for many analytical swelling models. However, these approaches often simplify the true complexity of soft soil behavior. For instance, they may assume linear elastic rebound, uniform soil properties, and purely vertical flow, all of which limit their accuracy in real excavation scenarios.

Soft soils are also prone to secondary compression or creep, particularly under sustained stress conditions after primary consolidation. This adds another layer of complexity to swelling predictions, as the soil may continue to deform over long periods, even after pore pressure has fully dissipated (Karol, 2003). However, this long-term deformation is not taken into account in the current analysis. Such deformation can be particularly damaging for foundation systems in excavated zones, where even small vertical displacements may lead to cracking, tilting, or uplift of structural elements.

Finally, the hydraulic conductivity of soft soils is low, often in the range of 10^{-9} to 10^{-11} m/s. This slows down both consolidation and swelling processes. In practical terms, swelling may not manifest immediately after excavation but instead progress over weeks or months, particularly in thick clay layers with minimal drainage. This delayed response complicates construction scheduling and highlights the importance of reliable prediction models (Holtz et al., 2011)

In summary, the swelling behavior of soft soils is controlled by a combination of mineralogy, pore pressure response, stress history, drainage characteristics, and soil structure. These factors must be fully understood and incorporated into modelling strategies to avoid conservative overdesign or unsafe underdesign in excavation projects.

2.2 Swelling Behavior in Excavation Pits

Swelling in excavation pits refers to the vertical upward displacement of soil at the base of an excavation caused by the release of overburden stress. This behavior, commonly observed in soft, saturated clay deposits, is especially critical in deep urban excavations where structural elements such as floor slabs, anchors, or tension piles interact with soil undergoing time-dependent deformation. Unlike traditional settlement analyses that focus on downward deformation under applied load, swelling occurs due to unloading, often producing significant uplift pressures that may lead to structural instability if not properly accounted for during design.

In deep excavations, the removal of overburden leads to a reduction in vertical total stress at the base. In soft soils, particularly clays with low permeability, this reduction triggers a delayed mechanical response. While the excess pore pressure may initially prevent immediate volume change, the gradual dissipation of this pressure allows the soil skeleton to expand, resulting in base heave. This mechanism is distinctly different from elastic rebound alone; it involves both

time-dependent deformation and redistribution of effective stress, especially in soils with a stress history involving over-consolidation (Finno et al., 2002)

Excavation-induced swelling becomes critical in engineering scenarios involving excavation stages or delayed slab construction. Field observations have shown that swelling often initiates shortly after excavation but can continue for weeks or even months depending on drainage conditions and soil thickness (Ou & Liao, 1999). The magnitude of swelling is influenced not only by soil type and thickness but also by the depth of excavation, rate of unloading, construction sequence, and the presence of structural elements such as diaphragm walls and piles. In particular, partial restraint from floor slabs or anchors can redistribute the swelling pressures laterally, resulting in complex stress paths that analytical models struggle to capture (Long, 2001).

Design guidelines such as CUR C202 (2014) attempt to quantify swelling pressure and its effects, typically using semi-empirical methods. However, these approaches assume simplified boundary conditions, often idealizing the swelling pressure as uniform across the excavation base. In reality, swelling is spatially variable and evolves over time. It can result in non-uniform uplift and differential movements that critically affect serviceability.

This has led to a growing agreement that numerical modelling, incorporating coupled stress pore pressure analysis and realistic geometry, is required for deeper insight into swelling mechanisms in the soft soil (Gibson & Ladd, 1998).

Swelling also interacts with the pile foundation system in complex ways. Tension piles may experience unexpected uplift forces if swelling is underestimated. Conversely, pile installation prior to excavation can induce additional over_pressures that modify the swelling response during subsequent unloading. Experimental studies and field measurements (Tan & Phoon, 2006) have demonstrated that pile-soil interaction under swelling conditions can produce nonlinear displacement profiles along the pile shaft, especially in layered soils. The role of pile spacing, diameter, and stiffness becomes important in how swelling pressures are distributed and resisted by the foundation system.

Furthermore, swelling may not manifest solely as a vertical displacement. In braced excavations, lateral ground movements caused by reduced horizontal stresses can also contribute to uplift forces, especially under low confining stress conditions at the excavation base (Clough & O'Rourke, 1990). This interaction between vertical and horizontal stress release often requires three-dimensional consideration, which most traditional two-dimensional analytical solutions cannot handle.

Finally, swelling is often not treated independently in design practice. It is sometimes grouped with general uplift analysis, or assumed to be negligible under drained conditions. However, swelling pressures even if moderate—can critically affect construction sequencing and load distribution on support elements. The timing of slab installation relative to the peak swelling response is particularly important; premature construction may result in upward soil pressures that cause cracking or delamination of the floor, while delayed construction may reduce heave but introduce other logistical complications.

2.3 Numerical Modelling of Excavation-Induced Swelling

Soft soils are known for their complex mechanical behavior, which includes non-linear, plastic, anisotropic, and time-dependent responses. These characteristics present a challenge for traditional analytical models, which often rely on simplified assumptions and linear behavior. As a result, analytical approaches may fail to fully capture the actual field response under excavation-induced unloading. In contrast, numerical modelling offers a more comprehensive and adaptable framework, particularly suited for simulating the time-dependent and non-uniform behavior of soils under complex loading conditions such as swelling (Persson, 2004 ;Bishop & Blight, 2016) .

Numerical models are capable of simulating the dissipation of excess pore water pressure, changes in effective stress, and the volumetric expansion associated with unloading. This makes them particularly effective for analysing swelling behavior in soft clay during and after excavation, as they can incorporate variations in permeability, boundary conditions, and staged construction sequences. As excavation alters the stress regime in the soil, leading to negative excess pore pressures and heave, numerical models can track these developments over time and space, enabling more accurate prediction of swelling pressure and heave magnitudes (Gens et al., 2018).

In addition to improved accuracy, numerical methods offer the ability to assess transient and non-linear responses. For example, rapid excavation or simultaneous structural loading can lead to complex soil reactions that evolve over time. These are difficult to address analytically, but can be captured effectively in numerical platforms such as PLAXIS using coupled stress–pore pressure analysis (Schanz et al., 2016). This is especially useful for evaluating how swelling affects structural elements like floor slabs or tension piles, which may experience uplift forces or bending due to uneven heave.

A key factor in successful numerical modelling is the selection of an appropriate constitutive soil model. Simple models, such as the Linear Elastic or Mohr-Coulomb model, are often insufficient to capture unloading and swelling behavior, as they assume constant stiffness and simplified failure criteria. These models generally treat soil response as either entirely elastic or perfectly plastic and fail to account for strain-dependent stiffness, which is critical in swelling scenarios. In contrast, advanced models such as the Hardening Soil model include stress-dependent stiffness, preconsolidation effects, and the ability to simulate softening or hardening during loading and unloading cycles (Brinkgreve et al., 2017).

As illustrated in Figure 2.1 , the stress–strain relationships of different material models show how their predictions diverge. In swelling-sensitive problems, especially those involving preconsolidated or overconsolidated clays, the choice of a model that accounts for non-linearity and stiffness variation is essential. The Hardening Soil model, for instance, allows simulation of heave due to unloading by incorporating swelling modulus and pore pressure dissipation over time.

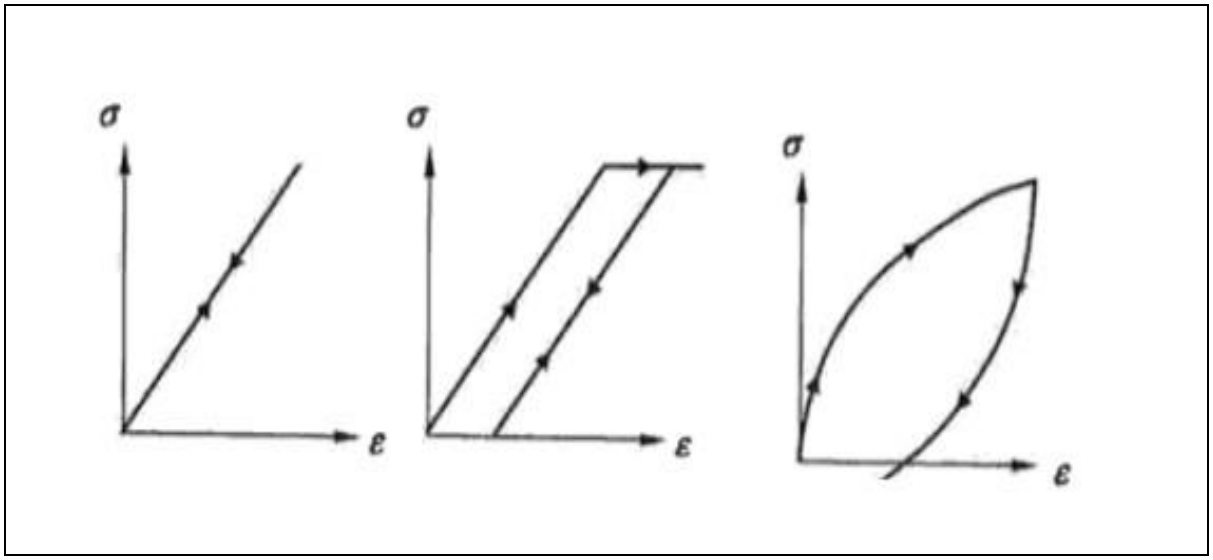

Figure 2.1 :Stress-strain relationship of different material models (Linear elastic, linear elastic-perfectly plastic, nonlinear) models, respectively from the left to the right (Persson, 2004).

Nevertheless, it is important to note that all numerical models rely on approximations and assumptions. Even advanced models require input parameters—such as stiffness moduli, unloading–reloading ratios, and creep indices—that may not be directly measurable or available. This introduces uncertainty in the results and necessitates careful calibration based on lab testing or field data. Additionally, higher fidelity models often require longer computation time and more rigorous validation (Brinkgreve, 2005).

Figure 2.2 compares the behavior of the Mohr-Coulomb and Hardening Soil models under stress-strain loading. The Mohr-Coulomb model shows a linear elastic–perfectly plastic response with a distinct yield point, whereas the Hardening Soil model exhibits a more gradual stiffness reduction and strain hardening, which more closely reflects real soft soil behavior under swelling conditions.

Ultimately, the strength of numerical modelling lies in its ability to simulate complex soil–structure interactions under excavation-induced unloading, including swelling effects. When calibrated appropriately, it provides insights not only into heave magnitude but also into time-dependent pore pressure changes and their impact on adjacent elements. This capability is essential for identifying mitigation strategies, evaluating design alternatives, and reducing over-conservatism in swelling pressure predictions, particularly in comparison with traditional analytical methods.

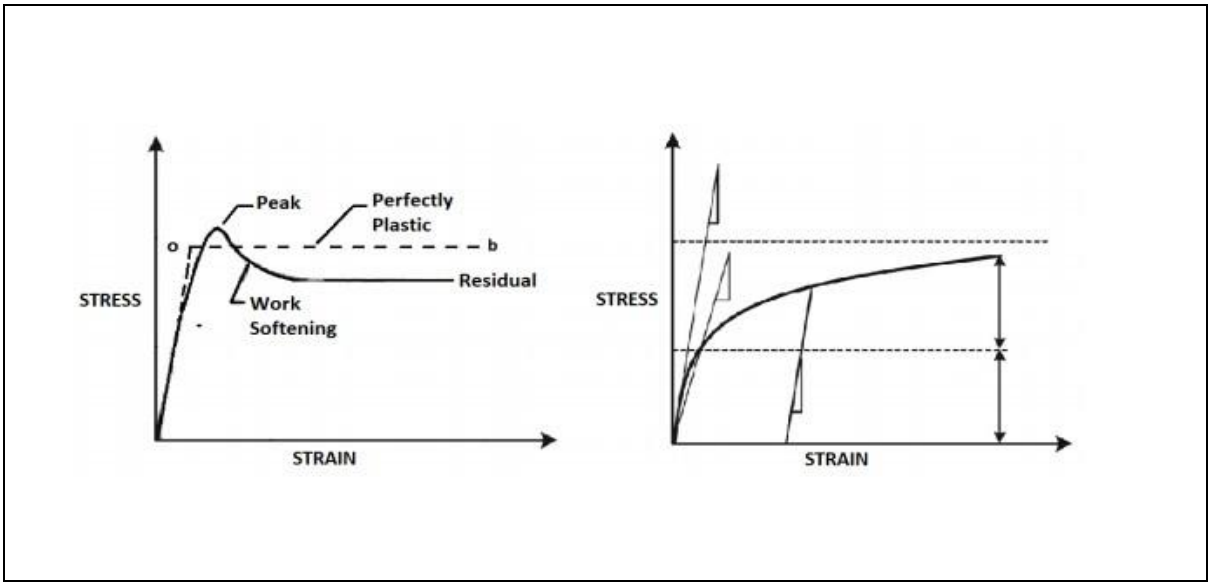

Figure 2.2: Stress-strain relationship (Hardening soil model, and Mohr-Coloumb model,), respectively from the left to the right (Schanz et al., 2016).

2.4 Pile Installation Effect

The long-term behavior of driven piles in clayey soils has been a subject of significant research, particularly concerning the increase in axial shaft resistance over time following installation. This phenomenon, often referred to as pile setup, occurs due to changes in soil-stress state and consolidation effects. As the pile penetrates the soil, it induces a displacement equal to its own volume, causing excess pore water pressure generation and a corresponding shift in the stress state (Basu P et al., 2014). The increase in pile capacity over time can be substantial, with studies indicating that the long-term bearing capacity can reach up to twelve times the initial capacity observed immediately after consolidation (Titi & Wathugala , 1999).

Understanding this time-dependent capacity gain is crucial for optimizing pile design and foundation performance, particularly in cohesive soil where consolidation has its effect in strength development. The assessment of pile capacity is typically conducted using pile load tests and analytical approaches, and increasingly, numerical modelling techniques. Numerical simulations provide valuable insights into pile-soil interaction mechanisms, capturing installation-induced effects that traditional methods may not fully account for (e.g., Wathugala & Desai, 1991 ;Basu et al., 2014). During installation, significant soil disturbance occurs in the vicinity of the pile, leading to remoulding effects and the generation of over_water pressure, particularly in saturated clayey deposits.

This disturbance alters the effective stress state, affecting both short-term and long-term load-bearing performance. Given these complexities, the selection of an appropriate numerical approach is essential to accurately model the installation effects on pile behavior, particularly in scenarios involving excavation pits, where soil movements and stress redistribution further influence the performance of the pile.

Additionally, pile installation plays a significant role in mitigating soil swelling that often arises due to excavation activities in clayey soils. In deep excavations, the removal of overburden stress leads to a reduction in the effective vertical stress, causing an increase in pore water pressure and subsequent swelling, which can negatively impact adjacent structures and foundation stability (Nelson & Miller, 1992). The presence of driven piles helps restrain the swelling in the soil, acting as vertical reinforcements that counteract heave-induced movements. However, if the heave-induced upward pressures exceed the pile's resistance or cause excessive bending moments, this may lead to structural damage such as cracking, joint failure, or uplift—particularly for lightly loaded or tension piles embedded in highly plastic clays. Furthermore, properly installed piles can enhance the overall stiffness of the soil mass, reducing the risk of differential movements and minimizing structural damage (Ng & Chiu, 2001).

Numerical Simulation of Pile Installation

The process of pile driving induces continuous changes in the stress distribution and void ratio near the pile-soil interface, leading to significant deformations and overpressure development. The displacement and shear strain generated during installation alter the soil's mechanical behavior, necessitating an advanced numerical approach to capture these dynamic changes. Finite Element (FE) modelling has emerged as an effective tool for simulating pile penetration, allowing for the incorporation of nonlinear soil behavior, frictional interactions, and elastoplastic deformations (Sheng et al., 2005). One of the major challenges in pile simulation is accounting for the evolution of excess pore water pressure, which dissipates over time as consolidation occurs, leading to an increase in shaft resistance. Additionally, the interaction between the pile and surrounding soil is highly complex, requiring appropriate interface modelling techniques to accurately represent the shear transfer mechanism. Traditional Mohr-Coulomb models may not sufficiently capture the remoulding effects observed in cohesive soils, making advanced constitutive models, such as the Hardening Soil Model , more suitable for capturing the nonlinear stress_ strain relationship.

Furthermore, when evaluating the effects of pile installation in excavation scenarios, it is essential to consider stress relaxation and lateral soil displacement, which influence the mobilization of shaft resistance. Numerical studies have demonstrated that pile setup effects are particularly pronounced in saturated clayey environments, where excess pore pressures require sufficient dissipation time to restore effective stress equilibrium. Therefore, numerical simulations must incorporate time-dependent consolidation models to accurately represent the long-term gain in pile capacity and the associated effects of soil strength recovery.

3 Analytical Solution for Excavation-Induced Swelling and swelling pressure in Soft Clay

This chapter presents the analytical framework used to estimate the vertical swelling of soft clay soils due to excavation-induced unloading. The objective is to provide a simplified, conservative prediction using the Koppejan method, which will later be compared with the numerical modelling results.

3.1 Theoretical background of the analytical method

In soft, saturated soils, excavation results in a reduction of total and effective vertical stresses at the base of the pit. This stress release can lead to an upward movement of the underlying soil, commonly referred to as swelling or heave. Accurately estimating this vertical deformation is essential for safe and reliable geotechnical design, particularly when structural elements such as floor slabs or piles are present.

One of the most recognized frameworks for analytically estimating swelling in Dutch geotechnical practice is the Koppejan method, which forms the core of the CUR C202 design guideline (CUR C202, 2014). This method is grounded in classical soil mechanics principles—particularly Terzaghi's one-dimensional consolidation theory—but extends them to account for unloading behavior. The key advantage of the Koppejan method lies in its ability to deliver conservative, layer-by-layer predictions of swelling without the need for complex numerical modelling.

Koppejan's Deformation Concept

The Koppejan method divides the vertical deformation due to unloading into three primary components:

- Immediate swelling (elastic deformation): This occurs almost instantly upon unloading and reflects the elastic rebound of soil grains due to stress release.
- Primary swelling: This is the time-dependent swelling that occurs as negative excess pore pressures dissipate following unloading. It mirrors the process of primary consolidation in reverse.
- Secondary swelling (or secular swelling): This component represents the long-term volumetric increase due to creep or structural rearrangement under sustained low stress levels.

This division is conceptually similar to the components of settlement under loading, where deformation progresses through immediate, primary, and secondary stages. Before presenting the swelling expression, it is instructive to recall the formulation for compression (settlement), which Koppejan also expresses in terms of strain. The corresponding expression for cohesive, compressible soils is given in equation 3.1:

$$-\varepsilon_v = \frac{s_v}{d} = \left(\frac{U(t)}{C_p} + \frac{1}{C_s}\ \log t\right) \ln \frac{\sigma'_{v,1}}{\sigma'_{v,0}} \tag{3.1}$$

Then, by analogy, the total vertical strain due to swelling can be expressed in equation 3.2 as:

$$\varepsilon_v = \frac{s_v}{d} = \left(\frac{U(t)}{A_p} + \frac{1}{A_s}\ \log t\right) \ln \frac{\sigma'_{v,1}}{\sigma'_{v,0}} \tag{3.2}$$

where:

- ε_v: vertical strain of the compressible layer (negative in compression) [–].
- s_v: vertical displacement (settlement or swelling) [m].
- d : (initial) thickness of the compressible layer [m].
- C_p: primary compression constant [–].
- C_s: secondary compression constant [–].
- A_p: primary swelling constant [–].
- A_s: secondary swelling constant [–].
- $U(t)$: degree of consolidation [–].
- $\sigma'_{v,0}$: initial effective stress at the middle of the layer [kN/m²].
- $\sigma'_{v,1}$: effective stress at the middle of the layer after unloading [kN/m²].
- t: time, typically for long-term swelling [days].

In many practical applications, especially for early-stage design, the secondary swelling term is either simplified or neglected due to lack of precise long-term creep data. This yields a simplified equation as shown in equation 3.3:

$$\varepsilon_v = \frac{s_v}{d} = \left(\frac{U(t)}{A_p}\right) \ln \frac{\sigma'_{v,1}}{\sigma'_{v,0}} \tag{3.3}$$

These calculations are typically applied layer-by-layer across the depth of the soil profile, and the total heave is obtained by summing up the contributions from each layer. The swelling coefficients and are usually derived from unloading-reloading oedometer tests, but in practice, empirical values are often used based on soil type, preconsolidation stress, and local experience.

Assumptions and Interpretation

The Koppejan method makes several assumptions to maintain its simplicity:

- The soil behaves as a 1D column with purely vertical strain.
- The swelling is governed entirely by changes in effective vertical stress.
- Lateral movements and anisotropy are not considered.
- Drainage conditions are idealized and uniform.

Despite these simplifications, the method provides useful upper-bound estimates of heave, making it a conservative and practical tool for preliminary design or for validating more advanced numerical simulations.

The method can also be extended to estimate swelling pressures when vertical movement is restrained, such as by a floor slab or pile cap. In such cases, the model relates the heave that would have occurred under free swelling to the resulting upward force developed when swelling is resisted. These force estimations are valuable for assessing tension loads on piles and potential uplift on structural elements.

Relevance to Excavation Design

In deep excavations, especially in soft clay regions, swelling can be significant and persistent. The unloading process leads to negative excess pore pressures, which dissipate slowly due to low permeability. The time-dependent nature of primary and secondary swelling aligns well with the staged construction of basements or tunnels, where structural elements may be installed before swelling is complete. Therefore, analytical models that can provide conservative estimates are essential to ensure safety without excessive overdesign.

In the context of this thesis, the Koppejan method—as implemented in the CUR C202 guideline—serves as the analytical basis for evaluating swelling-induced heave and comparing it against numerically simulated outcomes. This dual approach supports a more robust understanding of swelling behavior and informs the limitations of both simplified and advanced design methods.

3.2 Application of the Analytical Method

3.2.1 Overview of the Case Study

The analytical method described in Section 3.1 was applied to a hypothetical case study involving an excavation pit in a soft clay soil, representative of typical subsoil conditions encountered in urban areas of the Netherlands. The goal of the analysis was to estimate the vertical heave resulting from unloading due to excavation, using the Koppejan method as defined in the CUR C202 guideline.

The excavation geometry consisted of a 20-meter-wide pit with varying excavation depths of approximately 5, 6, and 7 meters, constructed in soft, low-permeability clay. The soft clay stratum varied in thickness between 6, 7, and 8 meters and was classified as normally consolidated.

The focus of the analysis was to determine the magnitude of swelling at the excavation base after the excavation, and to evaluate how this swelling would contribute to uplift forces on the structural elements. The analytical results would later be compared to those from a numerical model built in PLAXIS to assess the conservativeness and realism of the Koppejan-based predictions.

An Excel sheet containing the formulation of the Koppejan method was used. Key input parameters, excavation depths, ground water level, layer thicknesses were used to represent the

simple case, and swelling coefficients were derived from Table 2.b of NEN 9997-1 and adjusted to match the representative soil conditions.

The following sections outline the specific steps taken to apply the Koppejan method in this project, including soil profile definition, stress relief calculation, and final heave estimation.

3.2.2 The Geometry of the excavation pit

The method of calculating the swelling pressure depends on the shape of the excavation pit, where the pore water pressure, effective stress , and then the calculated swelling pressure can be approximated using 1D, 2D,and 3D geometry configurations as elaborated in Equations 3.4 and 3.5.

In Figure 3.1, the geometry of the excavation pit is used to indicate which approximation method can be used.

1.D : when the depth is very small compared to other dimensions of the excavation pit (h << b , h << L and b >>L).

2.D : when we dealing with a relatively rectangular excavation pit shape.

3D: When the excavation pit is more or less square shape.

$$\Delta p(t) = \frac{1}{\eta}\left(1 - U(t)\right).\Delta\sigma_{unl} \quad ; \quad \Delta p(t=0) = \frac{1}{\eta}.\Delta\sigma_{unl} \tag{3.4}$$

$$\Delta\sigma_1'(t) = \left[1 - \frac{1}{\eta}\left(1 - U(t)\right)\right].\Delta\sigma_{unl} \quad ; \quad \Delta\sigma_1'(t=0) = \left(1 - \frac{1}{\eta}\right).\Delta\sigma_{unl} \tag{3.5}$$

Where:

- $\Delta\sigma_{unl}$ Relief due to excavation / Change in total stress [kPa]
- $\Delta\sigma_1'$ Change in vertical effective stress [kPa]
- Δp Change in excess pore water pressure [kPa]
- U(t) Degree of consolidation as a function of time t [-]
- t Time [s]
- η The geometry factor depending on the geometry of the excavation pit [-]
  (For 1D η: =1 , for 2D:η =2 , for 3D:η =3)

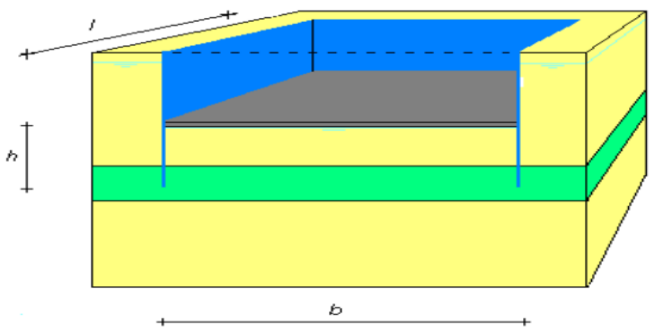

b: Excavation width (m)

L: Excavation length (m)

h = diaphragm length (m)

Figure 3.1: The Geometry of the excavation pit

3.2.3 Input Parameters and Soil Profile

This section presents the input parameters and soil profile used for the analytical evaluation of excavation-induced swelling as shown in Table 3.1: Soil Stratigraphy and Groundwater Levels (Representative Case). While multiple cases are considered in the overall analysis—consisting of three different clay layer thicknesses and three excavation depths, one representative case is presented here to illustrate the calculation procedure. The comparative results for all combinations are provided in Table *3.8*.

The representative soil profile consists of three distinct layers: a top sand layer, an intermediate clay layer, and a bottom sand layer. All layers are assumed to be normally consolidated. The clay layer is the primary focus of the swelling analysis, as it is compressible and low-permeability.

Before dewatering, the groundwater level (G.W.L) is assumed to be at a depth of −1.0 m throughout the profile. After excavation and dewatering, the G.W.L is lowered to -5.5 m in the top sand layer. The G.W.L within the clay layer is computed via vertical interpolation due to its partial drainage.

Table 3.1: Soil Stratigraphy and Groundwater Levels (Representative Case)

Soil Layer	Type	Thickness [m]	G.W.L [m] before lowering	G.W.L [m] after lowering
Sand	Normally Cons	6	-1	-5,5
Clay	Normally Cons	8	-1	Vertically Interpolated
Sand	Normally Cons	16	-1	-1

The mechanical and hydraulic parameters for each soil layer are presented in Table 3.2, including unit weights, effective friction angle, and soil compressibility and permeability characteristics relevant for swelling and consolidation analysis.

Table 3.2: Geotechnical Properties of Soil Layer

Soil Layer	γ_{unsat} [kN/m^3]	γ_{sat} [kN/m^3]	ϕ' [-]	A_p [-]	A_s [-]	Cv_{swell} [m^2/s]
Sand	18	20	32,5	4800	1,00E+09	1,600
Clay	17	17	17,5	120	1,00E+09	4,00E-07
Sand	18	20	32,5	4800	1,00E+09	1,600

3.2.4 Swelling Response Due to Excavation

This section presents the calculation of swelling deformation and associated swelling pressure resulting from excavation-induced unloading. The vertical effective stress is first evaluated before and after excavation at the mid-depth of each layer. The stress relief caused by excavation is then used to estimate the primary vertical swelling. The swelling response is assessed in two stages: free swelling before floor installation, and restrained swelling contributing to pressure on the structure.

The initial vertical effective stress and pore pressure values at the mid-depth of the sand and clay layers are listed in Table 3.3 as shown in Figure 3.2. These are used as initial conditions prior to excavation-induced unloading.

Table 3.3: Initial Vertical Effective Stress and Pore Pressure

Soil Layer	Soil layer Depth [m]	$\sigma'_{v,mid,ini}$ [kPa]	$U_{mid,ini}$ [kPa]
Sand	0-6	38	20
Clay	6-14	96	90

The excavation in this representative case is carried out to a depth of- 5.0 m, with the groundwater table correspondingly drawn down to −5.5 m as shown in Table 3.4.

Table 3.4: Excavation and Dewatering Conditions

Excavation Depth [m]	G.W.L [m] after lowering	Clay layer thickness [m]
-5	-5,5	8

As a result of excavation, stress relief occurs within the soil profile. The vertical effective stress at the mid-depth of each layer after excavation ($\sigma'_{v,mid,unl}$) is computed, along with the corresponding stress reduction ($\Delta\sigma'_{v,mid,unl}$). The primary swelling ($S_{v,prim}$), is then calculated using the analytical Koppejan formula as shown in Table 3.5.

Table 3.5:Stress Relief and Vertical Swelling After Excavation

Soil Layer	Soil layer Thickness [m]	$\sigma'_{v,mid,unl}$ [kPa]	$\Delta\sigma'_{v,mid,unl}$ [kPa]	$S_{v,prim,t=\infty}$ [m]
Sand	1	9	-54	0
Clay	8	19,5	-76,5	0,106

Following the excavation-induced stress relief and swelling estimates presented in Table 3.5, Figure 3.2 illustrates the redistribution of vertical effective stress and pore pressure with depth, both before and after excavation. This graphical representation helps visualize the impact of unloading on the stress conditions across the sand and clay layers.

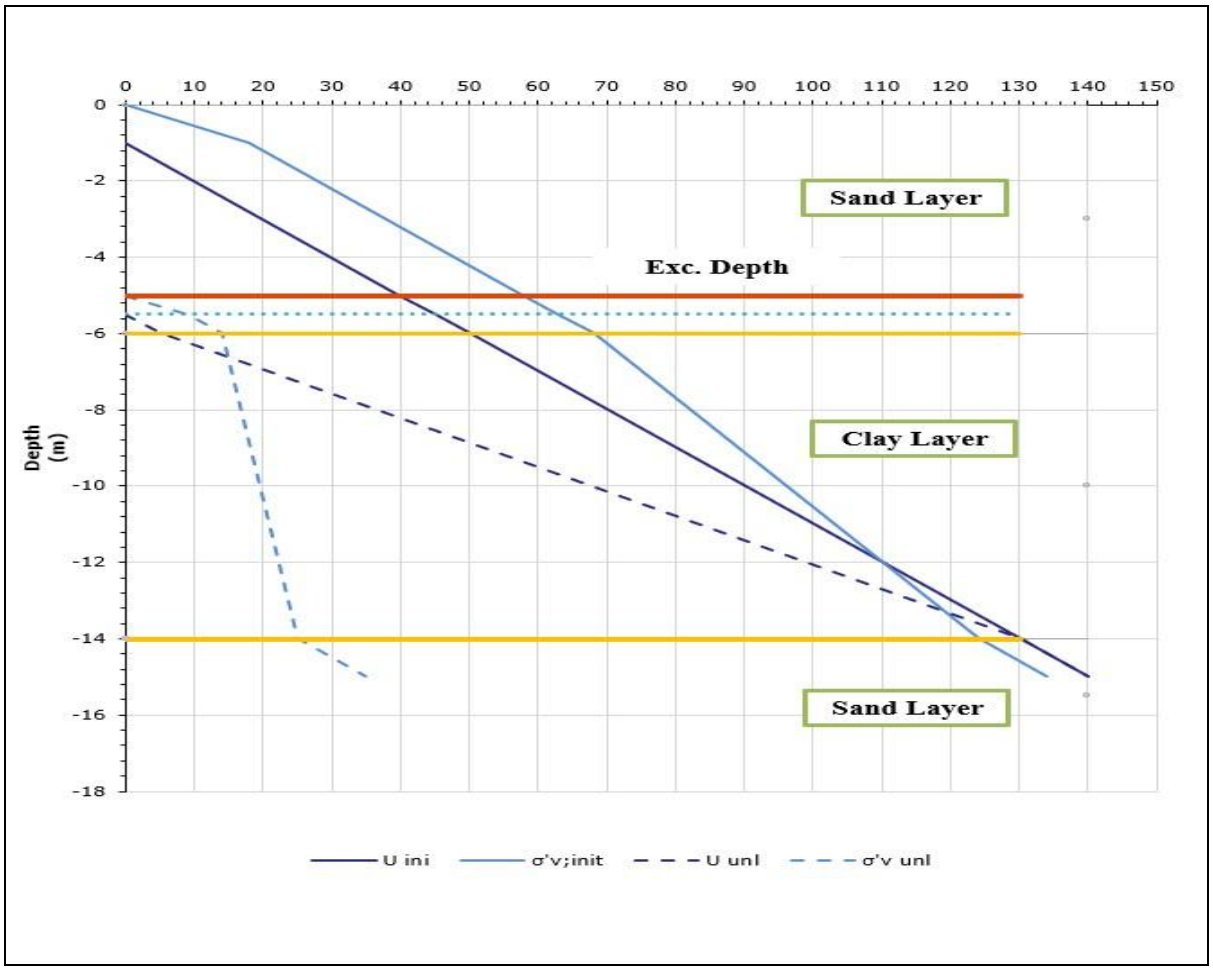

Figure 3.2:Redistribution of Effective Stress and Pore Pressure Due to Excavation

3.2.5 Time-Dependent Swelling and Swelling Pressure on the Floor

The primary swelling , previously computed, represents the total potential swelling of the clay layer at the end of consolidation when the degree of consolidation U(t)=100%. However, in reality, the clay begins to swell as soon as unloading occurs and continues to do so until a floor slab is installed and restrains further deformation.

To estimate the swelling that occurs during this free swelling phase, the Half-Time Method, as outlined in the CUR C202 Guideline, is adopted. This method assumes that half of the excavation duration contributes to the swelling process, as only the latter half of the excavation significantly affects the swelling clay. The total time during which free swelling occurs, $t_{free,swell}$ is given by equation 3.6:

$$t_{free,swell} = \frac{1}{2} t_1 + t_2 + t_3 \tag{3.6}$$

Where:

- t_1: Duration of the excavation [days].
- t_2: Waiting period after excavation and before floor installing [days].
- t_3: Duration of floor installation and curing [days].

During this period, the clay layer is free to swell. The amount of vertical swelling at the time of floor installation can be estimated by evaluating the degree of consolidation U(t) at $t_{free,swell}$ and applying it to the primary swelling as state in equation 3.7:

$$S_{v,(t_{free,swell})} = U_{(t_{free,swell})} * \ S_{v,prim,(\ t=\infty)} \tag{3.7}$$

To compute the degree of consolidation at the end of the free swelling period, the following time-dependent formulation is used. The solution is based on the vertical 1D consolidation theory (Terzaghi) and CUR C202 Guideline's approximation for vertical drainage with double drainage (drainage on both ends). The degree of consolidation is given by equation 3.8:

$$U_{(t_{free,swell})} = \sqrt[6]{\frac{T^3}{T^3+0{,}5}} \tag{3.8}$$

Where:

$$T = \frac{Cv_{swell} * t}{h^2} \ ; \quad h = \frac{d\ (clay)}{2} \tag{3.9}$$

- U(t): Degree of consolidation at time t [-].
- Cv_{swell} :Coefficient of consolidation for swelling [m²/s].
- t: Time during which free swelling occurs [s].
- h: Drainage path = half of the clay layer thickness for double drainage [m].
- T: Time factor [-].

After the floor is installed, further swelling becomes restrained and will instead contribute to a swelling pressure acting on the underside of the slab. This pressure can be estimated using the analytical swelling pressure expression from earlier equation (3.4).

This pressure build-up is time-dependent and continues until full consolidation is reached beneath the restrained slab.

For the representative case, the computed free swelling response and the resulting swelling pressure are summarized in the following tables. Table 3.6 presents the degree of consolidation at the end of the free swelling period, the corresponding vertical swelling deformation, and the parameters used in the calculation, while Table 3.7 provides the calculated swelling pressure acting on the underside of the slab after floor installation.

Table 3.6: Free Swelling Response at Time of Floor Installation (Representative Case)

$t_{free,swell}$ [day]	Cv_{swell} [m²/s]	d [m]	h [m]	T [-]	$U_{(t_{free,swell})}$ [%]	$S_{v,(t_{free,swell})}$ [mm]
45	4,00E-07	8	4	0,0972	35,2	38

Table 3.7: Swelling Pressure at Time of Floor Installation (Representative Case)

$\Delta\sigma_{unl}$ [kN/m^2]	η [-]	$U_{(t_{free,swell})}$ [%]	Swell pressure [kN/m^2]
58	1	35,2	37,6

The evolution of swelling and swelling pressure over time is illustrated in the Figure 3.3. It shows how the vertical swelling deformation increases with time, while the corresponding swelling pressure begins to develop only after the slab is installed (after 45 days), continuing to build up until full consolidation is reached.

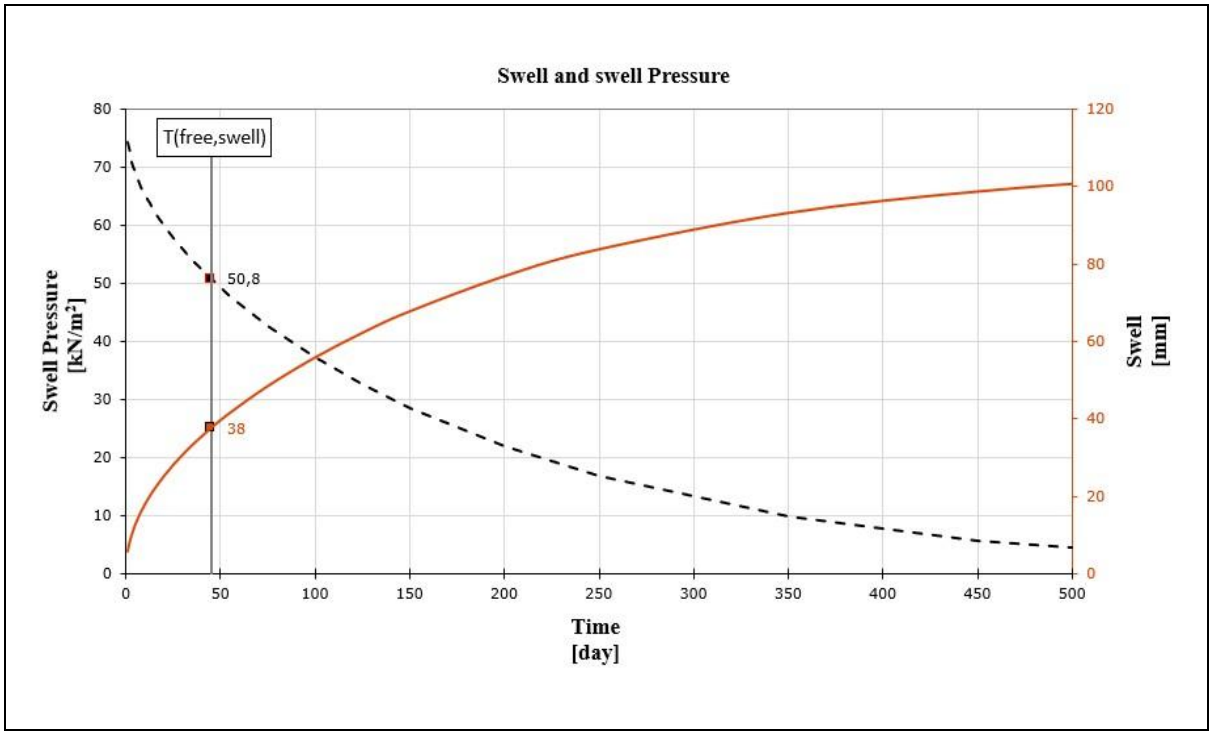

Figure 3.3:Time-Dependent Swell and Swelling Pressure

Table 3.8: Analytical Evaluation of Swelling Displacement and Swelling Pressure for Different cases

Clay layer Thickness [m]	Excavation depth [m]	Total Swelling [mm]	Free Swelling [mm]	Restricted Swelling [mm]	Swelling Pressure [kPa]
8	5	107	38	69	37,6
7	5	103	41,2	61,5	34,7
6	5	99	46,3	52,4	30,8
8	6	133	47	86	44,1
7	6	131	53	78	40,7
6	6	130	61	69	36,1

4 Numerical Modelling

4.1 Selection of suitable of a suitable numerical model

Soil, as a complex material, demonstrates diverse behaviours under varying stress conditions, including loading, unloading, and reloading. Moreover, below the plastic limit, it follows a non-linear pattern, with stiffness that depends on the applied stress (Kok et al., 2009). In order to represent the relation between stress and strain in the geotechnical engineering applications, what is known as constitutive soil modelling, consists of mathematical expressions that approximates soil and rock deformations is used (Onyelowe et al., 2023).

The finite element based program Plaxis 2D version 2024 is used to numerically analyse the heaving at the bottom of the excavation pit, where an advanced constitutive soil model is used to assess the soil displacements and stresses using different calculation stages.

4.2 Constitutive material model

Numerical Modelling is largely based on approximations, where the used constitutive soil model is implemented to reflect the real-behavior of the soil, but these assumptions can differ significantly from a model to another as stated by (Brinkgreve et al., 2017).

Brinkgreve (2022) presents several material model possibilities and limitations as shown in Table 4.1, as well as the applicability of these constitutive models to the type of loading as shown in Table 4.2.

Table 4.1 The suitable soil model for different geotechnical applications (A: is the best, B: is reasonable, C: is first order approximation). (Brinkgreve, 2022).

Model	Foundation	Excavation	Tunnel	Embankment	Slope
Linear Elastic	-	-	C	-	-
Mohr-Columb	C	C	C	C	C
Hardening Soil	B	B	B	B	B
HS small Strain	A	A	A	A	A
Soft Soil Creep	B	B	B	A	A
Soft Soil	B	B	B	A	A

Table 4.2:The applicability of these constitutive models to the type of loading (A: is the best, B: is reasonable, C: is first order approximation). (Brinkgreve, 2022).

Model	Primary compression	Unloading /Reloading	Shear/ Deviatoric loading	Compression + Shear	Tension + shear
Linear Elastic	C	C	-	-	-
Mohr-Columb	C	B	C	C	C
Hardening Soil	A	B	B	A	A
HS small Strain	A	A	A	A	A
Soft Soil Creep	A	B	B	A	B
Soft Soil	A	B	B	A	B

Constitutive models are used to describe the stress-strain behavior of soils by providing a framework for understanding how soil will behave under different loading conditions. Wood M.D (1990) suggests that considering the past history and future behavior of the soil and identifying an appropriate level of complexity is necessary in selecting a constitutive model. Brinkgreve et al. (2017) highlight the strengths and weaknesses of various material models, including the Mohr-Coulomb model, which is considered a rough approximation and not necessarily the most optimal, mainly due to its simplistic stress-strain relationship when compared with more advanced models (Hardening Soil model) .

Hardening soil model

Hardening soil model is an advanced soil model which is used to analyse the non-linear behavior of soil by taking into account a change of the stiffness modulus by a change of the soil stresses due to compression and/or shearing of the soil. Distinction can be made between the two main types of hardening. The shear hardening is used to model the irreversible strains due to primary deviatoric loading that is happening behind the retaining-walls in the case of an excavation pit and the compression hardening is used to model the irreversible plastic strains that may induced by developing the yield surface (Extending the elastic region) which is defined by the pre-consolidation stress if the case is loading, or staying at the elastic region when the mean effective stress P is decreases due to unloading so going below the pre-consolidation stress. In Figure 4.1 below, the two types of hardening that forms the Hardening soil model are illustrated.

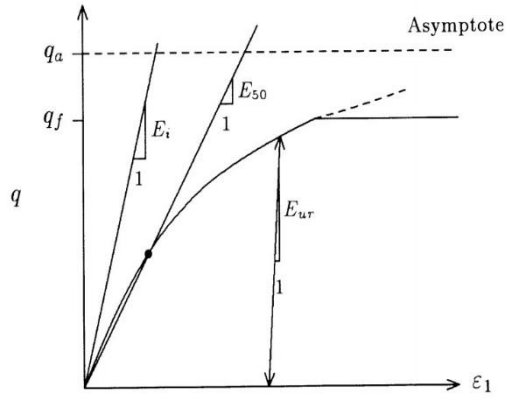

Hyperbolic /shearing Hardening soil (Schanz et al., 1999)

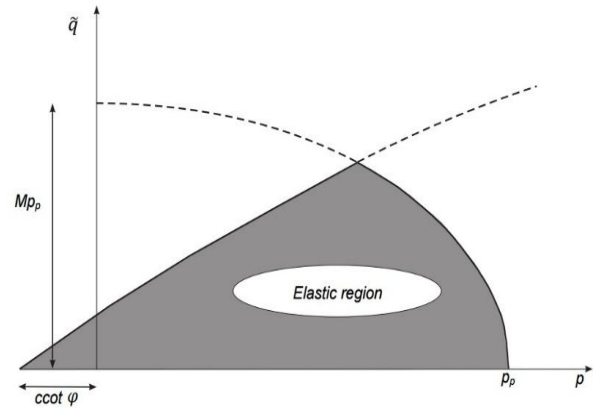

ccompression hardening (Plaxis 2D 2024.2 Material Models Manual 2D,n.d)

Figure 4.1:The Hardening Soil Model

Despite the model is based on isotropic but it has many advantages, such as the hyperbolic relation of stress-strain relationship during primary loading, distinction between primary- and un-/re-loading, memory for pre-consolidation and stress dependant stiffness (Brinkgreve et al., 2017). By taking into consideration the pre-consolidation pressure, the hardening soil model allows a more precise soil modelling. In Plaxis this can be performed by using OCR (over-consolidation ratio) or POP (pre-overburden pressure), see **Error! Reference source not found.**.

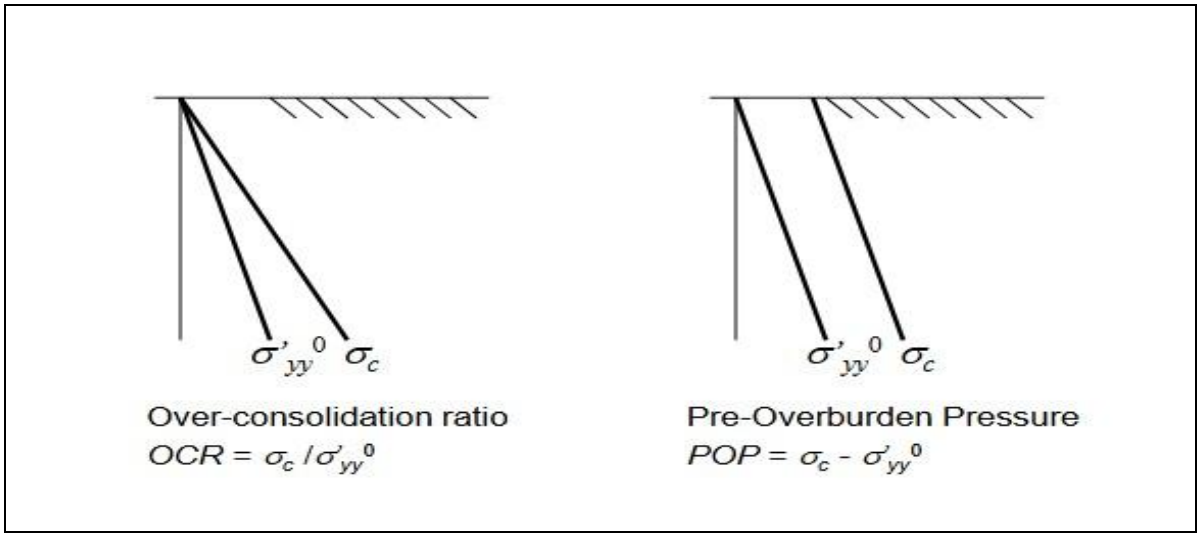

Figure 4.2: The definition of over consolidation ratio by OCR and POP.(Brinkgreve et al., 2010)

The incorporation of pre-consolidation pressure into the model is based on the observation that, when the stresses exceed the pre-consolidation pressure, the stress-strain that represents the stiffness of the soil gives a young's modulus that is smaller than the young's modulus if the case is for unloading or preloading when the stresses are below the pre-consolidation stress.

The hardening soil model consists of three main stiffness modulus; E_{ur}^{ref}, E_{50}^{ref}, E_{oed}^{ref}which are used to define the Elastic unloading/ reloading strain , the plastic straining due to primary deviatoric loading , and the plastic / elastic straining due to primary compression or unloading, respectively.

These modulus are stress dependent as they are changing by the change of the soil stress as shown in the following three equations. Eighth(Brinkgreve et al., 2010).

$$E_{ur}=E_{ur}^{ref}\left(\frac{\cos(\theta)-\sigma_3'*\sin(\theta)}{\cos(\theta)+p^{ref}*\sin(\theta)}\right)^m \quad (4.1)$$

$$E_{50}=E_{50}^{ref}\left(\frac{\cos(\theta)-\sigma_3'*\sin(\theta)}{\cos(\theta)+p^{ref}*\sin(\theta)}\right)^m \quad (4.2)$$

$$E_{oed}=E_{oed}^{ref}\left(\frac{cos(\theta)-\frac{\sigma_3'}{K_0^{nc}}*sin(\theta)}{cos(\theta)+p^{ref}*sin(\theta)}\right)^m \quad (4.3)$$

Where:

- E_{ur}^{ref} : Reference unloading / reloading stiffness modulus, corresponding to the reference confining pressure P^{ref}. [KN/m^2]
- E_{50}^{ref} : Reference secant stiffness modulus in standard drained triaxial tests corresponding to the reference confining pressure P^{ref}. [KN/m^2]
- E_{oed}^{ref}: Reference tangent stiffness for primary oedometer loading corresponding to the reference confining pressure P^{ref}. [KN/m^2]

In the above mentioned formulas the E^{ref} is the reference Young's modulus that is corresponding to the confining reference stress P^{ref} which is set to 100 kPa, as a default value in Plaxis. The factor m is the power for stress-level dependency of stiffness which is set 1 to for the soft soil and 0.5 for the sand. The stiffness is depending on the stress level (by depth) which is determined by the following formula as E_{ur}^{ref} and E_{50}^{ref} are depending on σ'_3, while E_{oed}^{ref} is depending on σ_1. (Brinkgreve et al., 2010).

$$\sigma_3 = K_0 * \sigma_1 \quad (4.4)$$

Besides the advantages of stress-dependency and memory of pre-consolidation stress, the HS model still has a number of limitations. Firstly, this model does not capture the softening behaviour caused by dilatancy effects (Brinkgreve & Broere, 2008) . In the HS model, the dilatancy continues to infinity, unless the dilatancy cut-off option is used. Moreover, the HS model does not take into account the increase of stiffness at small strain in comparison with reduced stiffness at large strain level. Lastly, this model also has a shortcoming in the region of small stress cycles due to an excessive accumulation of deformations in cyclic loading.

4.3 Geometry of the model

The numerical model represents a staged excavation process carried out in five phases to ensure stability and prevent soil collapse. The final excavation depth reached 5 meters, with each excavation phase followed by a consolidation stage to allow for dissipation of excess pore water pressure and soil settlement. To provide lateral support and maintain structural integrity, sheet piles were installed along the excavation perimeter. Additionally, struts in compression were incorporated at the surface level and at an intermediate depth of -2.5 meters. These struts played a crucial role in counteracting lateral soil pressures and minimizing excessive deformation, particularly during excavation stages where unsupported soil walls could lead to excessive movement or failure.

To manage groundwater conditions, dewatering was performed within the excavation pit, lowering the initial water table from -1 meter to -5.5 meters. This measure was necessary to reduce hydraulic pressures on the excavation walls and prevent potential instability due to uplift or excessive seepage. However, the piezometric water level in the sand layer beneath the clay deposit was maintained at -1 meter throughout all excavation stages to ensure realistic hydrostatic conditions and prevent uncontrolled seepage from deeper permeable layers.

The soil profile was modelled with a layered stratification, consisting of a 6-meter-thick sand layer at the surface, underlain by an 8-meter clay deposit, followed by a 16-meter deep sand

layer. This configuration was critical in accurately capturing the different mechanical responses of granular and cohesive materials under excavation-induced stress changes. The clay layer played a significant role in influencing ground deformation and excess pore pressure generation, while the underlying sand layers provided drainage paths, affecting consolidation behavior.
To further enhance the model's accuracy in representing soil-structure interaction, embedded beam elements were used to simulate the pile behavior. Embedded beams are particularly effective in numerical modelling as they allow for realistic representation of axial and lateral load transfer, while accounting for pile-soil interaction without requiring full 3D volume elements. The embedded pile was assigned volumetric expansion, meaning that its installation effects were simulated by introducing horizontal soil displacement around the pile, while neglecting vertical strains. This approach replicates the stress redistribution and excess pore water pressure buildup commonly observed in pile driving scenarios.

The volumetric expansion method was implemented to simulate the lateral soil displacement caused by pile penetration, capturing the effects of shear stress mobilization along the pile shaft and radial stress redistribution in the surrounding soil. This approach is particularly relevant in soft clays, where installation effects significantly influence pile setup, consolidation, and long-term axial resistance.

To ensure an accurate representation of soil-structure interaction, the numerical model was constructed with a domain size of 160 meters in length and 30 meters in soil stratification height. The vertical boundary conditions were set as closed, preventing lateral seepage of water, while the horizontal boundaries remained open, allowing interaction with surrounding permeable layers., The mesh density was set to a very fine resolution, ensuring high precision in capturing local deformations and stress variations near critical regions, such as the excavation walls, sheet pile-soil interface, and the embedded pile zone.

4.4 Soil Parameter

Accurate determination of soil parameters is essential for numerical modelling in geotechnical engineering, as it directly influences the reliability of simulations and design predictions. In this study, the Hardening Soil Model was adopted to represent the behavior of both clay and sand soils, capturing their stress-dependent stiffness and nonlinear deformation characteristics. To define the necessary input parameters for the model, Table 2.b of NEN 9997-1 was used as a reference, providing standardized geotechnical properties based on soil type and cone penetration test (CPT) bearing capacity (q_c).

The selection of soil parameters was guided by the stratification of the site, consisting of sand and clay layers, each. The bearing capacity (q_c) derived from CPT tests served as the basis for determining key soil parameters such as effective friction angle (ϕ'), cohesion (c'), stiffness moduli (E_{50}^{ref}, E_{oed}^{ref}, E_{ur}^{ref}), and Poisson's ratio (ν). Given the importance of accurately capturing stress-strain behavior and consolidation effects, the parameters were carefully assigned to reflect the true in-situ soil conditions.

Due to the absence of laboratory test data, conservative soil parameters were adopted from Table 2.b of NEN 9997-1. This approach ensures alignment with Dutch geotechnical design standards and provides a safe estimation of soil behavior under excavation and loading conditions, The determined model parameters are summarized in Table 4.3:

Table 4.3 :The soil model parameter

Soil Parameter		Sand Layer	Clay Layer
General	Soil model	Hardening Soil	Hardening Soil
	Drainage type	Drained	Undrained A
	q_c (MPa)	8	1.2
	γ_{unsat} (KN/m^3)	18	17
	γ_{sat}(KN/m^3)	20	17

Mechanical	c'_{ref} (kPa)	0	6,6
	θ'_{ref} (°)	32.5	17.5
	Ψ (°)	0	0
	E_{50}^{ref} (kPa)	50,00E+03	3400
	E_{oed}^{ref} (kPa)	50,00E+03	5360
	E_{ur}^{ref} (kPa)	150,0E+03	17,00E+03
	ν_{ur} (-)	0.2	0.15
	Power (m) (-)	0,5	0,9

	P_{ref} (kPa)	100	100
	K_0(nc) (-)	0,4627	0.6993
	R_f (-)	0,9	0.9
Ground water	Soil class	coarse	Medium fine
	Kx (m / day)	1	$3 * 10^{-5}$
	Ky (m / day)	1	$3 * 10^{-5}$
Interface	R_{inter}	0,7	0,6
Initial	OCR	1	1

4.5 Structural element parameter

4.5.1 Embedded Beam element

An embedded beam as structural element has been used to model the rows of the piles in order to transmit the loads or the displacements to the surrounding soil by using special interface elements where the interaction between the soil and the pile involve only the skin resistance in the case of heaving where there is no base resistance required.

Since the stress state and deformation generated around the piles are three-dimensional representations, it is impossible to model such structure realistically so, the 2D representation is considered a simple approach to deal with the row of piles in the out-of-plane direction " Z-direction " in the 2D plan strain model. The idea of using the embedded beam is that the pile (which is represented) by the beam is not setting up directly in the 2D mesh, but it is superimposed on the mesh while the mesh element of the soil is continuous. Also, the interface elements involve springs in the longitudinal and transverse direction and a slider in the longitudinal direction as shown in Figure 4.3.

An elastoplastic model is used to describe the behavior of the interface. The elastic behaviour of the interface should account for the difference in pile displacements and average soil displacements in the out-of-plane direction. This depends on the out-of-plane spacing in relation to the diameter and it occurs for relatively small displacement differences, while a failure criterion is used to distinguish the plasticity at the interface where permanent slip may occur.

For the interface, to remain elastic, the shear force $|t_s|$ at a particular point is given by:

$$|t_s| < T_{max} \tag{4.5}$$

For plastic behaviour the shear force $|t_s|$ is given by:

$$|t_s| = T_{max} \tag{4.6}$$

Where T_{max} is the equivalent local skin resistance.

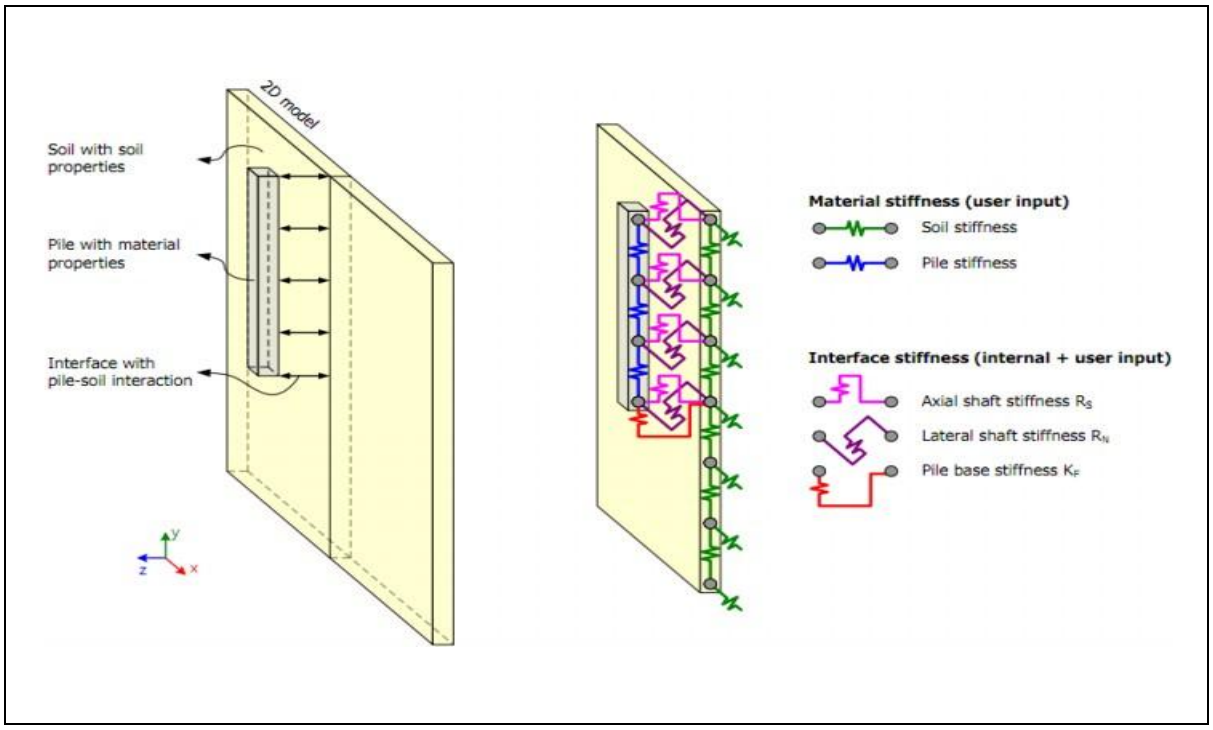

Figure 4.3: Embedded beam interaction with soil

The initial parameters are summarized in Table 4.4:

Table 4.4:The initial parameters of the embedded beam

Element parameter	Pile
Material type	Elastic
Unit weight γ (KN/m^3)	24
$L_{spacing}$ (m)	2.5/2
Cross section type	Solid square beam
E (kPa)	20,00E+06

To evaluate pile axial resistance, two methodologies were implemented:

1. The Dutch Method ((Axial Resistance Based on NEN 9997-1)):

The Dutch method, as defined in NEN 9997-1, is a widely used approach in the Netherlands for estimating pile capacity based on cone penetration test (CPT) results. This method provides an empirical framework for calculating axial shaft resistance (T_{max}) which is derived using CPT-derived frictional resistance values. The maximum axial shaft resistance per unit length of the pile is computed as shown in Table 4.5:

Table 4.5:The Dutch method for calculating of the axial shaft resistance

Soil Layer	q_c (kPa)	α(-)	$\tau_t = \alpha * q_c$ (kPa)	L (m)	W (m)	O = w * 4 (m)	As = L*O (m^2/m)	$T_{max} = As*\tau_s$ (kN/m)
Sand	8000	0.007	56	1	0.25	1	1	56
Clay	1200	0.01	12	1		1	1	12
Sand	8000	0.007	56	1	0.3	1.2	1.2	67.2
Clay	1200	0.01	12	1		1.2	1.2	14.4
Sand	8000	0.007	56	1	0.4	1.6	1.6	90
Clay	1200	0.01	12	1		1.6	1.6	19.2
Sand	8000	0.007	56	1	0.45	1.8	1.8	101
Clay	1200	0.01	12	1		1.8	1.8	22

Where:

q_c : The bearing capacity of the soil depending on the cone penetration test (kPa).

α : Empirical factor based on soil type and pile installation conditions (-).

τ_s : The shaft resistance of the soil based on the Dutch Method (kPa).

d : Length of the pile (1 m).

O : The circumference of the pile (m).

As : The lateral surface area of the pile for one meter (m^2).

T_{max} : The maximum axial shafter resistance of the pile for each one meter (KN/m).

2. Layer-dependent approach:

The Layer-Dependent option is utilized to link the local skin resistance of the pile to the shear strength parameters of the surrounding soil, specifically cohesion (c) and friction angle (ϕ). This approach also incorporates an interface strength reduction factor (R_{inter}), , which is defined in the material properties of the respective soil or rock layers (as specified in the interfaces of each soil).

The local shear stress resistance at the pile-soil interface (τ_i) is determined as follows:

$$\tau_i = c_i + \sigma_n' \tan \phi_i \tag{4.7}$$

$$c_i = R_{inter} * c_{soil} \tag{4.8}$$

$$\phi_i = R_{inter} * \phi_{soil} \tag{4.9}$$

Where:

- τ_i : Shear stress at the interface (kPa)
- c_i : Cohesion at the interface (kPa).
- ϕ_i : Friction angle at the interface (°).
- σ_n' : The principal effective stress (kPa).
- R_{inter} : The interface strength reduction factor.
- c_{soil} : Cohesion of the adjacent soil (kPa).
- ϕ_{soil} : Friction of the adjacent soil (°).

Since the pile load-bearing capacity is dependent on the stress conditions in the soil, its exact value is not predetermined but instead develops dynamically based on the surrounding soil behavior.
The special interface applied in the embedded beam behaves in a similar manner to an interface element along a structural wall, with the key distinction that it functions as a line interface rather than a sheet. This allows the model to accurately represent skin friction development along the pile shaft.

Calculation of Skin Resistance

The skin resistance (T_i), expressed as a force per unit depth, is given by:

$$T_i = 2 \pi R_{eq} \tau_i \tag{4.10}$$

Where:

- R_{eq} : Equivalent radius of the embedded pile (m).
- τ_i : Shear stress at the interface (kPa).

4.5.2 Methods of Embedded pile Installation (Volumetric Expansion)

Previous studies on pile installation modelling have frequently assumed that the pile is inserted into a pre-bored hole, reaching its final depth before applying a static load to simulate field load tests (e.g.,Trochanis M. A., 1991;Dijkstra J. et al., 2008). However, such pre-bored pile models fail to account for the over _water pressure generation that occurs during the actual driving process, particularly in saturated clayey soils. The penetration of displacement piles significantly alters the in-situ stress state and leads to volumetric expansion of the surrounding soil, primarily in the horizontal direction, due to the lateral displacement of soil. Therefore, a more realistic numerical approach should incorporate pile driving effects, ensuring that the induced strains and pore pressure buildup are accurately simulated. In fully saturated soft clay, the displacement of soil caused by pile penetration results in the rapid development of excess pore water pressure, which gradually dissipates over time, leading to increased shaft resistance (setup effect) (Randolph & Wroth, 1979). Many conventional modelling techniques assume vertical and radial symmetry, treating the volumetric expansion as an isotropic process. However, recent research has suggested that pile penetration-induced strains are predominantly horizontal, with minimal vertical displacement, particularly in plane strain conditions (Viggiani et al., 2012). By assuming zero vertical strain ($\varepsilon yy = 0$), the model simplifies soil deformation mechanics, focusing on the radial expansion effect which is simplified to horizontal expansion in 2D Plaxis model and its influence on stress redistribution. This approach aligns with the cavity expansion theory, which describes the soil response as a function of radial displacement and induced excess pore pressure (Salgado & Randolph, 2001). When a pile is driven into soft clay, the soil immediately surrounding the pile undergoes significant remoulding, leading to a temporary loss of strength, followed by a gradual strength recovery as pore pressure dissipates. Capturing this phenomenon in numerical simulations requires nonlinear soil constitutive models, such as the Hardening Soil Model, which better represent elastoplastic behavior and stress-dependent stiffness. Furthermore, neglecting vertical strain can be particularly useful in large-scale finite element models, where computational efficiency is a concern. By reducing the complexity of the soil deformation process, this assumption enables faster convergence while still maintaining accuracy in stress-strain predictions. However, its application is primarily valid in conditions where overburden stress is sufficiently high to constrain vertical movements, such as in deep foundations and offshore installations. Overall, adopting a horizontally dominated volumetric expansion model in pile driving simulations improves the realism of excess pore water pressure predictions and provides a more accurate representation of pile-soil interaction mechanisms. For calculating the volumetric expansion in one dimension, one meter of the centre-to-centre piles space was taken as shown in Figure 4.4, and the resulted volumetric expansions for each pile width are summarized in Table 4.6, where:

$$V_{pile} = w^2 * 1m \tag{4.11}$$

$$V_{spacing} = C.T.C^2 * 1m \tag{4.12}$$

$$\varepsilon_{xx} = \frac{V_{pile}}{V_{spacing}} * 100 \tag{4.13}$$

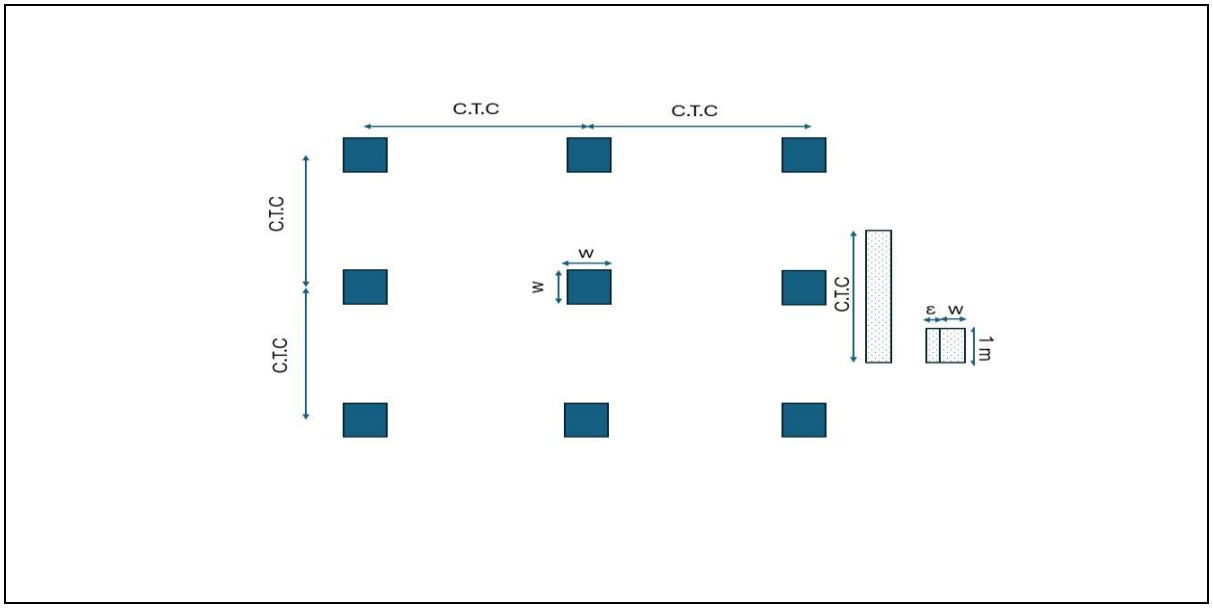

Figure 4.4: The vertical projection of the set of piles

Table 4.6: The volumetric expansion for each embedded pile width

C.T.C [m]	Pile width (W) [m]	Volumetric Expansion (VE) [%]
2.0 m	0.25	1.56
	0.3	2.25
	0.4	4
	0.45	5.1
2.5 m	0.25	1
	0.3	1.4
	0.4	2.56
	0.45	3.24

4.5.3 struts and sheet piles

Struts and sheet piles are commonly employed in excavation support systems to ensure lateral stability and load transfer. While sheet piles serve as retaining structures to hold back soil and water, struts act as compression members, counteracting the lateral earth pressures exerted on the excavation walls. The combination of these two components creates an effective support system that enhances excavation safety and reduces the risk of structural damage to nearby infrastructure. Table 4.7 and Table 4.8illustrate the parameters used to model strut and sheet-piles, respectively:

Table 4.7:The parameters of the strut element

Element parameter	strut
Material type	Elastoplastic
$L_{spacing}$ (m)	5
E (KN/m^3)	2,000E6

Table 4.8: The parameters of the sheet-pile element.

Element parameter	Sheet-pile
Material type	Elastic
Unit weight (KN/m/m)	2
EA (KN/m)	6,762E+06
EI (KN m^2/ m)	254,2E+02
ν(nu)	0.2
d (m)	0.6716

5 Numerical analysis

This chapter presents a comprehensive numerical study conducted using PLAXIS 2D to investigate soil-structure interaction and swelling behavior in a variety of scenarios. The primary objective of this analysis is to understand how different excavation support systems and geometric configurations influence ground deformations, with particular attention given to upward soil movement (swelling) in soft clay layers. The study involves several distinct cases, each representing a different level of structural complexity and support strategy, ranging from unsupported slopes to full excavation systems with piles and slabs.

5.1 Introduction to the Numerical Modelling Approach

The models simulate a typical stratigraphic profile consisting of sand–clay–sand layers, where the middle clay layer is particularly susceptible to swelling upon unloading during excavation. Each case has been designed to isolate specific factors influencing ground behavior. Case 1 focuses on an infinite slope with no structural elements, providing a baseline to validate the analytical method. Case 2 introduces sheet pile walls and struts, without the use of deep foundation elements, to examine how basic support systems affect swelling. Case 3 incorporates piles, both with and without installation effects, and explores different modelling approaches to axial resistance. Finally, Case 4 adds a floor slab to simulate the complete final stage of construction.

Table 5.1 as shown below is included to clearly outline the construction steps for each case and identify which stages apply to which configuration. This structured approach allows for a systematic evaluation of soil and structural response as elements are activated sequentially, closely mimicking real-world excavation practices. The staged analysis also enables detailed comparison between cases, helping to isolate the influence of individual elements such as sheet piles, struts, piles, and floor slabs.

The parametric studies performed in selected cases—such as variations in excavation width, clay layer thickness, pile geometry, and sheet pile embedment—offer additional insight into the sensitivity of the system to different design parameters. These results not only provide a deeper understanding of soil-structure interaction under excavation-induced stress changes, but also support the refinement of analytical methods through comparison with numerical data.

Table 5.1 Set of the calculation steps implemented in Plaxis 2D, version 2024.

Phase	Calculation type	Loading type	Time (d)	Case 1	Case 2	Case 3	Case 4	Case 5
Initial Phase	K0 procedure	Staged construction	0	✓	✓	✓	✓	✓
Install sheet pile	Plastic	Staged construction	0	-	✓	✓	✓	✓
Install strut	Plastic	Staged construction	0	-	✓	✓	✓	✓
Install pile(With or without Volumetric Expansion)	Plastic	Staged construction	10	-	-	✓	-	✓
Lowering water table (-5,5 m)	Plastic	Staged construction	0	✓	✓	✓	✓	✓
Consolidation	Consolidation	Staged construction	20	-	-	✓	✓	✓
Excavation (-2,5 m) +Strut	Plastic	Staged construction	10	✓	✓	✓	✓	✓
Consolidation	Consolidation	Staged construction	10	✓	✓	✓	✓	✓
Excavation (-3,75m)	Plastic	Staged construction	10	✓	✓	✓	✓	✓
Consolidation	Consolidation	Staged construction	10	✓	✓	✓	✓	✓
Excavation (-4,375m)	Plastic	Staged construction	10	✓	✓	✓	✓	✓
Consolidation	Consolidation	Staged construction	10	✓	✓	✓	✓	✓
Excavation (-4,6 m)	Plastic	Staged construction	5	✓	✓	✓	✓	✓
Consolidation	Consolidation	Staged construction	5	✓	✓	✓	✓	✓
Excavation (-5 m)	Plastic	Staged construction	5	✓	✓	✓	✓	✓
Resting	Consolidation	Staged construction	10	-	-	-	✓	✓
Install floor	Plastic	Staged construction	10	-	-	-	✓	✓
Final Consolidation	Consolidation	Staged construction	10^4-T	✓	✓	✓	✓	✓

5.2 Case 1: Infinite Model – No Structural Elements

The first numerical model represents an idealized case intended to isolate the behavior of the soil without any structural support. This model consists of a three-layered soil profile arranged in a sand–clay–sand sequence, with varying excavation widths. In order to maintain slope stability and prevent rotational failure, inclined slopes are used instead of vertical cuts. This configuration prevents collapse mechanisms such as sliding or overturning, allowing the soil to stand unsupported. No structural elements such as sheet piles, struts, or piles are included in this simulation, making it a purely geotechnical model aimed at understanding natural soil behavior.

This case serves as a baseline for verifying the analytical method developed for assessing soil swelling and deformation. By modelling the soil response without any external reinforcement, the simulation enables direct comparison with analytical predictions under simplified conditions.

The excavation depth is kept constant, while the width is varied to observe how it influences vertical and displacements within the soil body. The model boundaries are placed far enough from the excavation zone to minimize boundary effects, and the base of the model is fully restrained, with lateral boundaries fixed in the horizontal direction. Figure 5.1 below illustrates the case of Infinite model without any structural element

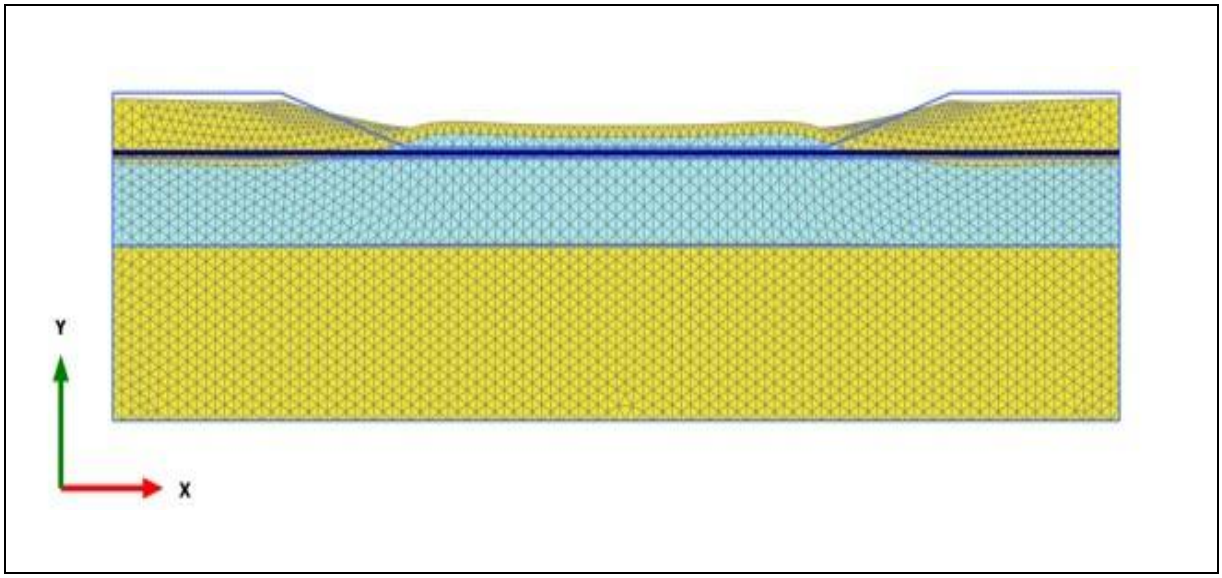

Figure 5.1:The configuration of the Plaxis model (Infinite model).

5.3 Case 2: 2D Model – Sheet pile and strut

The second case introduces structural support elements into the excavation system, specifically two sheet pile walls and struts, but without the inclusion of any piles as shown in Figure 5.2 . This configuration allows for the evaluation of how vertical deformations—particularly swelling—are influenced by basic support systems in the absence of deep foundation elements. The model retains the same soil stratigraphy as in the first case, with a sand–clay–sand sequence, and excavation is carried out vertically rather than with sloped sides, relying on the structural elements to maintain stability. The sheet pile wall is embedded sufficiently into the lower sand layer to provide lateral resistance, while the strut is positioned at the top of the wall to limit wall movement and distribute load. PLAXIS is used to simulate staged excavation with activation of the structural elements at appropriate depths.

To better understand the factors affecting swelling in this configuration, a parametric study was conducted by varying key geometric relationships in the system. First, the ratio of excavation width (W) to clay layer thickness (T) was investigated to assess how the relative size of the excavation affects swelling behavior. This was intended to reveal whether narrower or wider excavations in proportion to the clay layer would result in more significant vertical displacements due to stress relief. Second, the combined effect of excavation width (W) and excavation depth (H) was studied under different clay thicknesses to capture the influence of overall excavation geometry on the swelling magnitude and distribution. Finally, the embedded length of the sheet pile (L) into the lower sand layer was varied, examining the H/L ratio for different clay layer thickness with (H) as the excavation depth) to determine how deeper embedment contributes to controlling upward ground movement and improving system stability. This set of analyses was essential in identifying the sensitivity of the system to changes in geometry and in guiding design decisions for excavation support in similar ground conditions.

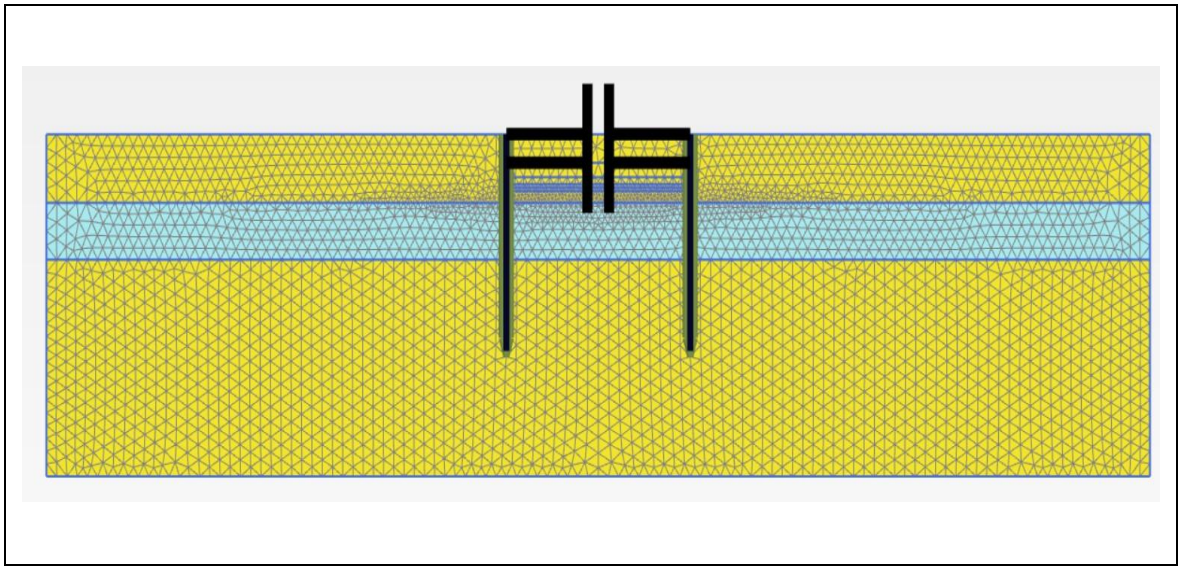

Figure 5.2:The configuration of the Plaxis model (sheet piles and struts).

5.4 Case 3: 2D Model – Sheet Pile, Strut, and Pile System

The third case builds upon the previous configurations by introducing deep foundation elements—vertical driven piles—into the excavation support system, in addition to the sheet pile wall and single strut. This expanded configuration as shown in Figure 5.3 enables a more comprehensive investigation into how deep foundation elements interact with soil during and after installation, and how they influence swelling behavior and stress redistribution at different stages of construction. The soil profile remains consistent with previous models, following a sand–clay–sand stratigraphy, and excavation is again carried out vertically. The sheet pile wall and strut serve as lateral support, while the vertical piles are intended to provide both vertical load transfer and additional confinement. Importantly, this case explores not just the structural presence of the piles, but also their installation effect, which is a critical factor often overlooked in practice.

To realistically simulate the ground disturbance caused by pile driving, a volumetric expansion was applied in the horizontal direction (xx-direction) as a proxy for the soil displacement induced during installation. This volumetric expansion varies with pile width (W) and pile spacing (c.t.c), accounting for the geometry and density of the pile group. Two pile spacings, c.t.c = 2 m and c.t.c = 2.5 m, were analysed in combination with pile widths of 0.25 m, 0.30 m, and 0.40 m, each associated with a different level of volumetric expansion. For comparison, equivalent cases were modelled without installation effects, allowing the same piles to be introduced as purely structural elements without accounting for the disturbance they create in the surrounding soil.

This setup enables a focused study on the role of pile installation in modifying the horizontal effective stress, swelling displacement, and swelling force within the system. By comparing cases with and without installation effects, the analysis quantifies how loading by piles and induced confinement from pile installation influence both the stress state and the resulting deformation after excavation. In addition, the final stage of consolidation is evaluated to assess how the installation effect alters the long-term equilibrium conditions in the soil.

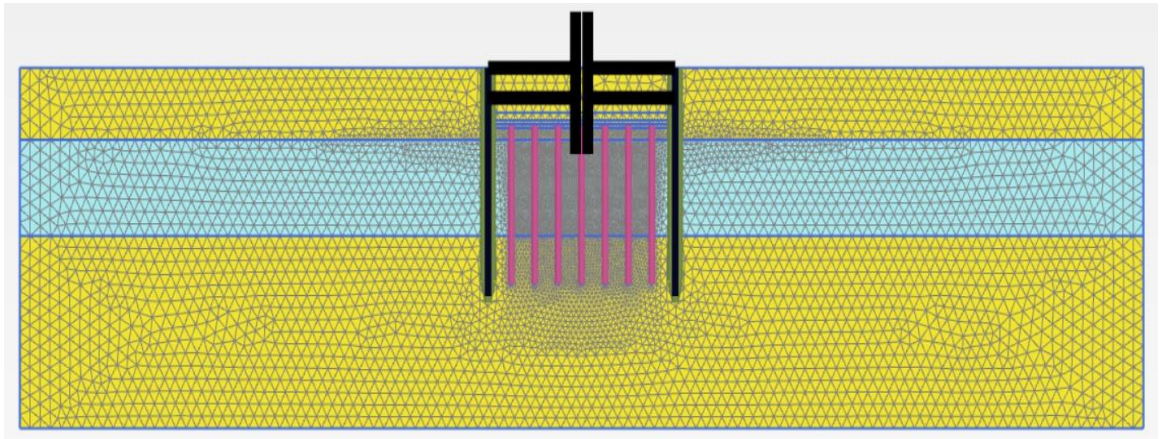

Figure 5.3:The configuration of the Plaxis model (sheet piles, struts, and the set of piles).

5.5 Case 4: 2DModel-Without Embedded Piles (Sheet Pile – Strut – Floor)

This case investigates a 2D excavation model supported by a sheet pile wall, a strut, and a floor slab, without the presence of piles. The objective is to assess how the inclusion of the floor element influences ground behavior, particularly swelling, under excavation-induced unloading. The soil profile remains the same, with a sand–clay–sand stratigraphy and vertical excavation.

The floor slab, placed at the excavation base, acts as a horizontal restraint, reducing the potential for upward clay heave. This reflects realistic construction scenarios where the floor is implemented early to enhance stability. The configuration of this case is illustrated in Figure 5.4 , showing the layout of structural elements within the excavation system.

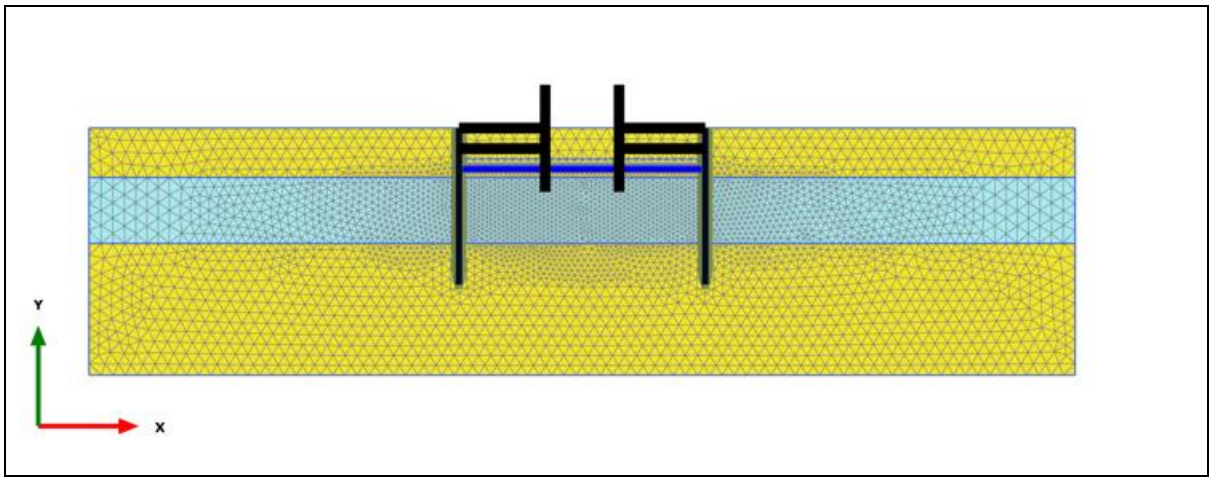

Figure 5.4:The configuration of the Plaxis model (sheet piles, struts, Floor).

5.6 Case 5: 2D Model- Full Structural System

This final case presents the most complete excavation support system, combining a sheet pile wall, top strut, base floor slab, and embedded vertical piles. The configuration, shown in Figure 5.5, represents a realistic deep excavation scheme where all structural elements work together to control soil deformation and swelling.

The soil stratigraphy remains consistent with earlier cases (sand–clay–sand), and excavation is performed vertically. The sheet pile and strut provide lateral restraint, the floor slab limits upward movement at the excavation base, and the embedded piles enhance vertical load transfer while confining the surrounding soil.

To realistically account for the effect of pile installation, a volumetric expansion was applied in the horizontal direction to simulate the soil displacement caused by driving. This expansion varies with pile width (W = 0.25 m, 0.30 m, 0.40 m, and 0.45 m) and spacing (c.t.c= 2 m and 2.5 m), reflecting different pile group geometries.

This setup enables a focused investigation of how the combined structural elements influence swelling behavior, stress redistribution, and ground stability during and after excavation.

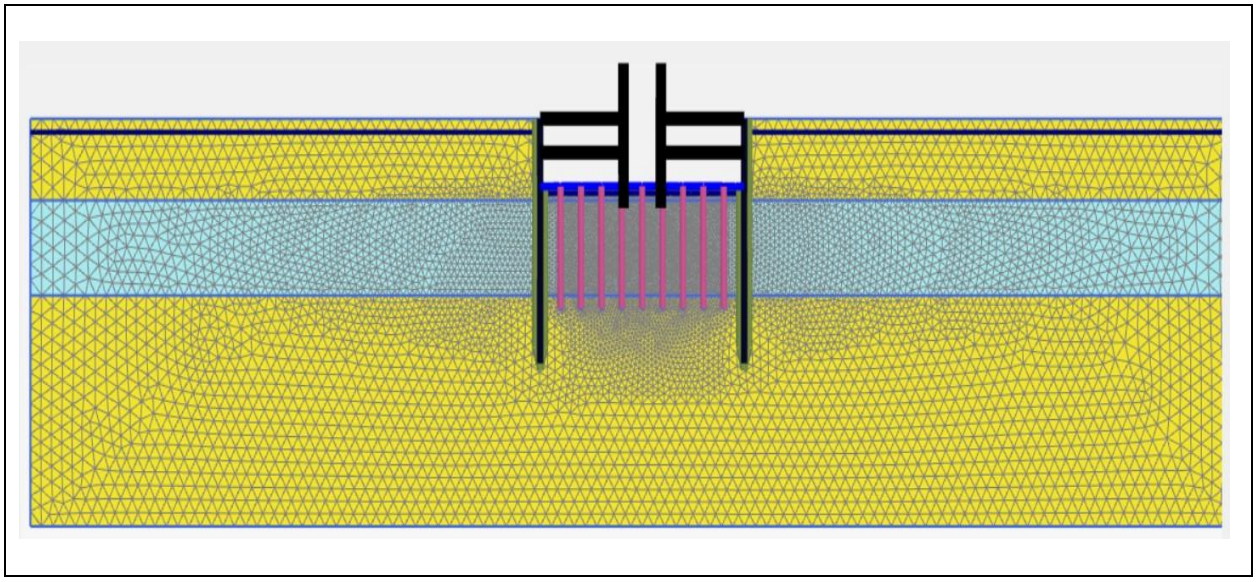

Figure 5.5: The configuration of the Plaxis model (sheet piles, struts, Floor, and Embedded piles).

6 Numerical modelling Results

6.1 Case 1 : 2D_ Model without structural element

6.1.1 Validation of the Numerical Modelling

In order to verify the reliability of the numerical approach used throughout this study, a validation exercise was conducted by comparing the results of a simplified numerical model against the analytical solution derived using the Koppejan method. The comparison focuses on the predicted swelling due to unloading following excavation in a soft clay layer, without the influence of any structural elements.

A reference case was selected to match the assumptions made in the analytical method:

- Excavation depth: 5.0 m
- Clay layer thickness: 8.0 m
- No structural support
- No pile installation or slab
- Volumetric expansion not applied

In this configuration, the analytical solution yielded a total vertical swelling of 106 mm, as calculated using the Koppejan method. The numerical model, built in PLAXIS 2D using the Hardening Soil model, was simulated under identical geometric and material conditions. The resulting maximum vertical heave predicted by the numerical analysis was approximately 99 mm as shown in **Error! Reference source not found.**.

The close agreement between the numerical and analytical results—differing by less than 7% demonstrates that the numerical model is capable of reliably capturing the vertical swelling behavior under excavation-induced unloading conditions. The minor discrepancy can be attributed to the simplifications inherent in the analytical approach, such as the assumption of 1D vertical strain and linear elastic rebound, which may neglect redistribution effects and stiffness nonlinearity.

This comparison serves as a validation of the modeling approach and confirms that the selected constitutive model, mesh configuration, and boundary conditions are appropriate for simulating swelling in soft clays. With the numerical model now benchmarked against analytical predictions, it can be confidently used in the subsequent chapters to evaluate more complex scenarios, including the influence of structural elements and pile installation effects.

6.1.2 Influence of the excavation widths on the swelling

This section presents the outcomes of the 2D model scenario, where no structural support elements—such as sheet piles, struts, or piles—are used. The soil body is assumed to maintain overall lateral stability due to the sloped geometry of the excavation (1:3 ratio), although some degree of rotation and stress redistribution may still occur. This configuration allows for an isolated investigation of the soil's natural response to excavation-induced unloading. The primary focus here is on vertical swelling and horizontal displacement behavior across varying excavation widths.

Five excavation widths were analysed: 30 m, 40 m, 50 m, 60 m, and 70 m, while maintaining consistent soil stratigraphy and boundary conditions. As illustrated in **Error! Reference s ource not found.**, the results reveal a decreasing trend in swelling with increasing excavation width. This trend initially appears contradictory to analytical expectations, which typically predict higher swelling magnitudes for wider excavations due to greater overall unloading.

To investigate this apparent contradiction, horizontal displacements were also evaluated at a reference point located at one-quarter of the excavation width (L/4) from the centre of the excavation pit. This reference location was kept consistent across all excavation widths. The results show that horizontal displacements decrease as excavation width increases, indicating that the soil body becomes more laterally restrained as the slope extends outward.

This behavior can be explained by the interplay between horizontal deformation and stress-induced vertical swelling. In narrower excavations (e.g., W = 30 m), the steeper slope geometry promotes greater inward movement of the surrounding soil toward the center. This horizontal displacement reduces lateral confinement at the base of the excavation, resulting in a localized decrease in effective stress and enabling the central clay to undergo vertical swelling more freely. Conversely, in wider excavations (e.g., W = 60–70 m), although a larger volume of soil is removed, the stress relief is distributed over a broader area due to the shallower slope. This distribution restricts the magnitude of horizontal soil movement near the center, thereby preserving lateral confinement and limiting stress relief. As a result, vertical expansion (swelling) is suppressed, leading to a lower heave despite the increased excavation width.

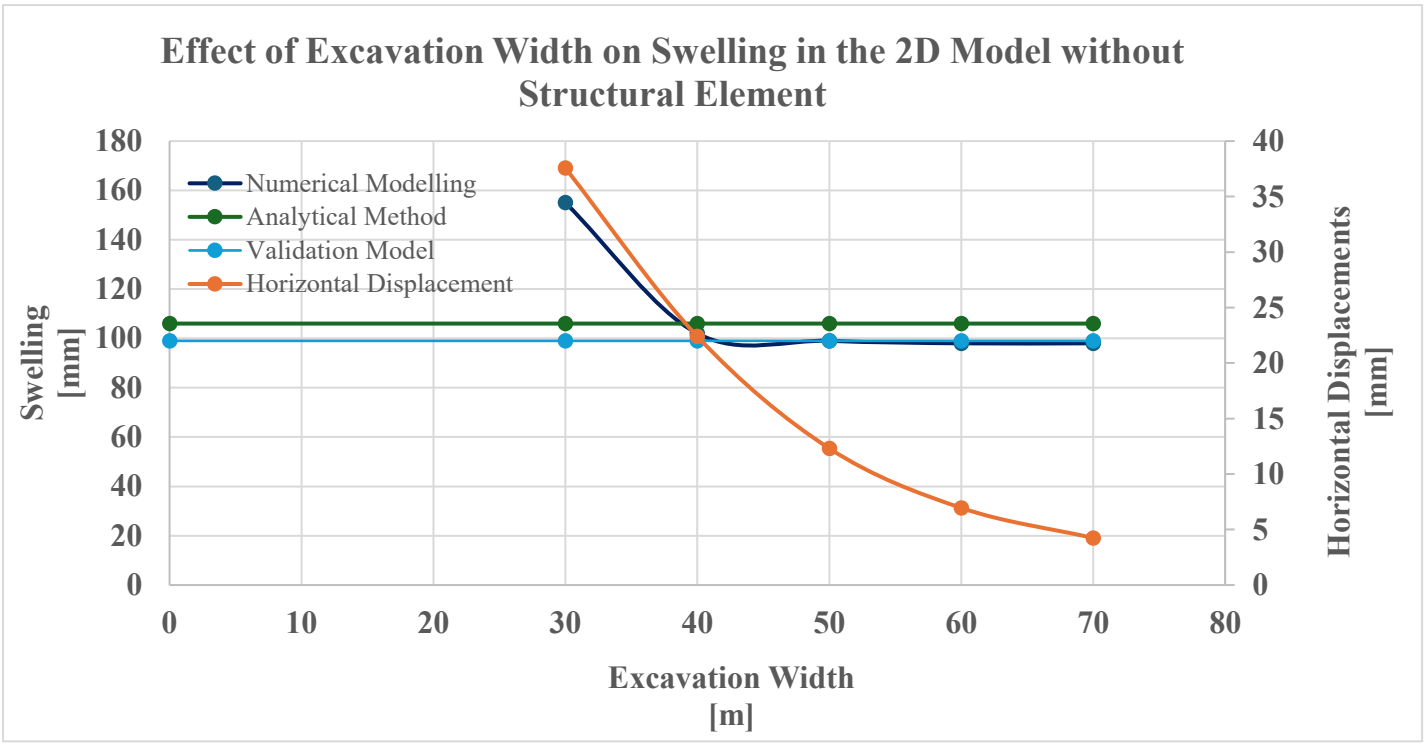

Table 6.1:Effect of Excavation Width on Swelling in the 2D Model without Structural Support.

6.2 Case 2: 2D_Model with sheet pile and strut

The results of this case focus on how swelling behavior is influenced by different geometric parameters of the excavation and the sheet pile. A parametric study was conducted to assess the effect of the excavation depth (H), excavation width (W), clay layer thickness (T), and the embedded length of the sheet pile into the sand (L) on swelling. The following subsections describe the trends observed in swelling based on these variations.

6.2.1 Influence of H/L (Excavation Depth / Embedded Length of Sheet Pile) on Swelling.

The parametric study conducted to evaluate the effect of sheet pile embedded length on swelling behavior reveals several consistent and important trends. The analysis considers excavation depths (H) of 5 m, 6 m, and 7 m, with embedded lengths of the sheet pile ranging from 1 m to 5 m (corresponding to H/L values from 1 to 7 depending on the case). For each excavation depth, simulations were carried out across varying clay layer thicknesses (T) from 5 m to 10 m. The results are plotted as H/L versus swelling for each clay layer thickness as shown in Figure 6.1,Figure 6.2, and Figure 6.3 .

Across all three cases, a clear and consistent pattern emerges: as the H/L ratio increases, the amount of swelling also increases, indicating that a shorter embedded length (L) results in less

effective control over upward soil movement. This is because a shallower embedment of the sheet pile into the underlying sand provides less passive resistance, allowing more vertical displacement to develop in the clay layer as it unloads. In contrast, longer embedded lengths (lower H/L) mobilize more of the supporting sand and help to confine the clay, reducing swelling near the excavation base.

Another consistent observation across all excavation depths is that swelling becomes more pronounced as the clay layer thickness (T) increases. For a given H/L value, a thicker clay layer exhibits higher swelling, which is attributed to its greater capacity to expand upon stress relief. This effect is magnified at greater excavation depths, where the volume of soil being removed—and thus the degree of stress unloading—is higher.

When comparing between excavation depths:

- At H = 5 m, swelling is the lowest across the board, but the sensitivity to changes in H/L remains significant. Increasing L noticeably reduces swelling, especially in thicker clay layers.
- At H = 6 m, swelling values are higher overall, and the benefits of increasing embedded length persist, though the difference between T values becomes more substantial.
- At H = 7 m, the effect of embedded length is even more critical. Swelling reaches its maximum in this case, particularly when T is 9–10 m. The rate of increase in swelling with H/L is more evident, and shallow embedment (small L) leads to a significant rise in vertical displacement.

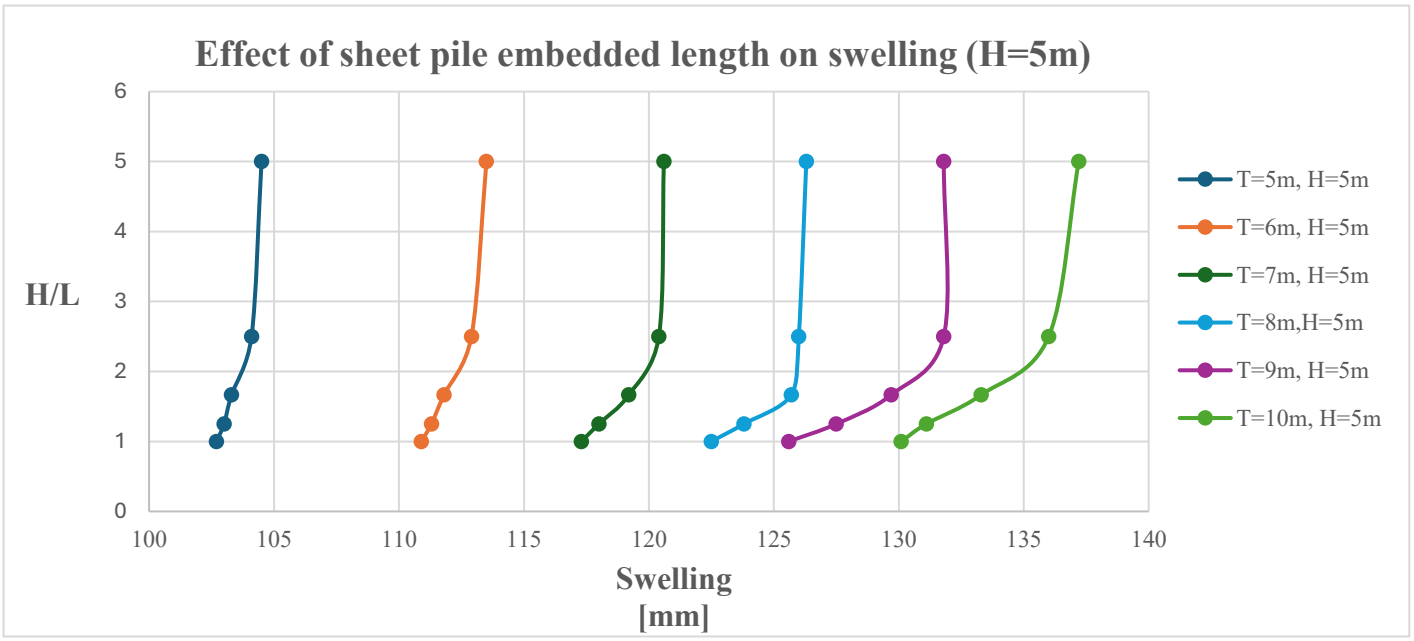

Figure 6.1:Effect of Sheet Pile Embedded Length on Swelling for H = 5 m and Various Clay Thicknesses (T).

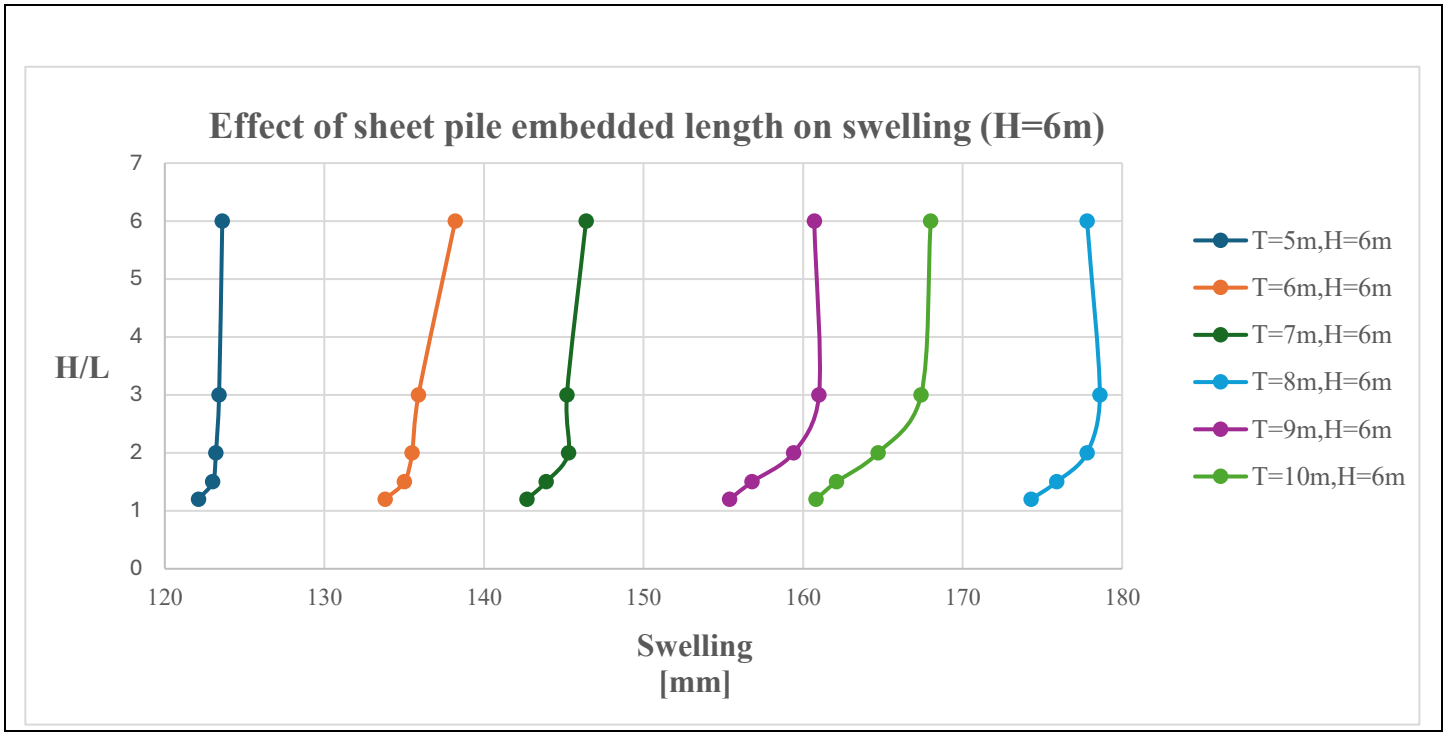

Figure 6.2:Effect of Sheet Pile Embedded Length on Swelling for H = 6 m and Various Clay Thicknesses (T).

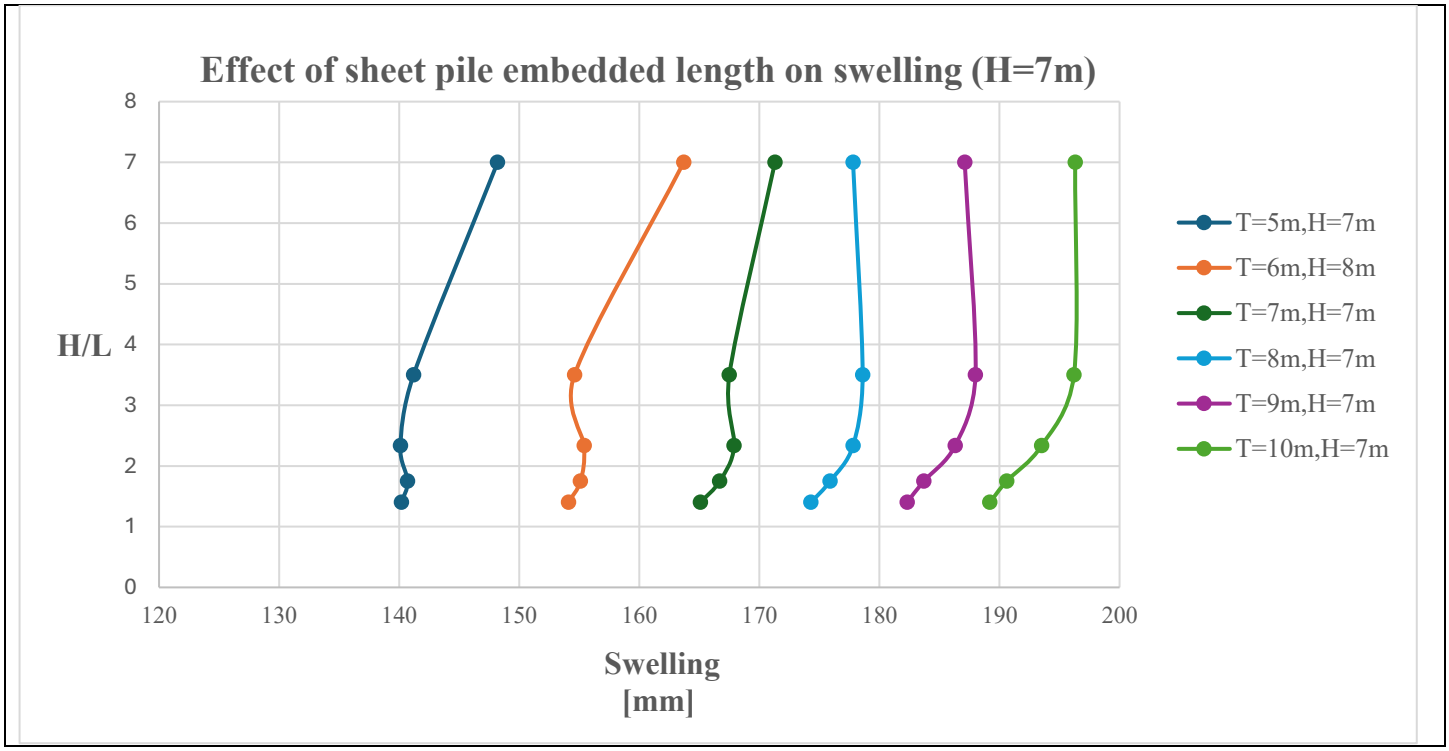

Figure 6.3:Effect of Sheet Pile Embedded Length on Swelling for H = 7 m and Various Clay Thicknesses (T).

6.2.2 Influence of W/H (Excavation Width / Excavation Depth) on Swelling

This section investigates how the ratio of excavation width (W) to excavation depth (H) influences the vertical swelling behavior in an excavation supported by a sheet pile wall and a single strut. Two excavation widths, 20 m and 30 m, were analysed for excavation depths ranging from 5 m to 7 m. The clay layer thickness was taken equal to the excavation depth in all cases, allowing consistent comparisons of swelling under equivalent soil conditions. The results are presented in terms of the W/H ratio plotted against swelling, as illustrated in Figure 6.4.

The findings show that as the W/H ratio increases, the magnitude of swelling decreases. In other words, narrower excavations tend to produce higher vertical displacements in the clay, whereas wider excavations are associated with reduced swelling. This trend contrasts with traditional analytical expectations, which suggest that a wider excavation—by removing more overburden—should result in greater upward rebound due to a larger stress release.

To explore this behavior further, horizontal displacements were examined along a consistent vertical cross-section directly in front of the sheet pile wall for both excavation widths. The results indicate that the surrounding soil undergoes noticeably more horizontal deformation in the narrower excavation. For example, in the case of W = 20 m with an excavation depth and clay thickness of 5 m, the recorded swelling was 97 mm, and the horizontal displacement at the selected location was 14.54 mm. Under the same conditions with W = 30 m, the swelling decreased to 88 mm, and the horizontal displacement was reduced to 10.84 mm.

These results suggest that the increased swelling observed in narrower excavations is closely linked to the greater extent of soil deformation toward the excavation. When the excavation width is smaller, the effects of stress relief are more concentrated, resulting in more localized movement of the surrounding soil. This concentrated deformation likely facilitates greater vertical expansion in the underlying clay. In wider excavations, the unloading effect is distributed over a broader area, which reduces the magnitude of soil movement and, consequently, the amount of swelling observed.

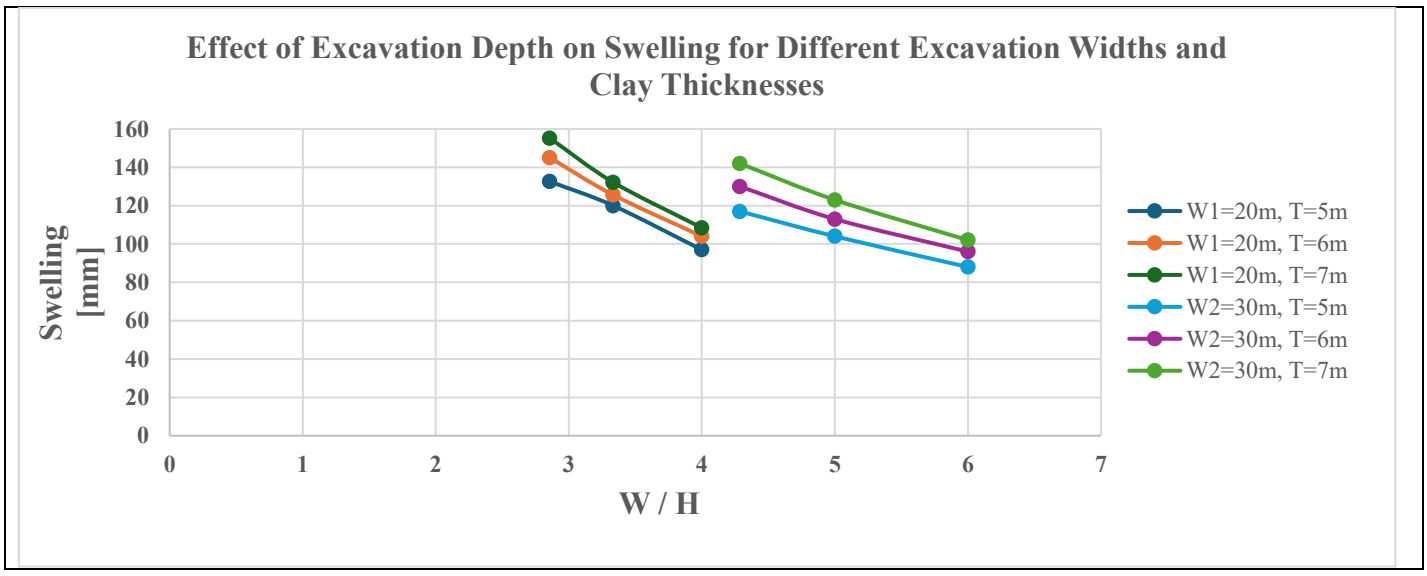

Figure 6.4: Effect of Excavation Width (W) and Clay Layer Thickness (T) on Swelling for Various W/H Ratios.

6.2.3 Influence of W/T (Excavation Width / Clay Thickness) on Swelling

This section investigates the effect of the ratio between excavation width (W) and clay layer thickness (T) on the swelling behavior of the soil in an excavation system without piles. The excavation depth is fixed at H = 5 m, while excavation widths of 20 m, 25 m, and 30 m are analysed for clay layer thicknesses ranging from 5 m to 10 m. The results are presented in terms of W/T ratios versus the corresponding swelling values, as shown in Figure 6.5.

The results reveal two key trends:

First, for each of the three excavation widths, swelling decreases as the W/T ratio increases. This indicates that for a given excavation width, reducing the clay layer thickness leads to a reduction in swelling. This behavior is consistent with theoretical expectations, as thinner clay layers have less capacity for vertical expansion upon unloading.

Second, for a fixed clay thickness (e.g., T = 5 m), increasing the excavation width from 20 m to 30 m leads to a noticeable reduction in swelling—from 102 mm to 90 mm, respectively. This observation appears to contradict conventional analytical theories, which typically predict increased swelling for wider excavations due to the larger area of stress relief. However, the numerical results suggest the opposite. This contradiction can be explained by considering the role of horizontal displacements: a cross-sectional analysis within the clay layer revealed that the horizontal displacement is greater in narrower excavations. Specifically, for W = 20 m, the displacement reached 19.58 mm, while it decreased to 13.84 mm for W = 30 m. The increased lateral movement in narrower excavations reduces confinement within the clay, facilitating greater vertical expansion. In contrast, wider excavations result in lower horizontal displacements, maintaining higher lateral restraint and thus limiting swelling.

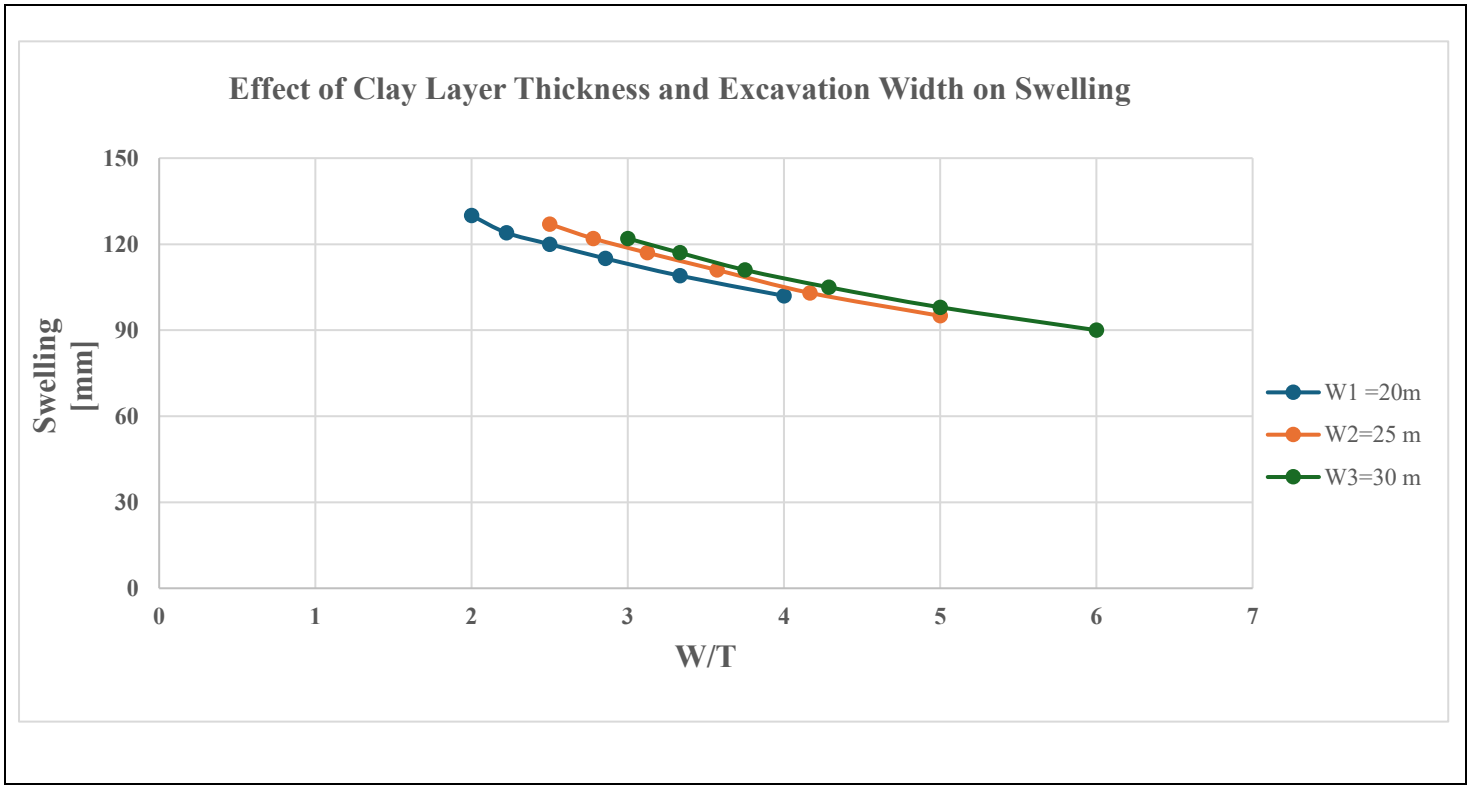

Figure 6.5:Effect of Excavation Width (W) and Clay Layer Thickness (T) on Swelling Expressed as W/T Ratio for H=5m.

6.3 Case 3: 2D_Model (sheet Pile – strut – pile system with and without Pile installation effect)

In this case, the analysis focuses on a more complete excavation support system that includes sheet piles, a strut, and vertical driven piles. The aim is to assess the influence of the pile element on soil swelling behavior, with particular emphasis on the effect of pile installation-a factor often neglected in simplified simulations. The excavation is supported laterally by a 19 m-long sheet pile wall and a horizontal strut, while vertical support is provided by piles driven to a depth of 13 m for all the numerical simulations.

Two sub-cases are considered in this analysis:

- Without pile installation effect, where the pile is introduced into the model without accounting for any soil disturbance during its installation.
- With pile installation effect, where the influence of soil displacement caused by pile driving is captured through a volumetric expansion approach.

To simulate the pile installation effect realistically, a controlled volumetric expansion in the xx-direction was introduced, reflecting the soil displacement caused by driving the pile into the ground. This expansion was varied based on the pile width and the spacing between piles, assuming that wider piles displace more soil during installation. Three different pile widths were analysed: 0.25 m, 0.30 m, and 0.40 m for c.t.c= 2,5m and 2m. The corresponding average volumetric expansion values applied in the model were 1.00%, 1.30%, and 2.56%, and 1,56 %, 2,25% and 4%, respectively.

These values were intended to mimic the degree of lateral soil movement expected from the pile driving process, acknowledging the radial displacement and stress redistribution it induces in the surrounding clay.

In contrast, for the case without the installation effect, the same pile geometries were introduced into the model with the volumetric expansion set to zero. This allows for a direct comparison between the actual pile presence (as a structural load-resisting element) and the additional soil disturbance introduced during its installation.

The comparison between these two cases helps to isolate the impact of installation-induced disturbance on the magnitude and pattern of swelling observed in the excavation zone. It also highlights the importance of considering pile-soil interaction during early construction stages, particularly in swelling-prone soils such as soft to medium clays. This setup forms the basis for the results discussed in the following section, which examine the variations in vertical soil movement under both modelling assumptions.

6.3.1 Influence of pile installation effect on the horizontal effective stress

To investigate the effect of pile installation on the horizontal stress state within the soil, a comparative analysis was conducted at the final stage of consolidation. Two different centre-to-centre spacings between piles were examined: 2.0 m and 2.5 m, in combination with three pile widths: 0.25 m, 0.30 m, and 0.40 m. The pile installation effect was incorporated using volumetric expansion (VE) to simulate the associated soil displacement.

For the configuration with c.t.c = 2.0 m, the applied volumetric expansions were:

- 1.56% for W = 0.25 m
- 2.25% for W = 0.30 m
- 4% for W = 0.40 m

For the wider pile spacing of c.t.c = 2.5 m, the VE values were slightly lower:

- 1.0% for W = 0.25 m
- 1.4% for W = 0.30 m
- 2.56% for W = 0.40 m

In all cases, reference simulations were also carried out without any installation effect (VE = 0%), representing piles inserted without soil disturbance.

As illustrated in Figure 6.6 , for c.t.c = 2.0 m, the effect of pile installation leads to a more pronounced increase in horizontal effective stress (σ'_3), especially in the clay layer. The closer spacing between the piles results in overlapping stress fields and stronger confinement, amplifying the lateral stress due to pile-induced soil displacement. In contrast, Figure 6.7shows that for c.t.c = 2.5 m, the influence of pile installation is still noticeable but less significant, owing to the greater spacing reducing the interaction between the stress zones of adjacent piles.

Overall, the results confirm that pile installation has a clear effect on the final horizontal stress state, with both pile width and spacing playing critical roles. Larger pile widths and tighter spacing increase the magnitude of induced lateral stress, while wider spacing reduces this interaction, leading to a less intense stress response in the surrounding soil.

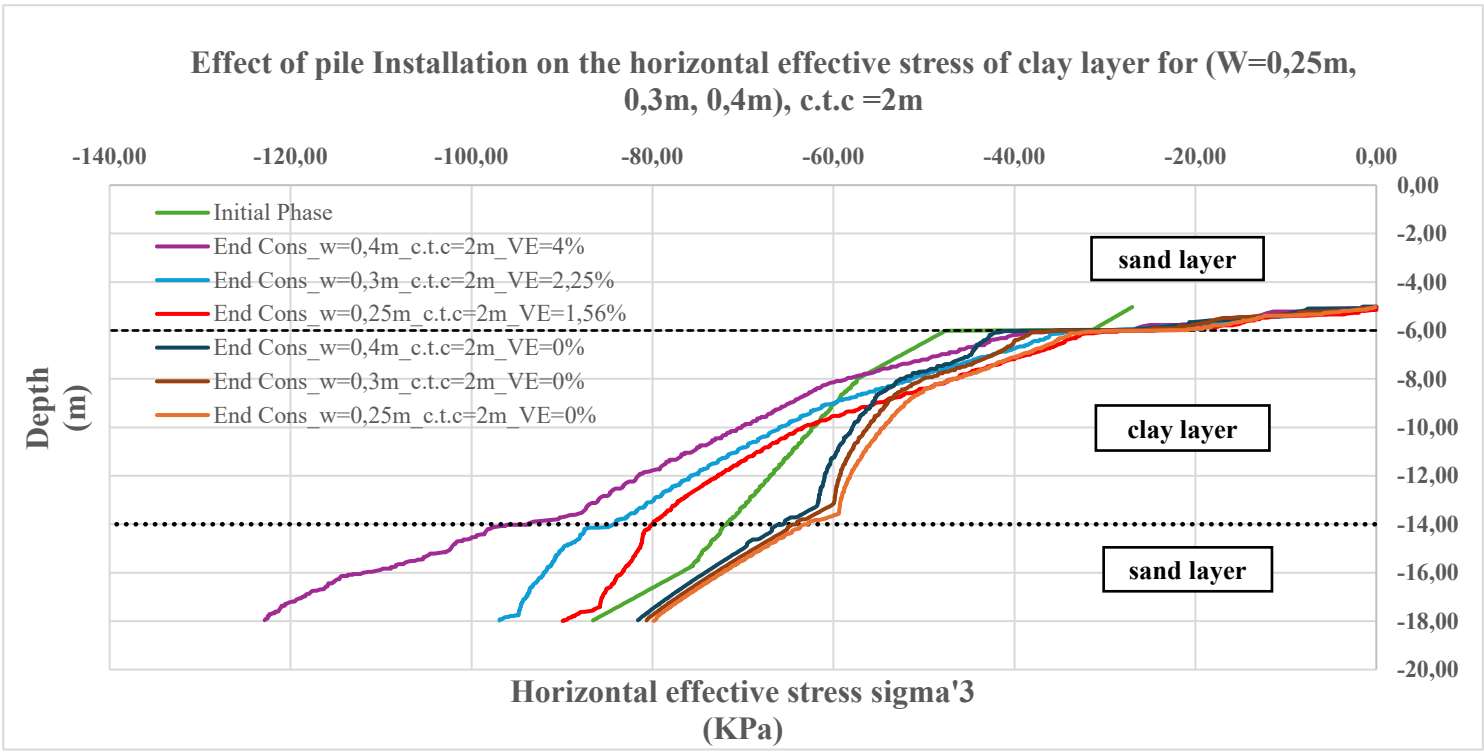

Figure 6.6: Comparison of the horizontal effective stress (With and without pile installation effect) for (W= 0.25, 0.3, 0.4m) , c.t.c=2m.

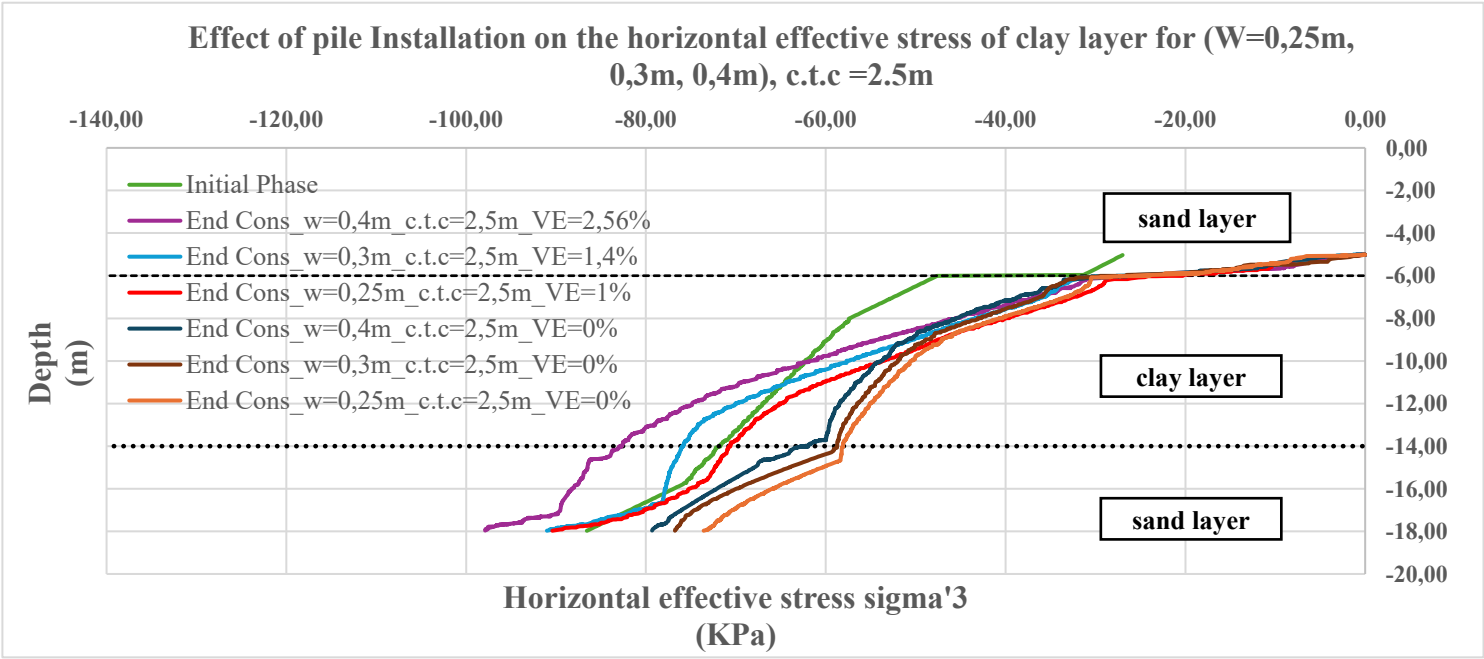

Figure 6.7:Comparison of the horizontal effective stress (With and without pile installation effect) for (W= 0.25, 0.3, 0.4m) , c.t.c=2.5m.

6.3.2 Influence of pile width and spacing on horizontal stress distribution due to pile installation effect

The results presented correspond to the final stage of excavation, capturing the influence of pile installation on horizontal effective stress within the soil mass for two pile spacing configurations: c.t.c = 2 m and c.t.c = 2.5 m. In both cases, horizontal effective stress (σ'_3) was evaluated for three different pile widths (0.25 m, 0.30 m, and 0.40 m), each represented by increasing values of volumetric expansion to simulate the ground disturbance caused by installation as shown in Figure 6.8. The findings reveal that horizontal effective stress increases notably in the presence of volumetric expansion, especially within the clay layer, which is the most sensitive to such stress changes due to its compressibility and low shear strength.

For the configuration with c.t.c = 2 m, the stress increase is significantly more pronounced than in the 2.5 m case. This is attributed not only to the closer spacing between individual piles but also to the greater number of piles included in the system (nine piles compared to seven in the wider-spaced setup). The increased number of piles results in a larger cumulative volumetric disturbance in the soil mass, leading to a more increase in horizontal effective stress.

The wider piles (particularly the 0.40 m width) amplify this effect further, as their installation displaces more soil laterally, intensifying confinement around the pile shafts and within the surrounding clay. The distribution of this stress extends vertically throughout the clay layer and even into the underlying sand stratum, reflecting the increase of the stress-state in sand.

The case with c.t.c = 2.5 m exhibits a similar but less intense pattern. The reduced number of piles in this configuration limits the total volumetric disturbance, resulting in a more moderate increase in horizontal effective stress.

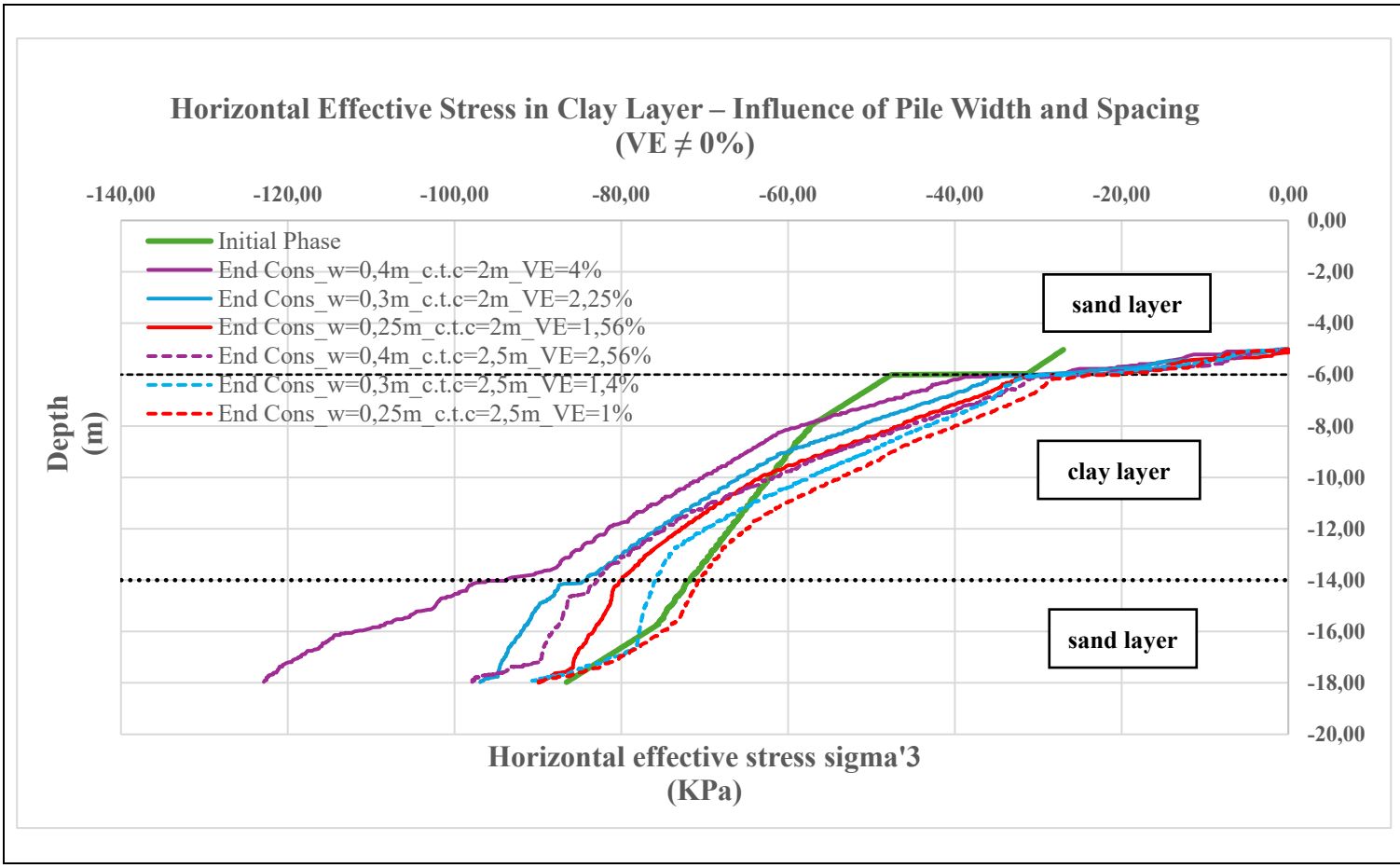

Figure 6.8: Comparison of Horizontal Effective Stress in the Clay Layer for Different Pile Widths and Spacings Under Volumetric Expansion (VE ≠ 0%)

6.3.3 Influence of pile installation effect on the swelling for different Pile widths and spacings

This section analyses the impact of pile installation on vertical ground swelling, evaluated at the end of excavation and final consolidation. The analysis considers three pile widths **(**W = 0.25 m, 0.30 m, 0.40 m, 0.45m**)** and two pile spacing configurations (c.t.c = 2.0 m and 2.5 m), comparing conditions with and without pile installation. Installation effects are simulated using volumetric expansion. The results, presented in Table 6.2 and Figure 6.10**,** highlight the complex interaction between soil confinement, horizontal stress build-up, and subsequent vertical deformation during unloading.

To understand the swelling behavior, it is essential to consider the preceding changes in horizontal effective stress (σ'_3), as illustrated in Figures 6.7 and 6.8. Pile installation, especially at closer spacing (c.t.c = 2 m), increases horizontal confinement within the clay layer due to radial soil displacement. This lateral confinement leads to a corresponding increase in vertical effective stress. Consequently, when the soil is unloaded during excavation, the difference between initial and final vertical effective stress becomes greater, resulting in increased swelling. This vertical movement is a combination of consolidation-induced settlement (due to dissipation of excess pore water pressure) and heave, driven by lateral displacement of the soil mass.

For c.t.c = 2.0 m**,** the swelling results align with the stress interpretation. The highest swelling increase (+ 68 %) is observed for W = 0.45 m, where the corresponding volumetric expansion is also largest (VE = 5,1%). This case exhibits the greatest rise in horizontal effective stress, which intensifies the vertical rebound during unloading. Similarly, for W = 0.4m, 0.3m and 0.25 m, the swelling increases by 50%, 7% and 3.22%**,** respectively, in accordance with their lower VE values (4%, 2.25% and 1.56%).

In contrast, the behavior for c.t.c = 2.5 m is more moderate. The increase in horizontal stress due to installation is less pronounced (as shown in Figure 6.8), and the corresponding swelling increments are smaller: 28% for W = 0.45 m, 14,7% for W = 0.40 m, 2.63% for W = 0.3m and 2,5% for W=0,25m. This reduction is attributed to the larger spacing between piles, which reduces the cumulative volumetric disturbance and lowers the level of confinement. As a result, the unloading-induced swelling becomes less sensitive to the installation effect.

Figure 6.9, further illustrates the relationship between swelling and volumetric expansion. While the swelling response for c.t.c = 2.0 m generally increases with VE, an interesting deviation is observed in this configuration without a floor slab: the measured swelling is lower for c.t.c = 2.0 m compared to c.t.c = 2.5 m across all pile widths. This contrasts with the trend seen in the full model (with floor), where closer pile spacing consistently leads to greater vertical deformation for larger pile widths.

In the model without a floor, the induced lateral stress from pile installation at closer spacing is not effectively confined at the top boundary, resulting in less vertical rebound.

Table 6.2:Swelling Results for Different Pile Widths and Spacings with and without Pile Installation Effect

Spacing (c.t.c) (m)	Pile width (m)	Swelling (with pile installation) (mm)	Swelling (without pile installation) (mm)	Change %
2.0 m	0.45m	37	22	+68%
2.0 m	0.40 m	33	22	+50%
2.0 m	0.30 m	30	28	+7 %
2.0 m	0.25 m	32	31	+3.22%
2.5m	0.45m	41	32	28%
2.5 m	0.40 m	39	34	+14,7%
2.5 m	0.30 m	39	38	2,63%
2.5 m	0.25 m	41	40	+2,5%

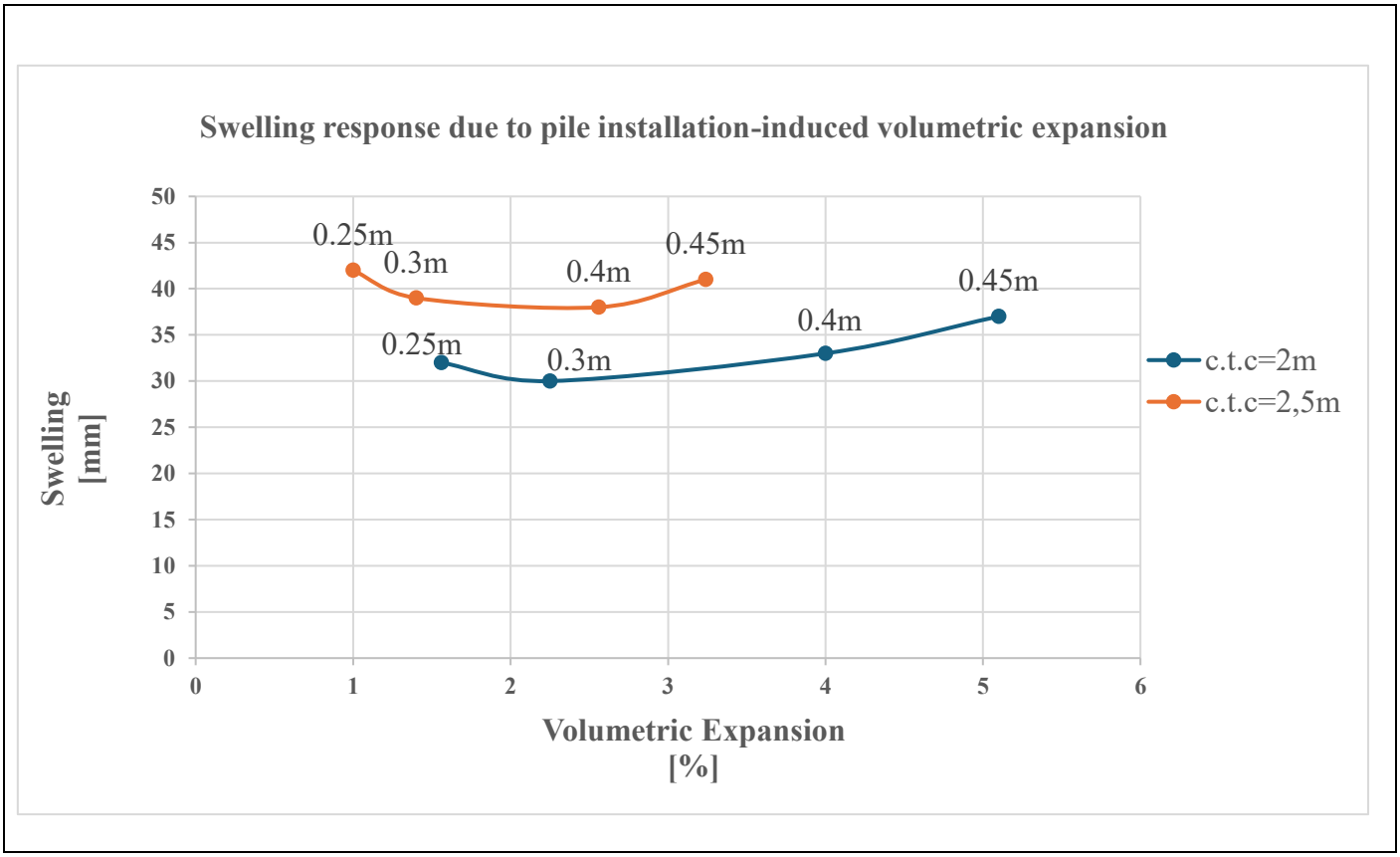

Figure 6.9: Swelling Response as a Function of Volumetric Expansion for Different Pile Spacings (c.t.c = 2.0 m and 2.5 m)

6.4 Case 4: 2D_Model,Without Piles (Sheet Pile – Strut – Floor)

6.4.1 Influence of Excavation Width on Swelling

This section investigates the effect of excavation width (W) on the swelling behavior of soft clay soil in a 2D excavation model supported by a sheet pile wall, a strut, and a floor slab (excluding piles). The excavation depth was kept constant at 5 m, and the clay layer thickness was fixed at 8 m. Four excavation widths were analysed: 15 m, 20 m, 25 m, and 30 m. The numerical modelling was performed for three different floor stiffness values:

- E1 = 25.7 × 10^6 kPa
- E2 = 2 E1 = 51.4 × 10^6 kPa
- E3 = 2 E2 = 102.8 × 10^6 kPa

Swelling and swelling pressure results obtained from numerical modelling were compared with the analytical method, which assumes a fixed swelling value of 106 mm and swelling pressure of 37.6 kPa, independent of excavation geometry or structural stiffness.

Swelling Behavior with Varying Excavation Widths

The results shown in Figure 6.10 indicate that vertical swelling increases with excavation width in all stiffness cases. For the least stiff floor (E1), the swelling increased from 55.7 mm at W = 15 m to 100.9 mm at W = 30 m. For the stiffest floor (E3), swelling ranged from 48.6 mm to 80.9 mm. This trend reflects the broader stress relief in wider excavations, allowing more of the clay layer to expand vertically.

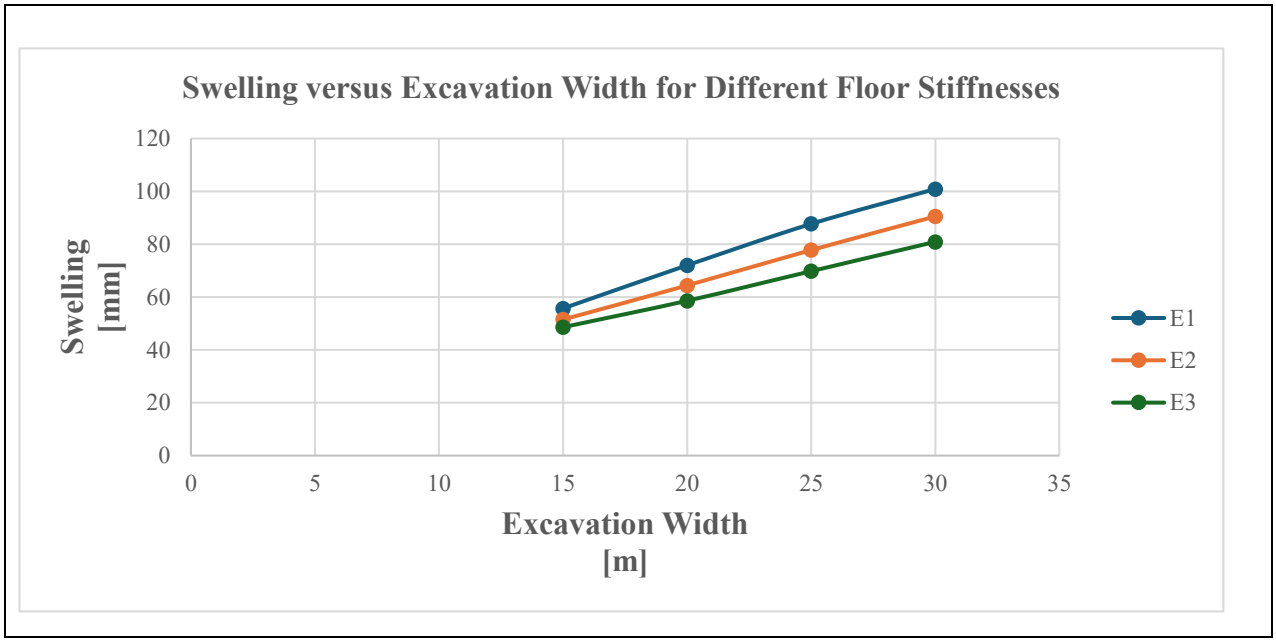

Figure 6.10: Swelling versus Excavation Width for Different Floor Stiffnesses (E1, E2, E3)

Swelling Pressure with Varying Excavation Widths

Swelling pressure, defined as the upward pressure exerted by the expanding soil on the floor slab, shows an inverse trend in Figure 6.11 . As excavation width increases, swelling pressure decreases across all stiffness cases. For example, in the E1 case, pressure decreases from 19.42 kPa at 15 m to 3.52 kPa at 30 m. Stiffer slabs show higher pressures because they mobilize more resistance, thus reflecting more stress transfer from the soil.

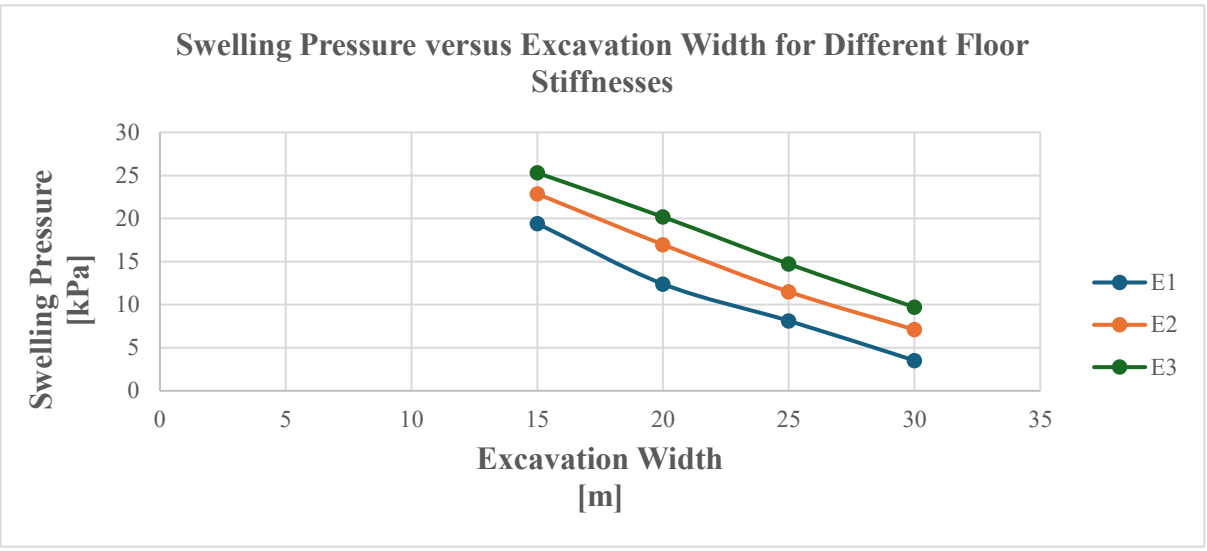

Figure 6.11:Swelling Pressure versus Excavation Width for Different Floor Stiffnesses (E1, E2, E3)

Comparison with Analytical Method

Table 6.3 presents a detailed comparison between the numerical modelling results and the analytical predictions for both swelling and swelling pressure across varying excavation widths and floor stiffness levels. The analytical method assumes constant values for swelling (106 mm) and swelling pressure (37.6 kPa). In contrast, the numerical results reveal a clear sensitivity to floor stiffness and excavation width.

As the excavation width increases, the discrepancy between the two methods becomes more pronounced. For example, at W = 30 m, the analytical model overestimates the swelling pressure by more than 90% in the E1 configuration. A similar trend is observed for swelling, particularly in cases with stiffer slabs (e.g., E3), where numerical values are significantly lower than the analytical assumption. These findings highlight the limitations of the analytical approach, which neglects the influence of stress redistribution, unloading geometry, and soil–structure interaction.

Table 6.3: Comparison Between Numerical and Analytical Results for Swelling and Swelling Pressure Across Different Excavation Widths and Floor Stiffnesses

Numerical Modelling				**Analytical Method**		**Comparison**	
W [m]	E [kPa]	S [mm]	Swelling pressure [kPa]	S [mm]	Swelling pressure [kPa]	% Diff (swelling)	% Diff (swelling pressure)
15	2,57E+07	55,7	19,42	106	37,6	47,5	48,4
20	2,57E+07	72,03	12,4	106	37,6	32	67,0
25	2,57E+07	87,7	8,12	106	37,6	17,3	78,4
30	2,57E+07	100,9	3,52	106	37,6	4,8	90,6
15	5,14E+07	51,5	22,86	106	37,6	51,4	39,2
20	5,14E+07	64,4	16,97	106	37,6	39,2	54,9
25	5,14E+07	77,8	11,5	106	37,6	26,6	69,4
30	5,14E+07	90,5	7,1	106	37,6	14,6	81,1
15	1,082E+08	48,6	25,3	106	37,6	54,2	32,7
20	1,082E+08	58,6	20,18	106	37,6	44,7	46,3
25	1,082E+08	69,8	14,72	106	37,6	34,2	60,9
30	1,082E+08	90,9	9,7	106	37,6	16,5	74,2

6.5 Case 5 : 2D Model- Full Structural System – Sheet Pile, Strut, Floor, and Embedded Piles

6.5.1 Influence of Sheet Pile and Embedded Pile Depth Ratio (L/D) on Swelling

This section presents the results of a parametric study focused on the interaction between the embedded depth of the sheet pile (L) and the embedded length of the vertical piles (D), expressed as the L/D ratio, and their effect on swelling. The analysis was conducted within the full structural support configuration (sheet pile, strut, floor slab, and embedded piles), with a constant pile spacing of 2 m (centre-to-centre) and a pile width of 0.25 m. The excavation depth was fixed at H = 5 m, and the study was repeated for three different clay layer thicknesses (T = 6 m, 7 m, and 8 m) to account for soil variability.

For each clay thickness, three embedded depths of the sheet pile were investigated: L = 3 m, 4 m, and 5 m. Corresponding to each L value, the depth of the embedded piles (D) was varied from 2 m to 5 m,

The swelling results, plotted in Figure 6.12 , reveal several consistent trends across all clay thicknesses:

- Swelling increases as the L/D ratio increases, regardless of clay thickness. This indicates that for a fixed sheet pile depth, shallower piles lead to more swelling. Conversely, when the pile depth increases relative to the sheet pile embedment, the system becomes more effective in confining the soil, thereby reducing upward deformation.
- Across all cases, higher clay layer thicknesses (T = 8 m) are associated with greater swelling magnitudes, which is consistent with the increased potential for volumetric rebound in thicker clay deposits under unloading.

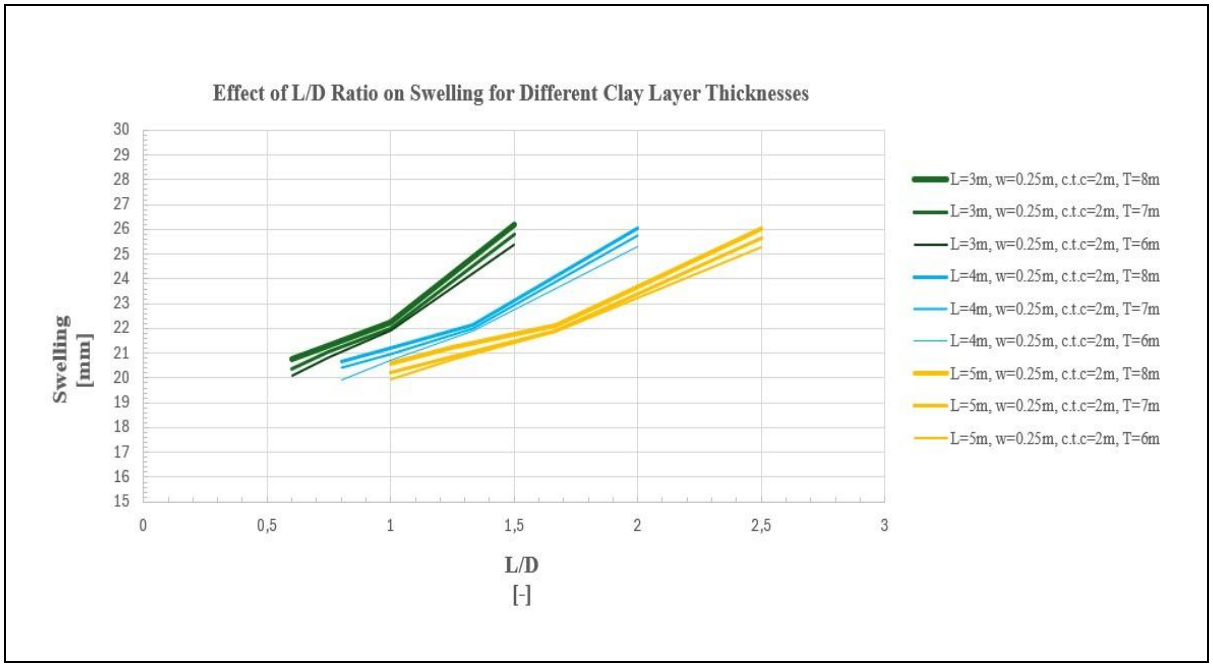

Figure 6.12: Effect of L/D Ratio on Swelling for Different Clay Layer Thicknesses (T = 6 m, 7 m, 8 m), with Pile Spacing c.t.c = 2 m and Pile Width w = 0.25 m.

6.5.2 Influence of Pile Width and Spacing on Horizontal Effective Stress due to Pile Installation Effect (with Floor Slab)

This section presents the results of the final excavation stage for Case 5, in which all structural elements—sheet pile wall, strut, floor slab, and embedded piles—are included. The focus is on evaluating the influence of pile installation-induced ground disturbance on the distribution of horizontal effective stress (σ'_3) in the presence of the floor slab. Two centre-to-centre pile spacings **(**c.t.c = 2 m and c.t.c = 2.5 m**)** were considered, in combination with four pile widths (W = 0.25 m, 0.30 m, 0.40 m, and 0.45 m**).** The installation effect was simulated using volumetric expansion (VE) to represent the radial soil displacement caused during pile insertion.

For the configuration with c.t.c = 2.0 m, the applied volumetric expansions were:

- 1.56% for W = 0.25 m
- 2.25% for W = 0.30 m
- 4% for W = 0.40 m
- 5,1% for W=0,45m

For the wider pile spacing of c.t.c = 2.5 m, the VE values were slightly lower:

- 1.0% for W = 0.25 m
- 1.4% for W = 0.30 m
- 2.56% for W = 0.40 m
- 3.24% for W=0,45 m

Reference cases with VE = 0% were also simulated to represent pile insertion without soil disturbance, enabling a direct comparison of the effects induced by installation.

As illustrated in Figure 6.13, a clear increase in horizontal effective stress is observed with increasing VE, particularly within the clay layer. The effect is most pronounced for the widest pile (W = 0.45 m) with the highest VE of 5.1%, where the curve shows significant lateral stress enhancement compared to the reference case. The trend is consistent: larger pile diameters produce greater radial soil displacement, intensifying horizontal confinement and enhancing σ'_3.

Additionally, the closer spacing (2 m) results in overlapping stress zones between adjacent piles, amplifying the cumulative effect of confinement. The presence of the floor slab further reinforces the lateral stress build-up, leading to a more confined stress field compared to earlier configurations without the slab.

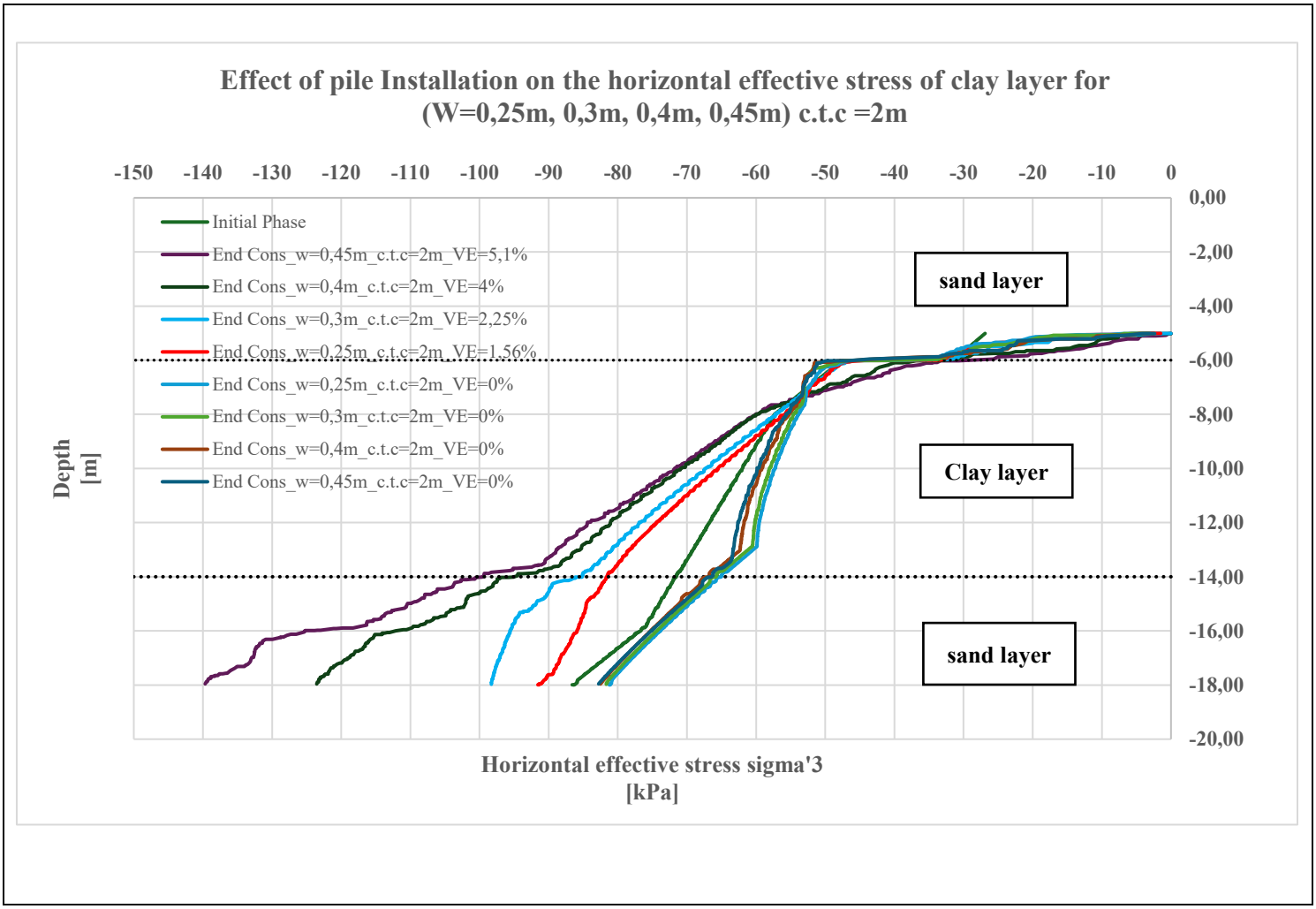

Figure 6.13: Effect of Pile Installation on the Horizontal Effective Stress of the Clay Layer for W = 0.25–0.45 m, c.t.c = 2 m, with Floor Slab

In the wider spacing configuration (c.t.c = 2.5 m), the horizontal effective stress also increases with volumetric expansion, but the overall magnitude of the increase is reduced relative to the 2 m case. This is shown in Figure 6.14 , where the influence of pile installation is still evident—especially for W = 0.45 m with VE = 3.24%—but the curves display less lateral stress build-up than those in the closer spacing.

This difference is attributed to the reduced number of piles across the same excavation width, which limits the interaction between overlapping stress zones. Consequently, while the stress enhancement remains visible—particularly within the clay—the overall confinement is less intense than in the denser configuration. Still, the floor slab contributes to maintaining a confined state, preventing stress loss at the excavation boundary.

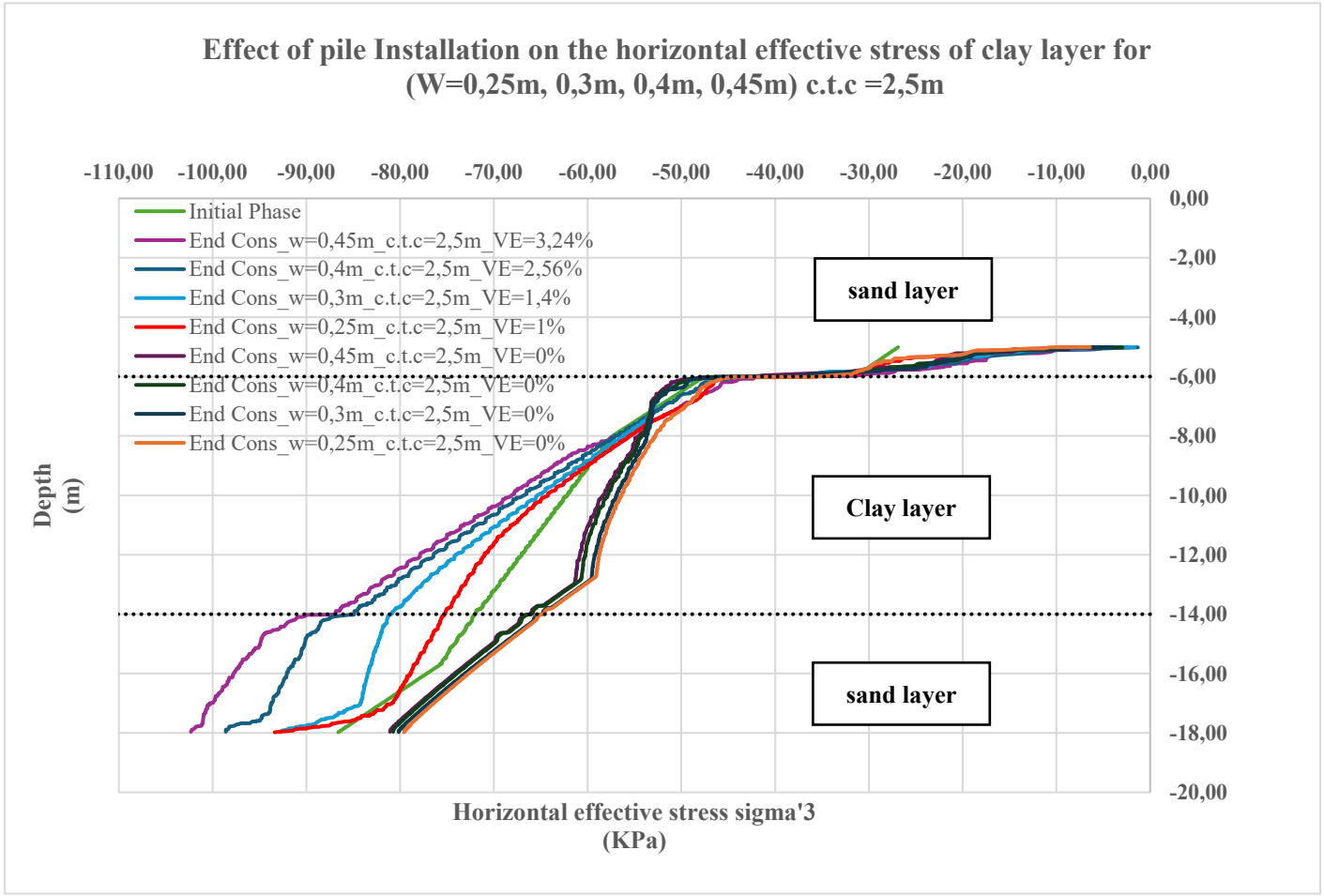

Figure 6.14: Effect of Pile Installation on the Horizontal Effective Stress of the Clay Layer for W = 0.25–0.45 m, c.t.c = 2.5 m, with Floor Slab

To further highlight the influence of pile spacing on stress development, Figure 6.15, shows only the cases where pile installation effects were simulated (i.e., VE ≠ 0%) for both c.t.c = 2 m and c.t.c = 2.5 m, across all pile widths.

The results clearly illustrate that for a given pile width, the configuration with closer spacing (2 m) consistently produces higher horizontal effective stresses (σ'_3) than the wider spacing (2.5 m). This is particularly evident for W = 0.45 m, where the stress curve for c.t.c = 2 m, VE = 5.1% lies significantly to the left of its counterpart for c.t.c = 2.5 m, VE = 3.24%, reflecting a stronger lateral confinement effect in the denser pile arrangement. This behavior is consistent across the other pile widths as well, highlighting how pile density intensifies stress interaction, especially within the confined clay layer.

Interestingly, the figure also reveals that certain combinations of pile width and spacing result in comparable stress profiles, suggesting a compensatory relationship between these two parameters. For instance, the horizontal effective stress generated by W = 0.45 m, c.t.c = 2.5

m, VE = 3.24% is closely aligned with the response of W = 0.30 m, c.t.c = 2.0 m, VE = 2.25%, despite the differences in width and spacing. Similarly, the stress curve for W = 0.25 m, c.t.c = 2.0 m, VE = 1.56% is nearly equivalent to that of W = 0.30 m, c.t.c = 2.5 m, VE = 1.4%. These parallels indicate that reducing pile spacing can compensate for smaller diameters, and vice versa, in achieving similar horizontal stress levels.

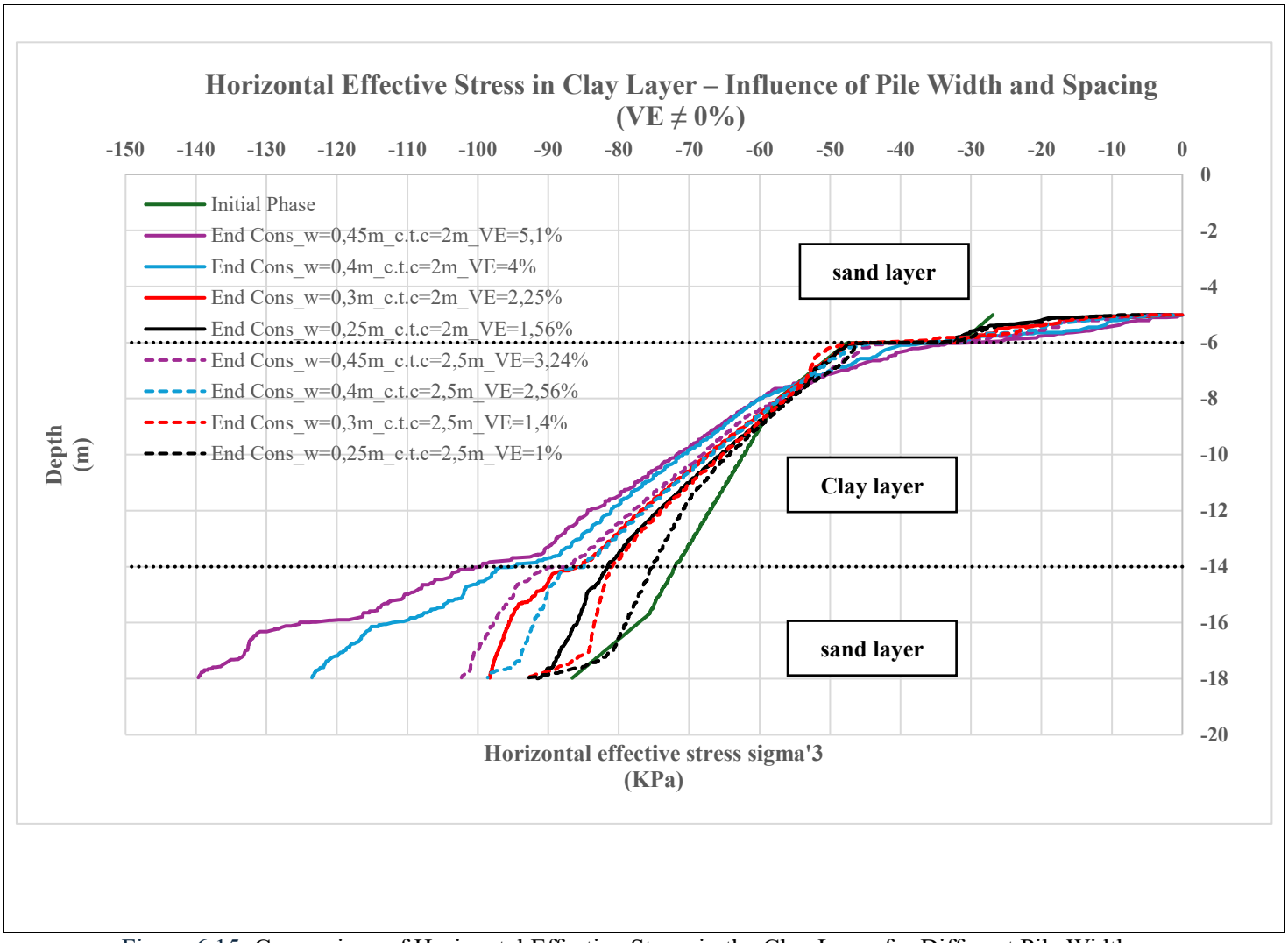

Figure 6.15: Comparison of Horizontal Effective Stress in the Clay Layer for Different Pile Widths and Spacings Under Volumetric Expansion (VE ≠ 0%)

6.5.3 Influence of Volumetric Expansion and Pile Spacing on Swelling and Excess Pore Water Pressure

This section interprets the vertical swelling observed beneath the floor slab in relation to the horizontal tensioning effect induced by pile installation, and the concurrent dissipation of negative excess pore water pressure resulting from consolidation. Both mechanisms interact and contribute to the total measured swelling response. The extent to which each dominates depends on the pile width, pile spacing, and the evolving pore pressure conditions.

The installation of piles generates a horizontal tensioning effect in the clay layer between adjacent piles. This increase in horizontal effective stress (σ'_h) leads to a corresponding rise in vertical effective stress (σ'_v) due to stress redistribution under undrained conditions. Upon excavation, this increase in σ'_v results in a larger effective stress drop at the excavation base, particularly in more confined configurations. As a result, the swelling becomes more pronounced due to both: (i) the dissipation of negative excess pore water pressure developed during consolidation, and (ii) the vertical soil displacement imposed by the installation-induced stress field.

This behavior is clearly reflected in the swelling results for the complete model (Figure 6.18). For pile widths W = 0.40 m and W = 0.45 m, the swelling is consistently greater in the c.t.c = 2 m configuration compared to the corresponding cases at c.t.c = 2.5 m. The closer pile spacing intensifies the tensioning effect and increases confinement, which in turn amplifies the upward displacement of soil following excavation.

Moreover, an analysis of the water pressure evolution (Figure 6.16 and Figure 6.17) provides further insight. For W = 0.45 m, the under_pressure typically associated with unloading is significantly reduced—nearly neutralized—by the upwardpressure during pile installation. In such cases, swelling cannot be attributed to pore pressure dissipation alone. Instead, it results predominantly from the mechanical uplift caused by intense horizontal tensioning in the confined soil mass. The same interpretation likely holds for W = 0.40 m.

In contrast, for W = 0.25 m, the swelling mechanism exhibits a more classical response. The pore pressure data reveal that while the larges part of the under_pressure is offset by the pile installation effect, a substantial portion of negative excess pore water pressure remains and dissipates gradually. This dissipation drives vertical rebound in the clay layer. Additionally, the tensioning effect—though weaker than for larger piles—still contributes to the observed swelling. Therefore, the mechanism here is a combination of pore pressure dissipation and moderate mechanical tensioning.

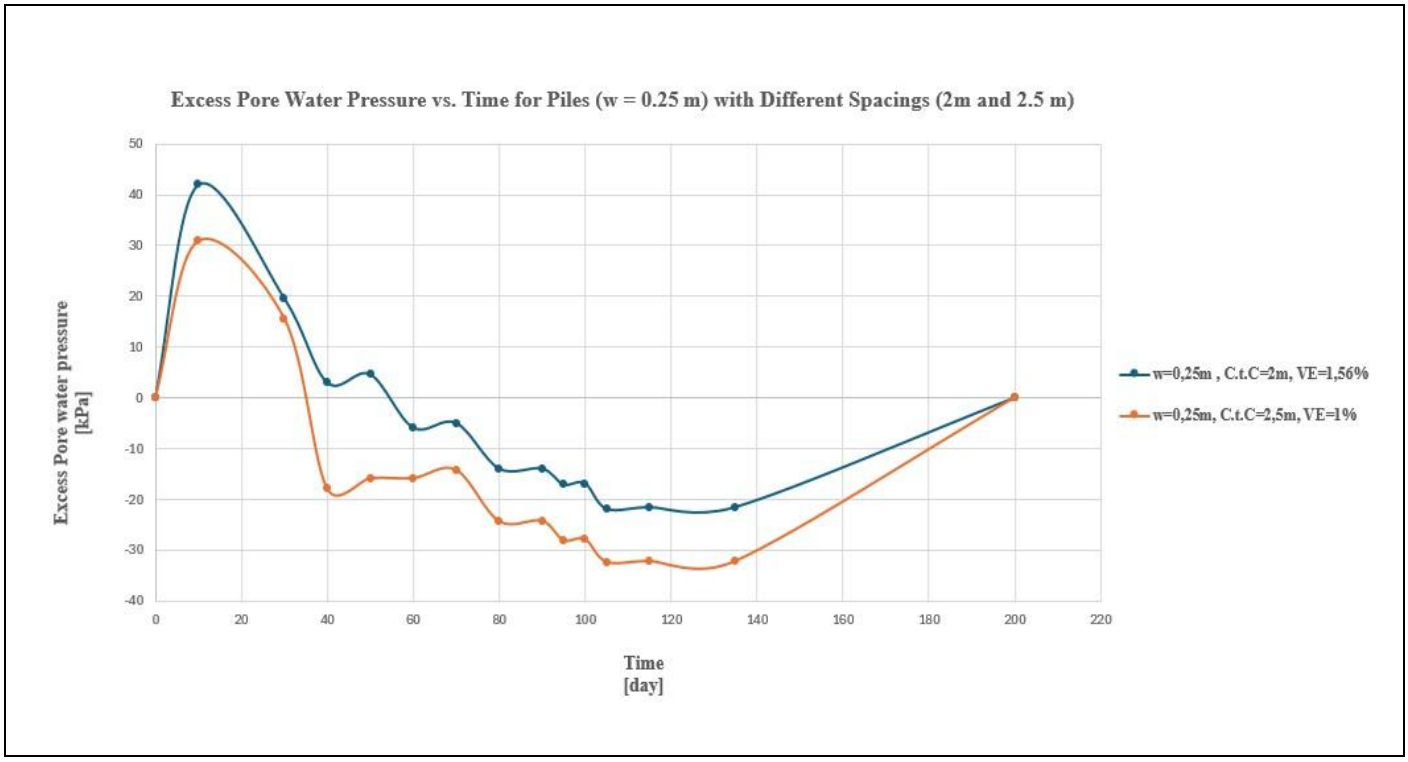

Figure 6.16: Water Pressure vs. Time for Piles (w = 0.25 m) at Different Pile Spacings (c.t.c = 2 m and 2.5 m)

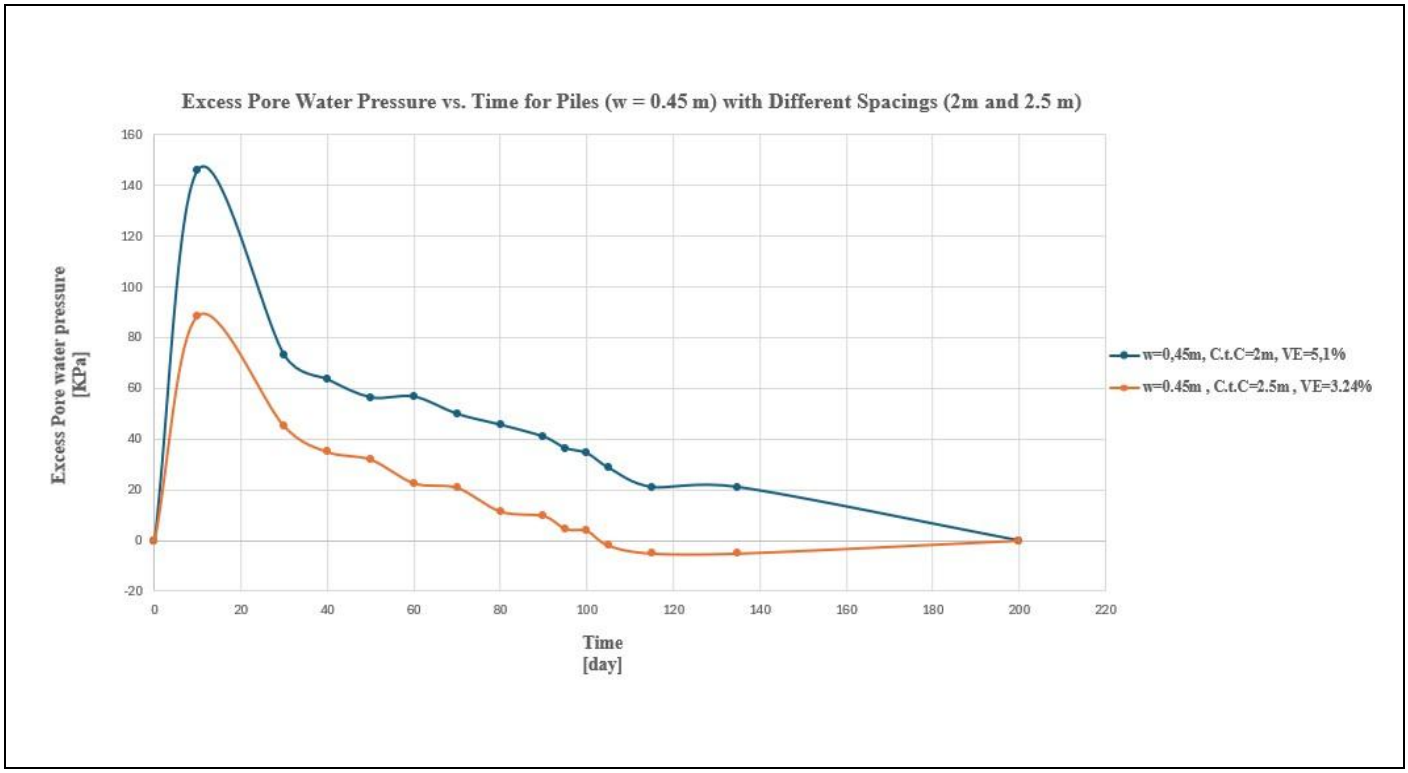

Figure 6.17: Water Pressure vs. Time for Piles (w = 0.45 m) at Different Pile Spacings (c.t.c = 2 m and 2.5 m)

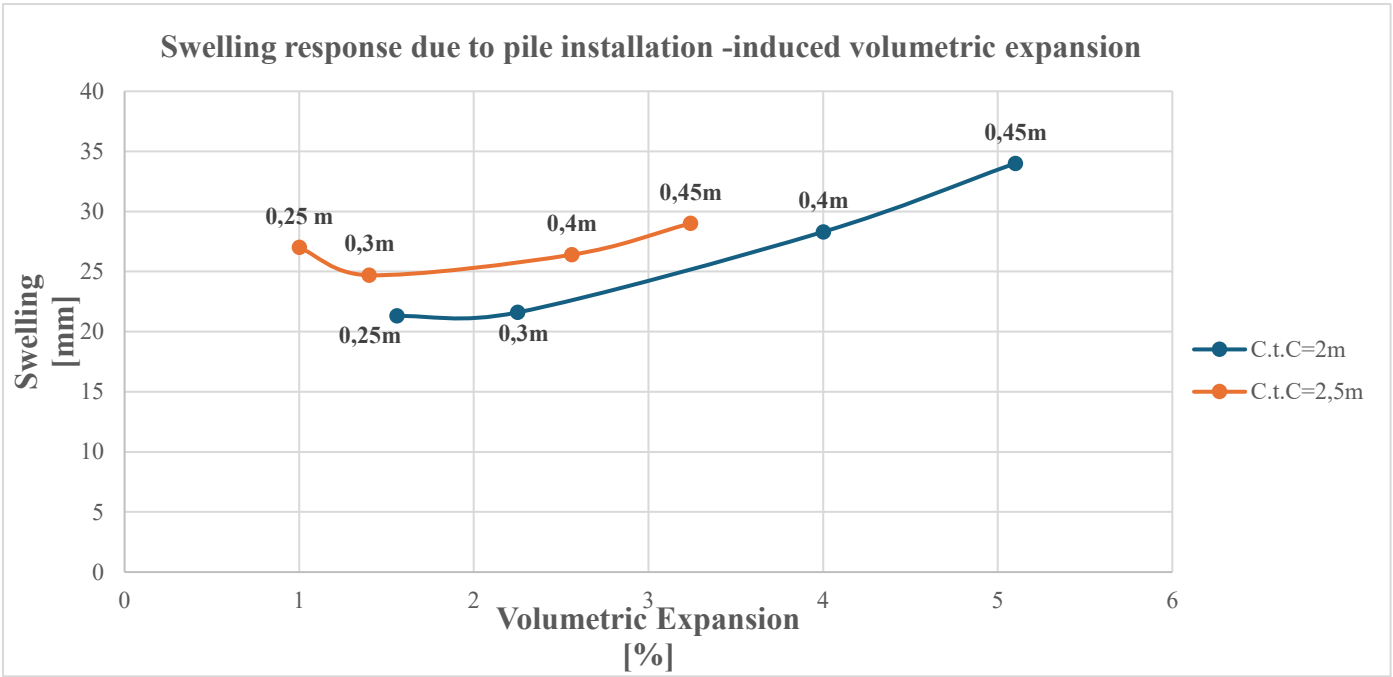

Figure 6.18: Swelling vs. Volumetric Expansion Due to Pile Installation for Piles with Varying Widths and Spacings (C.t.C = 2 m and 2.5 m)

6.5.4 Evaluation of Swelling and swelling Pressure on Floor Slab: Numerical Modelling vs. Analytical Predictions

This chapter evaluates the swelling pressure acting on the floor slab under various structural scenarios, focusing on the role of embedded piles and installation-induced volumetric expansion. The study covers two pile spacings: c.t.c = 2 m and c.t.c = 2.5 m. Each configuration is analysed to assess the reduction in swelling pressure and the accuracy of analytical predictions compared to numerical modelling.

The five scenarios in this case used to get the results:

1. involves a very stiff floor and a very stiff anchor, used solely to determine the maximum possible swelling pressure under fully restrained conditions.
2. introduces a realistic floor and anchor system without piles and without volumetric expansion. The stiffness of the anchor is calibrated for each pile width so that the elastic vertical deformation of the floor equals the elastic deformation of the corresponding pile. This setup allows the extraction of the swelling pressure under equivalent deformation conditions.
3. represents the full 2D model with realistic piles and floor, without volumetric expansion. This is the realistic scenario where the effect of pile presence on reducing swelling pressure is captured. A direct comparison between Case 3 and Case 2 enables quantification of the reduction due to piles.
4. replicates the structure of Case 2 but incorporates volumetric expansion. Again, no piles are included, and the anchor stiffness is calibrated for each width to reproduce the same elastic deformation as the pile. This configuration isolates the swelling pressure contribution from volumetric expansion without pile influence.
5. includes all structural elements—realistic piles and floor—and incorporates volumetric expansion. This is the realistic case where both pile presence and installation effects are considered. The comparison between Case 5 and Case 4 helps to quantify the swelling pressure reduction due to piles under realistic installation-induced conditions.

The results show that for both pile spacings, the incorporation of piles leads to a clear reduction in swelling pressure. The effect is more pronounced for the smaller spacing (c.t.c = 2 m), particularly for larger pile widths.

Table 6.4 presents the swelling pressure values for the c.t.c = 2 m case across all five scenarios. It is observed that for Case 4 and Case 5, which include volumetric expansion, the pile installation effect results in a more substantial reduction in swelling pressure on the floor compared to Case 2 and Case 3 (without volumetric expansion). For instance, at w = 0.45 m, the piles absorb the entire swelling load, resulting in zero pressure on the floor slab.

Table 6.5 presents the results for the c.t.c = 2.5 m configuration. A similar trend is evident: the presence of volumetric expansion (Case 4 vs. Case 5) enhances the pile's effectiveness in reducing swelling pressure. However, for this wider spacing, the piles are less effective compared to the c.t.c = 2 m case. Even at w = 0.45 m, some pressure remains on the floor, indicating that the reduced confinement between piles limits the stress relief capacity.

Table 6.6 illustrates that for a pile spacing of c.t.c = 2 m, the analytical method substantially overestimates the swelling values, with differences ranging between approximately 55% and 70% when compared to the numerical results. Table 6.7 further shows that the swelling pressure on the floor is markedly overpredicted, with the deviation reaching up to 100% for a pile width of 0.45 m. For the wider spacing of c.t.c = 2.5 m, Table 6.8 reveals a similar trend, with the analytical method overestimating the swelling magnitude by approximately 60% to 65%. Finally, Table 6.9 demonstrates that the swelling pressure is also overestimated in this configuration, although the discrepancy is lower than in the c.t.c = 2 m case—amounting to roughly half the difference observed for w = 0.45 m.

Table 6.4: Numerical Evaluation of Swelling Pressure on the Floor for c.t.c = 2.0 m: Effect of Pile Installation and Volumetric Expansion

Width [m]	Swelling pressure (1) [kPa]	Swelling pressure (2) [kPa]	Swelling pressure (3) [kPa]	Reduction due to piles [%]	Swelling pressure (4) [kPa]	Swelling pressure (5) [kPa]	Reduction due to piles [%]
0.25	32	24.8	14.6	41	25.1	13.6	45.8
0.3	32	25.4	12.95	49	25.6	8.03	68.6
0.4	32	26.9	13.22	50.8	25.5	2.9	88.6
0.45	32	27.2	13.35	50.9	24.8	0	100

Table 6.5: Numerical Evaluation of Swelling Pressure on the Floor for c.t.c = 2.5 m: Effect of Pile Installation and Volumetric Expansion

Width [m]	Swelling pressure (case 1) [kPa]	Swelling pressure (case 2) [kPa]	Swelling pressure (case 3) [kPa]	Reduction due to piles [%]	Swelling pressure (case 4) [kPa]	Swelling pressure (case 5) [kPa]	Reduction due to piles [%]
0.25	32	23,9	17.9	25.1	23.9	17.4	27.2
0.3	32	24,5	16.4	33.1	24.5	15.4	37.1
0.4	32	25,4	16.6	34.6	25.4	11.6	54.3
0.45	32	25,9	17.2	33.6	25.5	9.1	64.3

Table 6.6:Comparison of Swelling– Analytical vs. Numerical (c.t.c = 2 m)

Swelling [mm]			
Width [m]	Analytical Method	Numerical Modelling	% Diff (swelling)
0.25	106	32	69.8
0.3	106	30	71.7
0.4	106	33	68.9
0.45	106	37	56.1

Table 6.7: Comparison of Swelling Pressure – Analytical vs. Numerical (c.t.c = 2 m)

Swelling pressure [kPa]			
Width [m]	Analytical Method	Numerical Modelling	% Diff (swelling pressure)
0.25	20.4	13.6	33.3
0.3	20.4	8.03	60.6
0.4	20.4	2.9	85.8
0.45	20.4	0	100

Table 6.8: Comparison of Swelling– Analytical vs. Numerical (c.t.c = 2.5 m)

Swelling [mm]			
Width [m]	Analytical Method	Numerical Modelling	% Diff (swelling)
0.25	106	42	60.4
0.3	106	39	63.2
0.4	106	38	64.2
0.45	106	41	61.3

Table 6.9: Comparison of Swelling Pressure – Analytical vs. Numerical (c.t.c = 2.5 m)

Swelling pressure [kPa]			
Width [m]	Analytical Method	Numerical Modelling	% Diff (swelling pressure)
0.25	20.4	17.4	14.7
0.3	20.4	15.4	24.5
0.4	20.4	11.6	43.13
0.45	20.4	9.1	55.4

7 Discussion

This chapter offers a reflection on the findings of this study by comparing them with existing research, identifying limitations in the adopted methodologies, and highlighting areas for further investigation. The focus is placed on the analytical assumptions, numerical simplifications, and model sensitivities that may influence the observed results.

The phenomenon of excavation-induced heave in soft clays has long been acknowledged in geotechnical engineering, with seminal works by Terzaghi (1943) and Nelson & Miller (1992) emphasizing the role of stress relief and time-dependent consolidation. The swelling behaviours observed in this study, particularly the heave magnitudes and development of under_pressure conditions in the clay, are broadly in line with these theoretical foundations. However, this study contributes further depth by explicitly incorporating the effects of pile installation, modeled using volumetric expansion—a method previously explored by Basu et al. (2014) and Wathugala & Desai (1991). The inclusion of such mechanisms is essential for capturing realistic stress path changes during pile penetration.

The analytical method, based on the Koppejan approach, served as a preliminary tool for estimating vertical swelling. Nonetheless, its one-dimensional formulation, assuming uniform vertical unloading, neglects horizontal stress redistribution, boundary constraints, and soil-structure interaction. The sensitivity of this approach is evidenced by a change in the shape factor from 1.0 to 2.0, which increased the predicted swelling from 106 mm to 118 mm. This illustrates the limitations of relying on fixed empirical parameters that fail to reflect complex excavation geometries or loading scenarios. Moreover, the method does not account for the mitigating effects of structural inclusions such as floor slabs or embedded piles, which are crucial for redistributing stress and influencing pore pressure responses.

While the numerical analysis yielded more realistic results and accommodated complex geometries and staged construction, it involved several simplifications. The use of plane strain conditions excludes out-of-plane deformations and load paths—an acceptable approximation for symmetrical, elongated excavations, but potentially inaccurate for irregular layouts. Furthermore, although volumetric expansion effectively simulated stress changes from pile installation, it does not replicate the actual displacement history during pile driving or jacking. The Hardening Soil model employed in PLAXIS relies heavily on accurate calibration; in this study, some parameters were assumed based on empirical correlations due to the lack of site-specific laboratory tests, which introduces additional uncertainty.

Several important factors remain unaddressed or simplified. Time-dependent swelling due to consolidation was not modeled, although it can significantly affect long-term deformation and swelling pressure. The influence of thixotropy or strength regain in soft clays following remoulding, which could impact pile behavior and long-term heave, was also not considered.

Although the use of 2D modeling was suitable for the scope of this study, it inherently fails to capture three-dimensional stress redistribution and interactions. Moving towards 3D simulations would allow for better representation of excavation geometries, boundary effects, and pile group interactions.

Ultimately, the comparison between analytical and numerical methods revealed significant differences in the estimation of swelling and swelling pressures, especially as the complexity of the modeled support systems increased. In configurations involving embedded piles, the

analytical method overestimated vertical heave by up to 70% and floor slab pressure by nearly 100% in some cases. These discrepancies highlight the limitations of relying solely on simplified methods, which can lead to overly conservative designs and increased construction costs. Conversely, failing to account for stress redistribution or installation effects may lead to unsafe underestimation of deformation.

This research emphasizes the importance of integrating both analytical and numerical approaches. While analytical models remain valuable for early-stage assessments and parametric studies, detailed design in soft clays with complex support systems requires advanced numerical simulations. Future work should aim to incorporate time-dependent behavior, thixotropy, and three-dimensional modeling to enhance the predictive accuracy and practical applicability of excavation-induced swelling analyses.

8 Conclusions and recommendations

This thesis investigated the mechanisms and magnitudes of excavation-induced swelling in soft clay conditions, emphasizing the role of structural elements such as piles and floor slabs, as well as the influence of pile installation effects. A combination of analytical and numerical methods was employed to gain a comprehensive understanding of swelling behavior under varying design configurations and soil-structure interactions.

The analytical method employed was based on a simplified hypothesis model, serving as a reference for comparison with numerical simulations. It predicted a swelling of 106 mm and a swelling pressure of 37.6 kPa for the reference case without piles. Upon including piles, the swelling pressure reduced to 20.4 kPa, highlighting the mitigating effect of pile installation.

In the 2D numerical model without structural elements, the predicted swelling was 99 mm, showing only a 7% deviation from the analytical result. This close agreement served as a validation of the analytical method for the simplified reference case, supporting its use as a baseline for comparison in more complex configurations. A parametric study on excavation width revealed an inverse trend—swelling slightly decreased with increased width (98 mm to 102 mm), except for the narrowest case (155 mm). This behavior was linked to greater horizontal inward soil displacement in narrow excavations, emphasizing the need to consider horizontal deformation when using analytical models.

In the sheet pile and strut system (without slabs or piles), greater excavation depths (H) increased swelling, while deeper sheet pile embedment lengths (L) reduced it. Increased clay thickness also led to more swelling due to higher unloading volumes. A W/H ratio analysis revealed that wider excavations led to reduced swelling, contrary to typical expectations, due to increased horizontal displacement near the sheet pile wall.

In the system with sheet pile, strut, and piles (with/without volumetric expansion), increasing pile width at 2.0 m spacing significantly raised swelling (up to 68%) compare to the situation without pile installation effect and horizontal stress, especially for w = 0.45 m. For 2.5 m spacing, swelling increases were moderate (28%). Without the floor slab, the lower confinement allowed more lateral stress dissipation, reducing vertical swelling at closer pile spacing.

In the full system case including sheet pile, strut, and floor slab a detailed comparison was conducted between analytical and numerical results for an excavation width of 30 m. Three different floor stiffness values were considered: E1 (baseline stiffness), E2 = 2E1, and E3 = 2E2, to investigate the influence of slab rigidity. The results demonstrated that increased excavation width led to greater swelling, consistent with stress relief mechanisms. While stiffer floor slabs resulted in higher swelling pressure, they also exhibited reduced vertical swelling due to increased resistance against deformation. The analytical method consistently overestimated both swelling and pressure, with the discrepancy becoming more pronounced for stiffer slabs:

- E1: Swelling overestimated by 4.8%, pressure by 90.6%
- E2: Swelling overestimated by 14.6%, pressure by 81.0%
- E3: Swelling overestimated by 16.5%, pressure by 74.2%

In the complete structural configuration, which includes sheet pile walls, struts, a floor slab, and embedded piles, the inclusion of piles demonstrably reduced the swelling pressure acting on the floor slab. For both pile spacings investigated, the presence of piles contributed to a clear mitigation of upward pressure. At a closer pile spacing of c.t.c = 2.0 m, the application of volumetric expansion to simulate pile installation led to a more pronounced reduction in floor pressure compared to the case without volumetric expansion. For example, at a pile diameter of w = 0.45 m, the piles fully absorbed the induced heave, resulting in zero swelling pressure transmitted to the slab.

In contrast, for a wider pile spacing of c.t.c = 2.5 m, although a similar trend was observed, the reduction in swelling pressure was less effective. For the same pile diameter (w = 0.45 m), a residual pressure remained acting on the floor, indicating incomplete load absorption by the piles.

The analytical method was found to significantly overestimate both swelling and swelling pressure, particularly for the smaller pile spacing. For c.t.c = 2.0 m, the overestimation of vertical swelling ranged from approximately 70% at w = 0.25 m to 55% at w = 0.45 m. The associated swelling pressure was considerably overpredicted, reaching up to 100% for the largest pile diameter.

For c.t.c = 2.5 m, the analytical overestimation of swelling remained notable, ranging between 60% and 64% across all pile widths. However, the overprediction of swelling pressure was comparatively lower, with values ranging from 14.7% at w = 0.25 m to 55.4% at w = 0.45 m. These results highlight the improved performance of closer pile spacing in controlling swelling-induced loads and the limitations of the analytical method in accurately capturing the interaction between pile spacing, pile diameter, and volumetric expansion effects.

Recommendations:

Based on the outcomes of this study, the following recommendations are proposed to guide both future research and practical applications in the design of deep excavations in soft clays:

- Preference for Numerical Modeling: Numerical methods, particularly finite element modeling, should be prioritized when assessing excavation-induced swelling, especially in cases involving pile installation effects. While analytical approaches like the Koppejan method offer useful preliminary insights, they lack the capacity to account for complex soil-structure interactions, boundary effects, and stress redistribution.
- Pile Installation Modeling: Volumetric expansion should be explicitly incorporated into numerical models to represent the stress alterations induced by pile installation. This method effectively captures the change in effective stress and associated swelling. Failure to account for these effects may result in significant underestimation of structural demands. Further research could explore whether alternative approaches, such as the Material Point Method (MPM) or advanced 3D modeling techniques, provide improved accuracy over current FEM-based tools.
- The arrangement of pile groups, especially in terms of spacing and diameter, is essential for effective control of excavation-induced swelling. Reducing the distance between piles and increasing their diameter improves soil confinement, thereby minimizing vertical heave and alleviating stress on structural components. It is important for designers to assess these factors in an integrated manner, as their combined influence governs the overall effectiveness of the system.
- Consideration of Floor Stiffness and Soil-Structure Interaction: Structural elements such as floor slabs significantly influence the redistribution of swelling pressure. Stiffer slabs tend to attract higher swelling pressure but also reduce vertical displacement. Therefore, accurate representation of structural stiffness in numerical models is essential for realistic predictions of stress concentrations.
- Future studies should move beyond two-dimensional assumptions and incorporate three-dimensional effects, particularly for non-uniform excavation geometries and pile arrangements. In addition, long-term consolidation behavior and staged construction sequences should be examined to reflect realistic site conditions and to improve prediction of time-dependent swelling phenomena.

Reference

Atkinson, J. H., & Bransby, P. L. (1978). The Mechanics of Soils: An Introduction to Critical State Soil Mechanics. McGraw-Hill.

Basu P, Prezzi M., & Salgado R. (2014). Shaft Resistance and setup factors for piles jacked in clay. J. Geotech. Geoenviron. Eng., 140 (3).

Bishop, R. E. D., & Blight, G. E. (2016). The Theory of Soil Mechanics. McGraw-Hill.

Brinkgreve, R. B. (2005). Selection of soil models and parameters for geotechnical engineering application. In Soil constitutive models.

Brinkgreve, R. B. (2022). Testing & Modelling of Soil Behaviour (CIEM2000) Possibilities and limitations of models.

Brinkgreve, R. B., et al. (2016). PLAXIS 2D Reference Manual. Delft University of Technology.

Brinkgreve, R. B. J., & Broere, W. (2008). Plaxis 2D. 2008. Version 9.

Brinkgreve, R. B. J., & person. (2010). Plaxis manuals, 2D-version 10. Delft University of Technology, The Netherlands.

Brinkgreve, R. B., Swolfs, W., & Kumarswamy, S. (2017). Material models manual [Computer software manual].

Clough, G. W., & O'Rourke, T. D. (1990). Construction-induced movements of in-situ walls." Design and Performance of Earth Retaining Structures,ASCE. 439–470.

Desai, C. S., & Zaman, M. M. (1984). Advanced constitutive modelilng and finite element analysis of geotechnical problems. International Journal for Numerical and Analytical Methods in Geomechanics, 8(3), 225–248.

Finno, R. J., Bryson, L. S., & Hashash, Y. M. A. (2002). Response of deep excavations supported by diaphragm walls in soft clay. Journal of Geotechnical and Geoenvironmental Engineering, 128(9), 749–761.

Fox, E. N. (1948). The Mean Elastic Settlement of Pile Groups." Géotechnique. 1(1), 2–17.

Gens, A., Potts, D. M., & Santos, C. (2018). Risk and Uncertainty in Geotechnical Modelling. Geotechnical Engineering Journal, 52(3), 268–278.

Gibson, R. E., & Ladd, C. C. (1998). Design and analysis of excavations and retaining structures in soft clays. Proc. Geotech. Conf., ASCE.

Holtz, R. D., Kovacs, W. D., & Sheahan, T. C. (2011). An Introduction to Geotechnical Engineering (2nd ed.).

Karol, R. H. (2003). Chemical Grouting And Soil Stabilization, Revised And Expanded. CRC Press.

Knappett, J., & Craig, R. F. (2012). Craig's soil mechanics (8th . ed.). Abingdon, Oxon: Spon Press.

Kok, S. T., Huat, B. B. K., Noorzaei, J., Jaafar, M. S., & Gue, S. S. (2009). A case study of passive piles failure in open excavation. DFI Journal - The Journal of the Deep Foundations Institute, 3(2), 49–56.

Leroueil, S., & Hight, D. W. (2003). Behaviour and properties of natural soils." In Tan et al. (Eds.), Characterisation and Engineering Properties of Natural Soils. Balkema.

Long, M. (2001). Database for retaining wall and ground movement due to deep excavations. Journal of Geotechnical and Geoenvironmental Engineering, 127(3), 203–224.

Long, M., & Menkiti, C. (2007). Geotechnical properties of Dublin Boulder Clay. Quarterly Journal of Engineering Geology and Hydrogeology, 40(1), 55–74.

Mitchell, J. K., & Soga, K. (2005). Fundamentals of Soil Behavior (3rd ed.). John Wiley & Sons.

Nelson, J. D., & Miller, D. J. (1992). Expansive Soils: Problems and Practice in Foundation and Pavement Engineering. John Wiley & Sons.

Ng, C. W. W., & Chiu, C. F. (2001). Effects of Pile Groups on Adjacent Slope Stability. Journal of Geotechnical and Geoenvironmental Engineering, 4(127), 330–336.

Ng, C. W. W., & Wang, Z. (2001). A numerical investigation of excavation-induced soil movements. Computers and Geotechnics, 28(1), 1–27.

Onyelowe, K. C., Ebid, A. M., Ramani Sujatha, E., Fazel-Mojtahedi, F., Golaghaei-Darzi, A., Kontoni, D. P. N., & Nooralddin-Othman, N. (2023). Extensive overview of soil constitutive relations and applications for geotechnical engineering problems. In Heliyon (Vol. 9, Issue 3). Elsevier Ltd. https://doi.org/10.1016/j.heliyon.2023.e14465

Ou, C. Y., & Liao, W. C. (1999). Evaluation of excavation-induced soil heave in clay. Canadian Geotechnical Journal, 36(4), 681–692.

Ou, C.-Y. (2006). Deep Excavation: Theory and Practice (1st ed.). CRC Press.

Persson, J. (2004). The unloading modulus of soft clay: a field and laboratory study. Gothenburg: Department of Geo-Engineering, Chalmers University of Technology.

Powrie, W. (2014). Soil Mechanics: Concepts and Applications, Third Edition (3rd ed.). CRC Press.

SBRCURnet. (2014). Design Guideline for Swelling Pressure. CUR Commissie C168, The Netherlands.

Schanz, T., Vermeer, P. A., & Dümmler, W. (2016). Numerical Simulation of Geotechnical Problems. International Journal for Numerical and Analytical Methods in Geomechanics, 40(12), 1735–1751.

Schanz, T., Vermeer, P., & Bonnier, P. (1999). The hardening soil model: formulattion and verification. Beyond 2000 in computational geotechnics. 281–296.

Sheng D., Eigenbrod K. D., & Wriggers P. (2005). Finite element analysis of pile installation using large-slip frictional contact. Journal of Computer and Geotechnics, 32, 17–26.

Tan, T. S., & Phoon, K. K. (2006). Characterisation and Engineering Properties of Natural Soils, Vol. 1.

Terzaghi, K. (1943). Theoretical Soil Mechanics. Wiley, New York.

Terzaghi, K., & Peck, R. B. (1967). Soil Mechanics in Engineering Practice.

Titi H., & Wathugala G. W. (1999). Numerical procedure for predicting pile capacity setup/freeze. J. Transport. Res. Board, 1663, 23–32.

Wathugala G. W., & Desai C. S. (1991). Hierarchical single-surface model for anisotropic hardening cohesive soils. Proc. 7th International Conference of the International Association for Computer Methods and Advances in Geomechanics, 1249–1254.

Wood M.D. (1990). “Soil Behavior and Critical State Soil Mechanics. Cambridge University Press .

Zienkiewicz, O. C., sdsd, & www. (1980). Analysis of consolidation problems by finite elements. Géotechnique, 30(2), 159–182.

Appendix

Case 1: 2D Model without structural elements

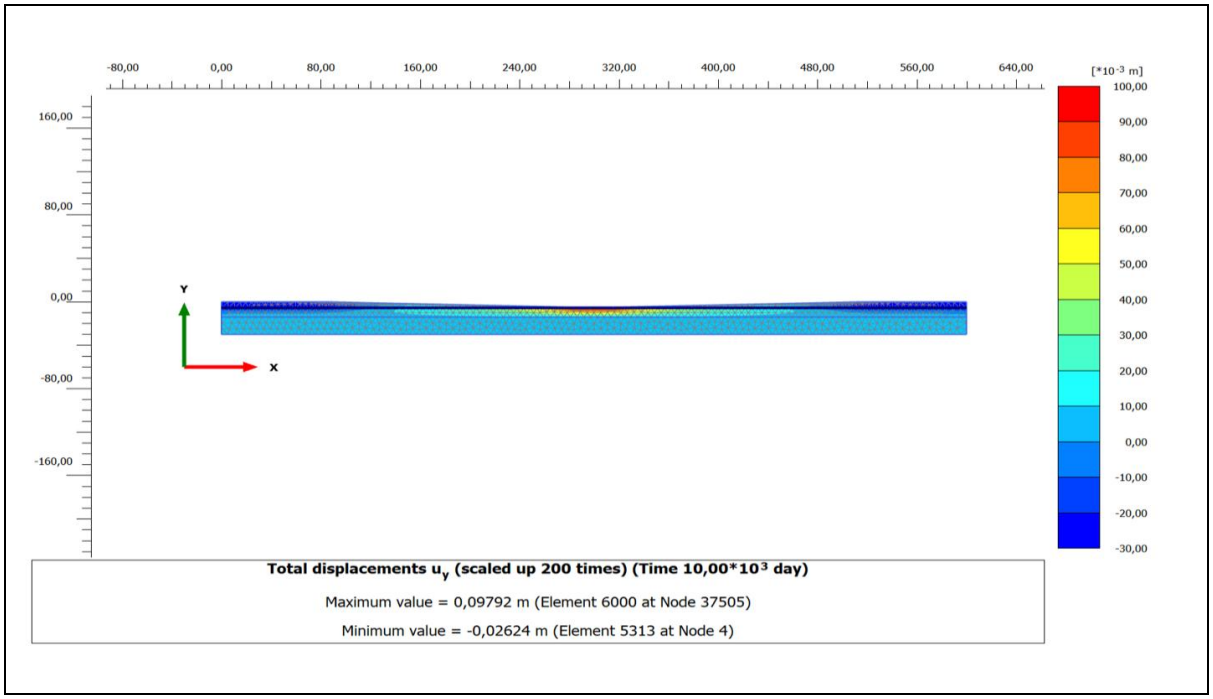

Figure 1 : Swelling deformation in the Validation Model.

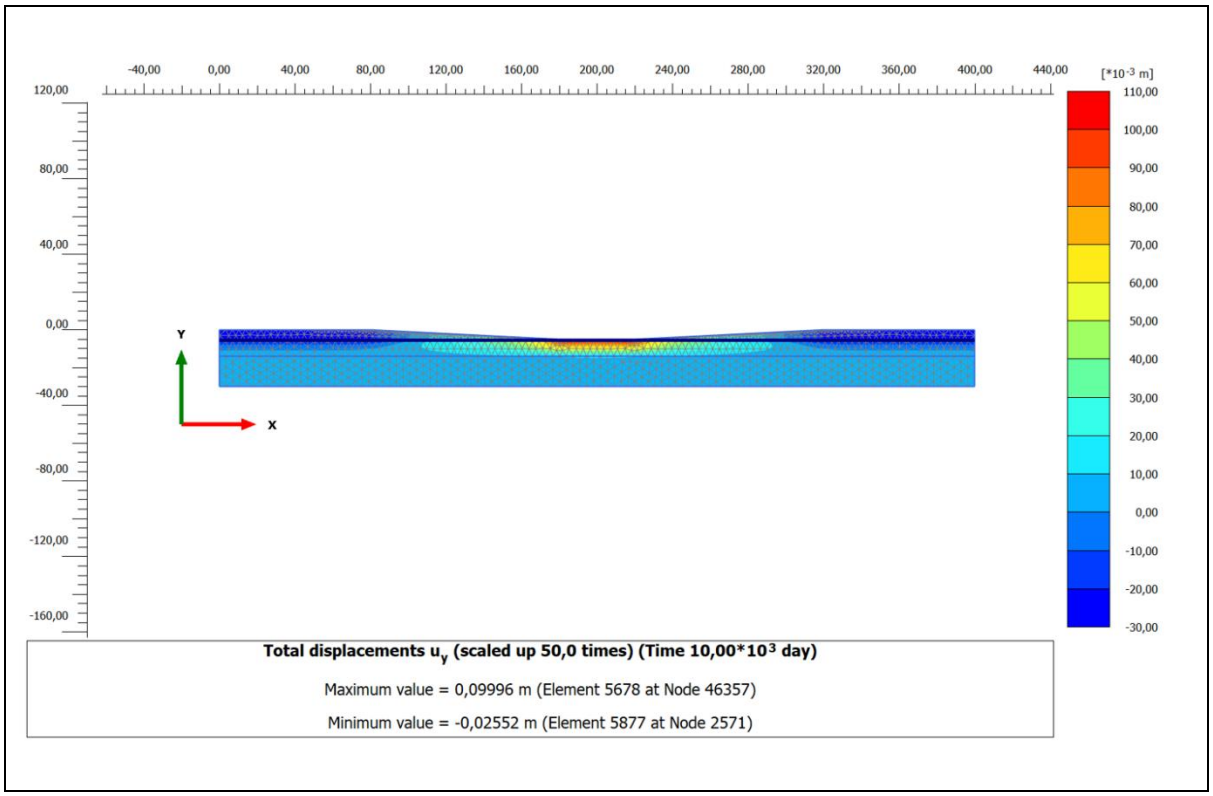

Figure 2: Swelling deformation for case 1 (W=40m).

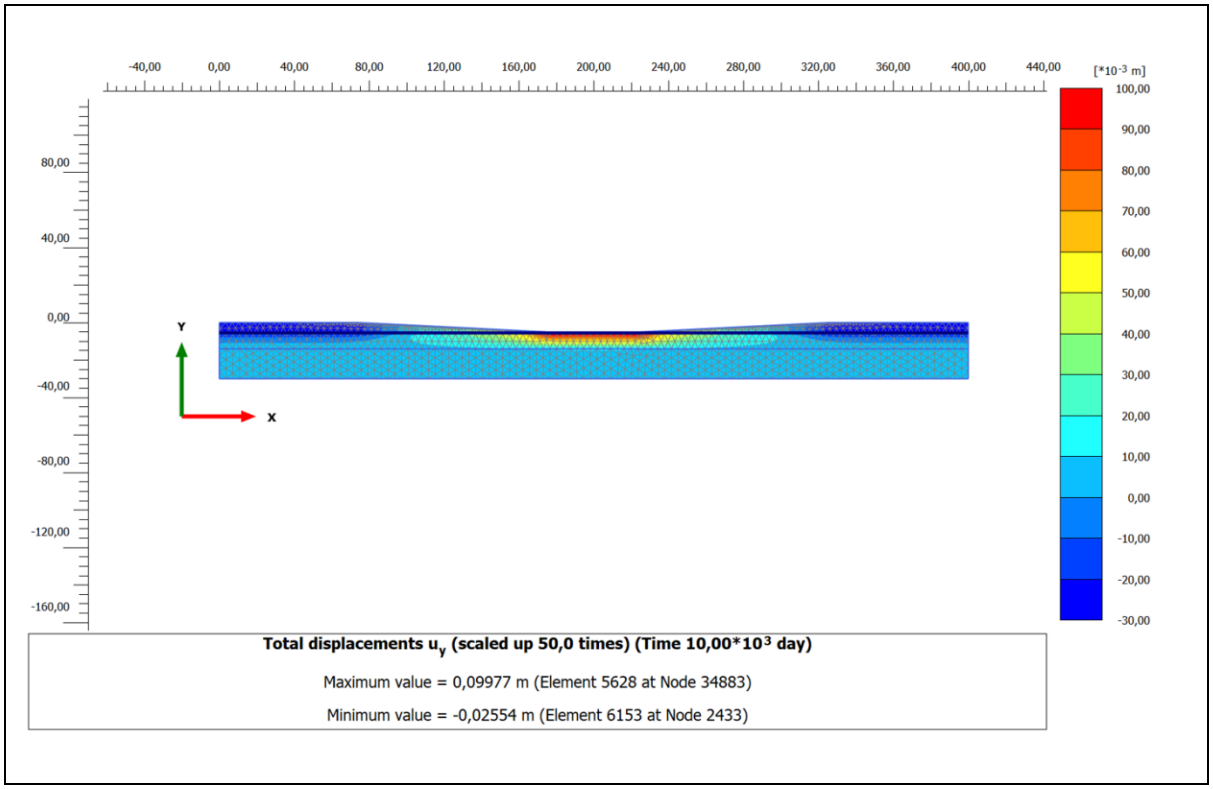

Figure 3: Swelling deformation for case 1 (W=50m).

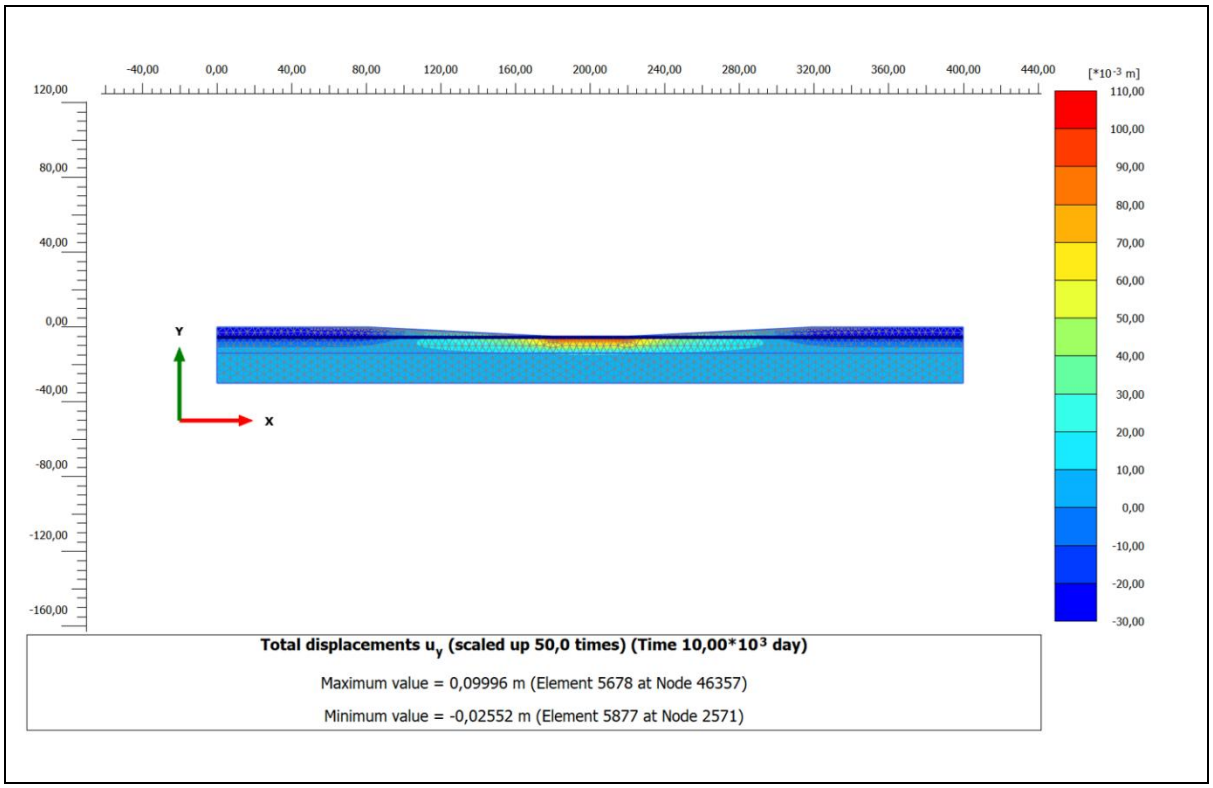

Figure 4: Swelling deformation for case 1 (W=60m).

Case 3: 2D_Model (sheet Pile – strut – pile system with and without Pile installation effect)

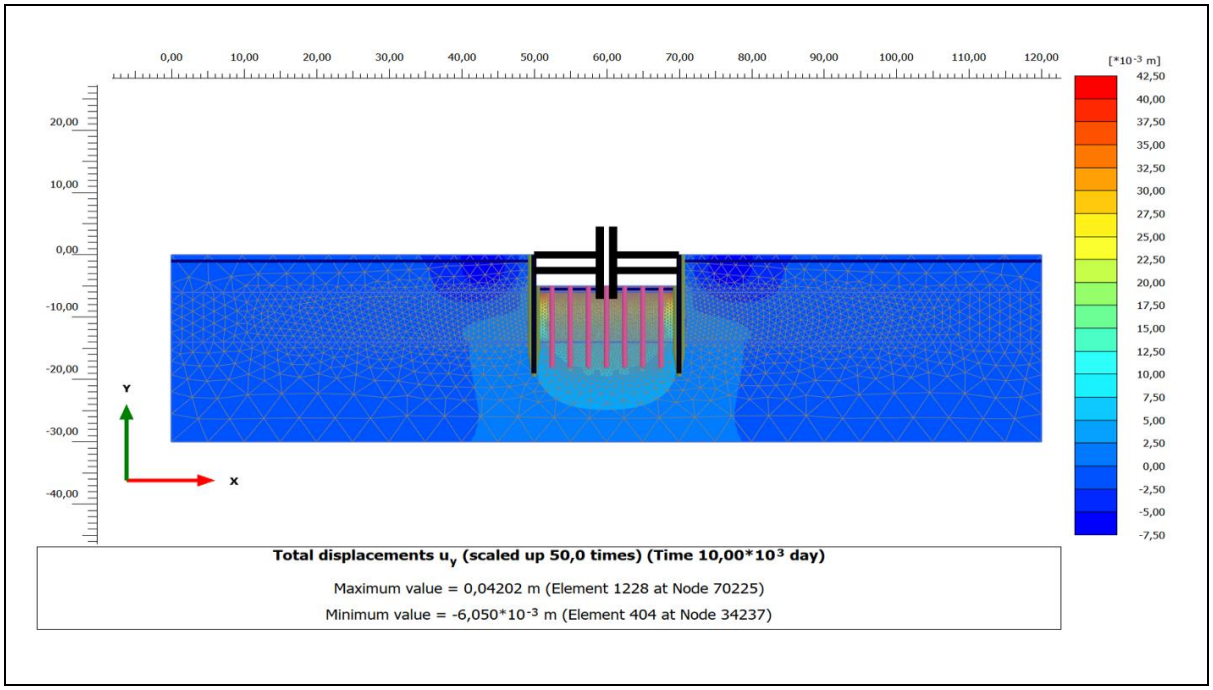

Figure 5: Swelling deformation for case 3 (w=0.25m, and c.t.c=2.5m).

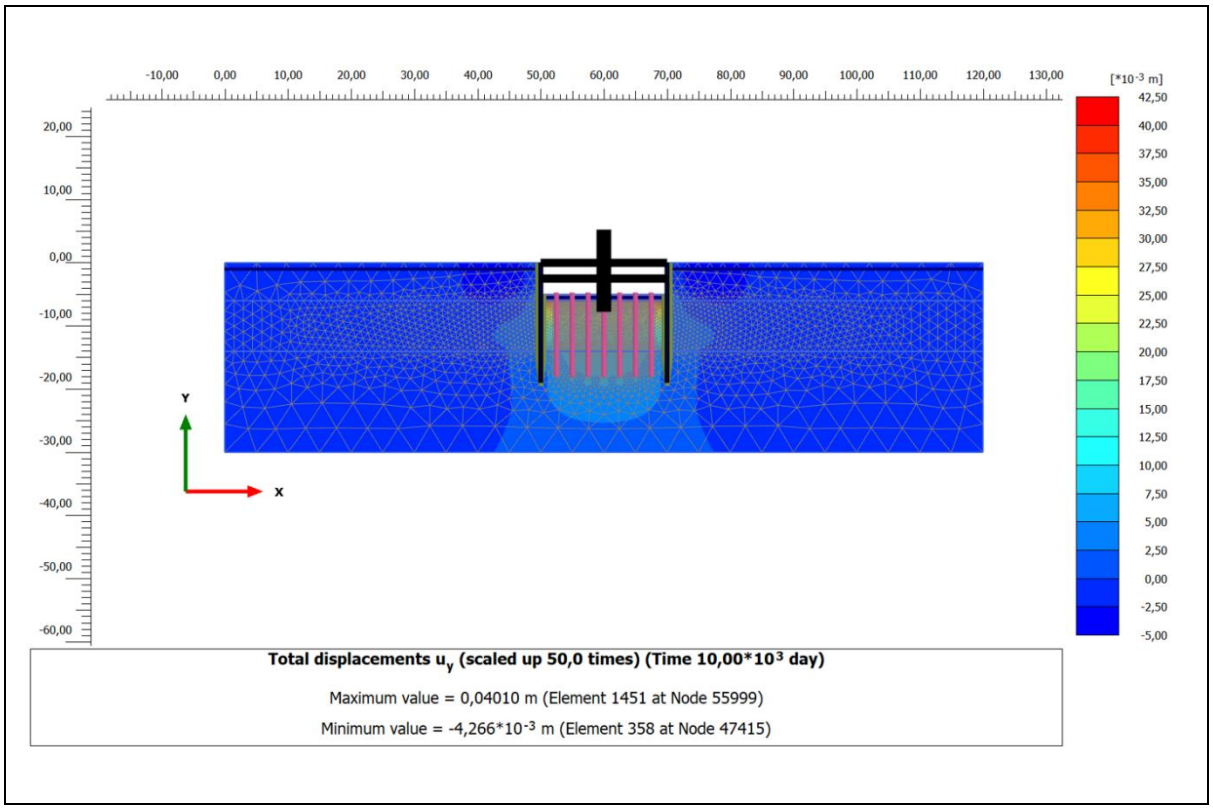

Figure 6: Swelling deformation for case 3 (w=0.3m, and c.t.c=2.5m).

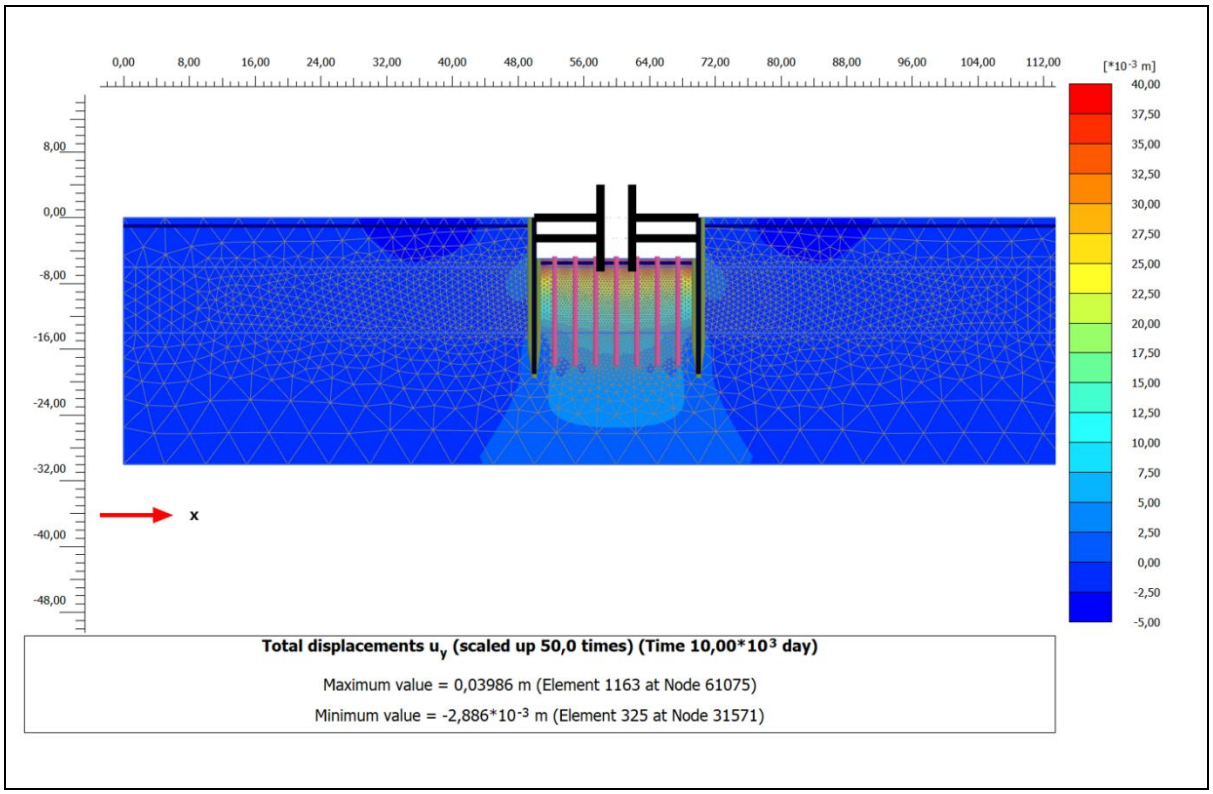

Figure 7: Swelling deformation for case 3 (w=0.4m, and c.t.c=2.5m).

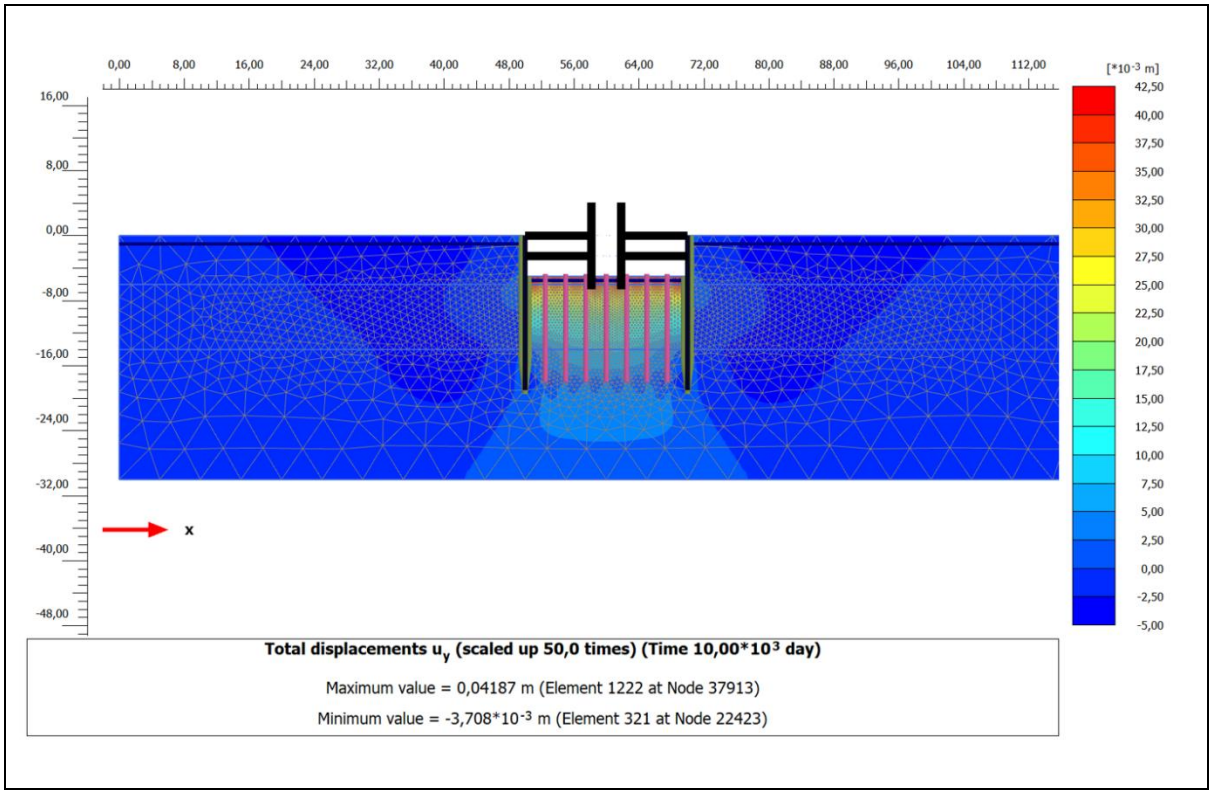

Figure 8: Swelling deformation for case 3 (w=0.45m, and c.t.c=2.5m).

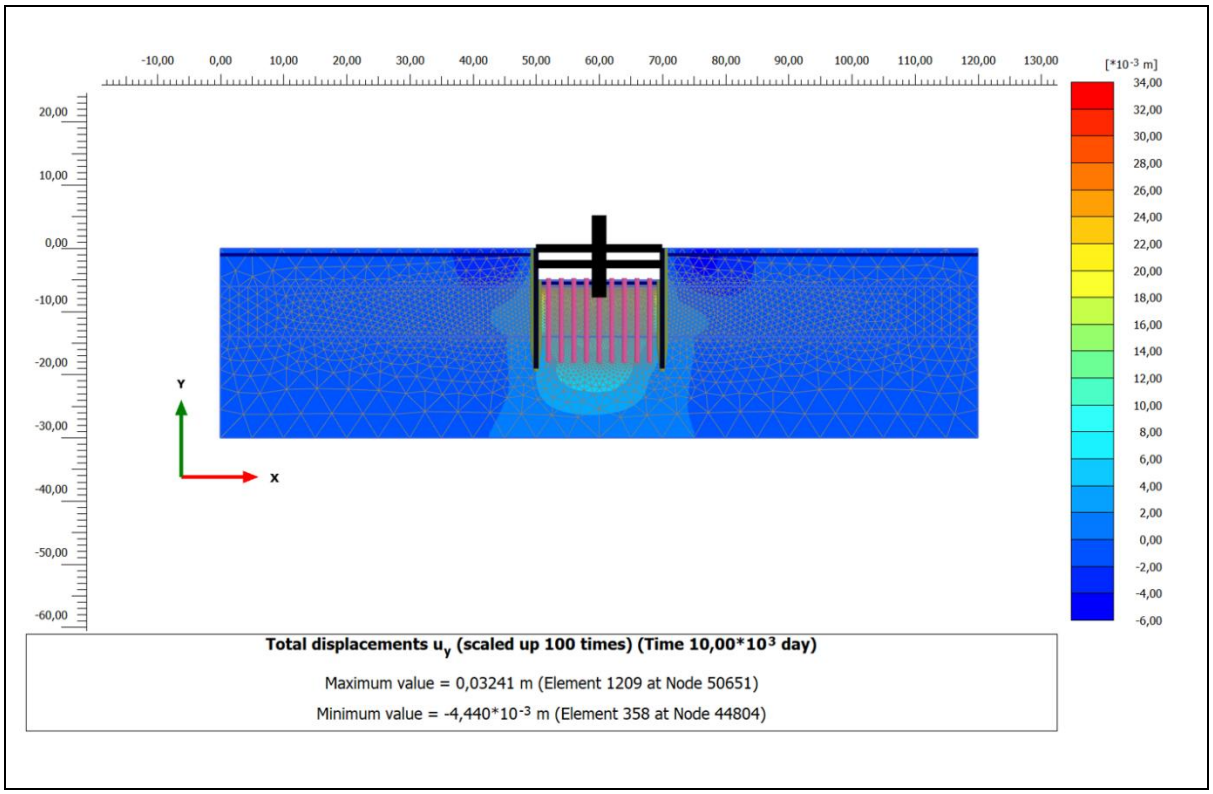

Figure 9: Swelling deformation for case 3 (w=0.25m, and c.t.c=2m).

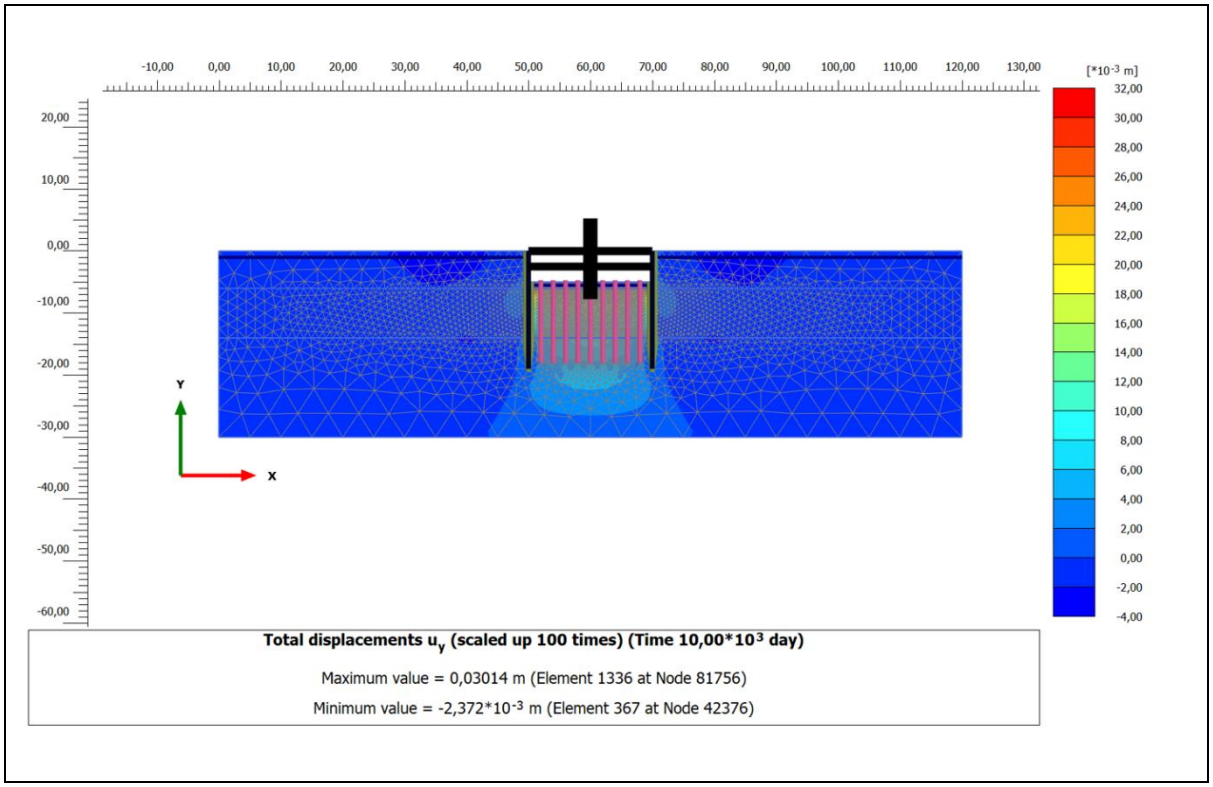

Figure 10: Swelling deformation for case 3 (w=0.3m, and c.t.c=2m).

Case 4: 2D_Model without Piles (Sheet Pile – Strut – Floor)

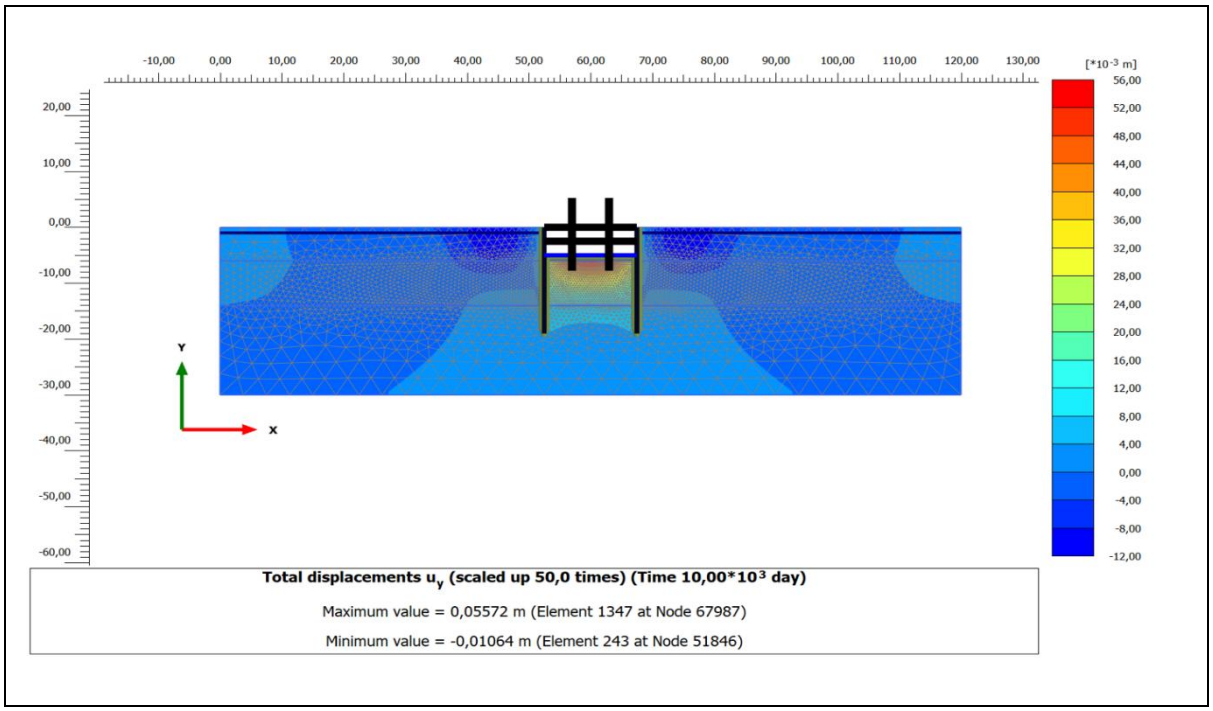

Figure 11: Swelling deformation for case 4 (E1, W=15m).

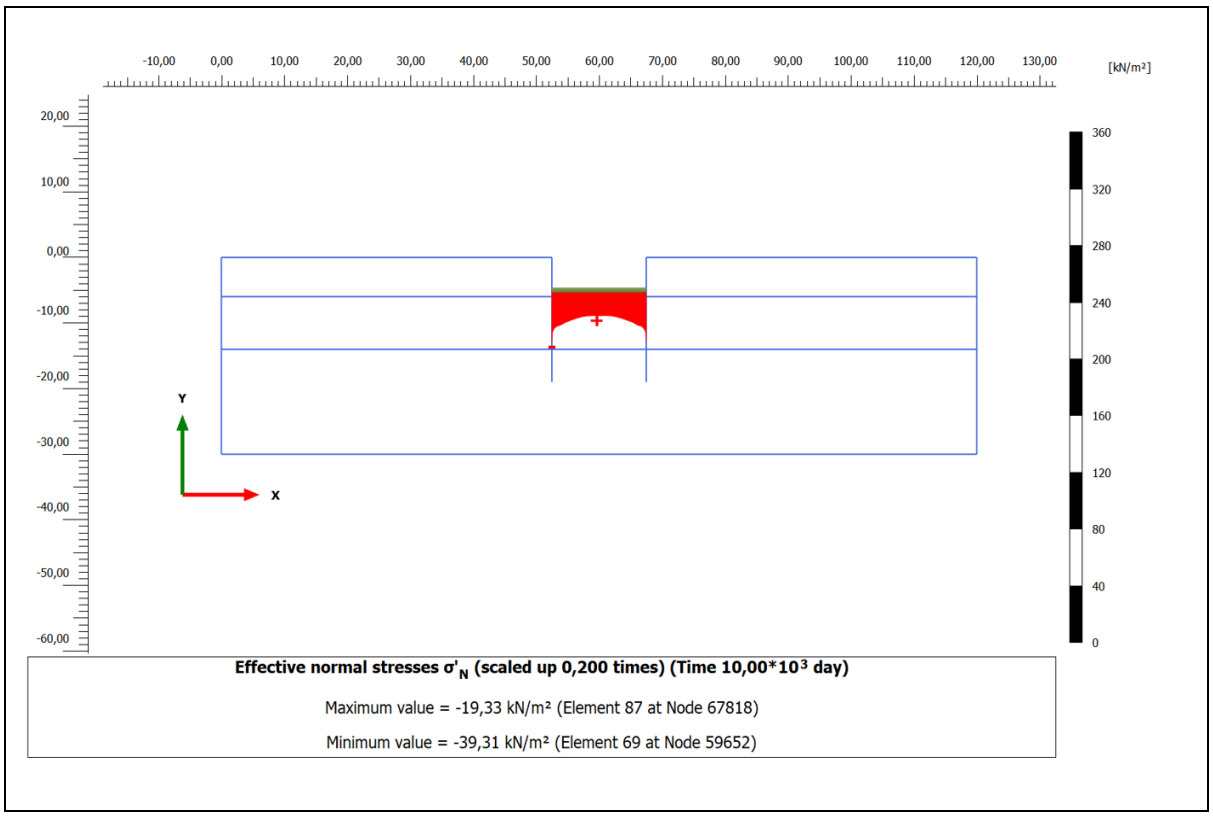

Figure 12: Swelling pressure for case 4 (E1, W=15m).

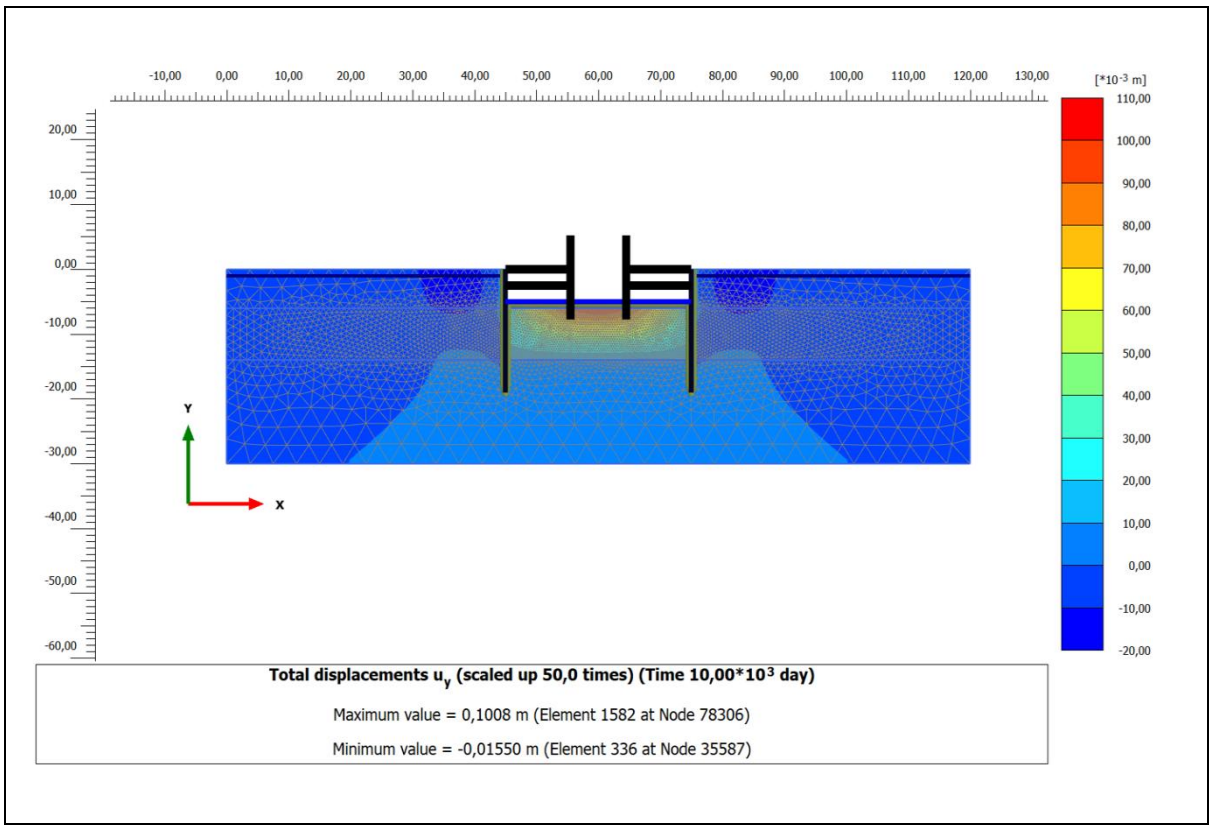

Figure 13: Swelling deformation for case 4 (E1, W=30m).

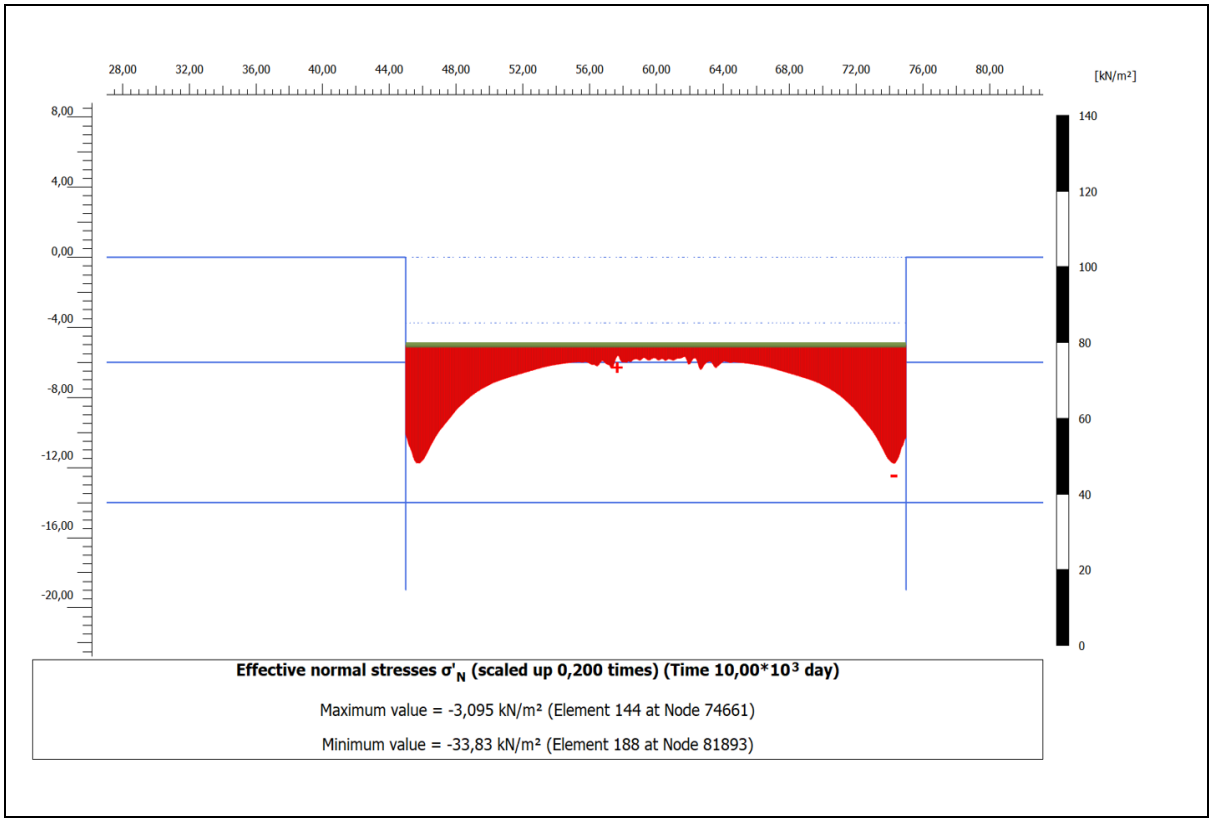

Figure 14: Swelling pressure for case 4 (E1, W=30m).

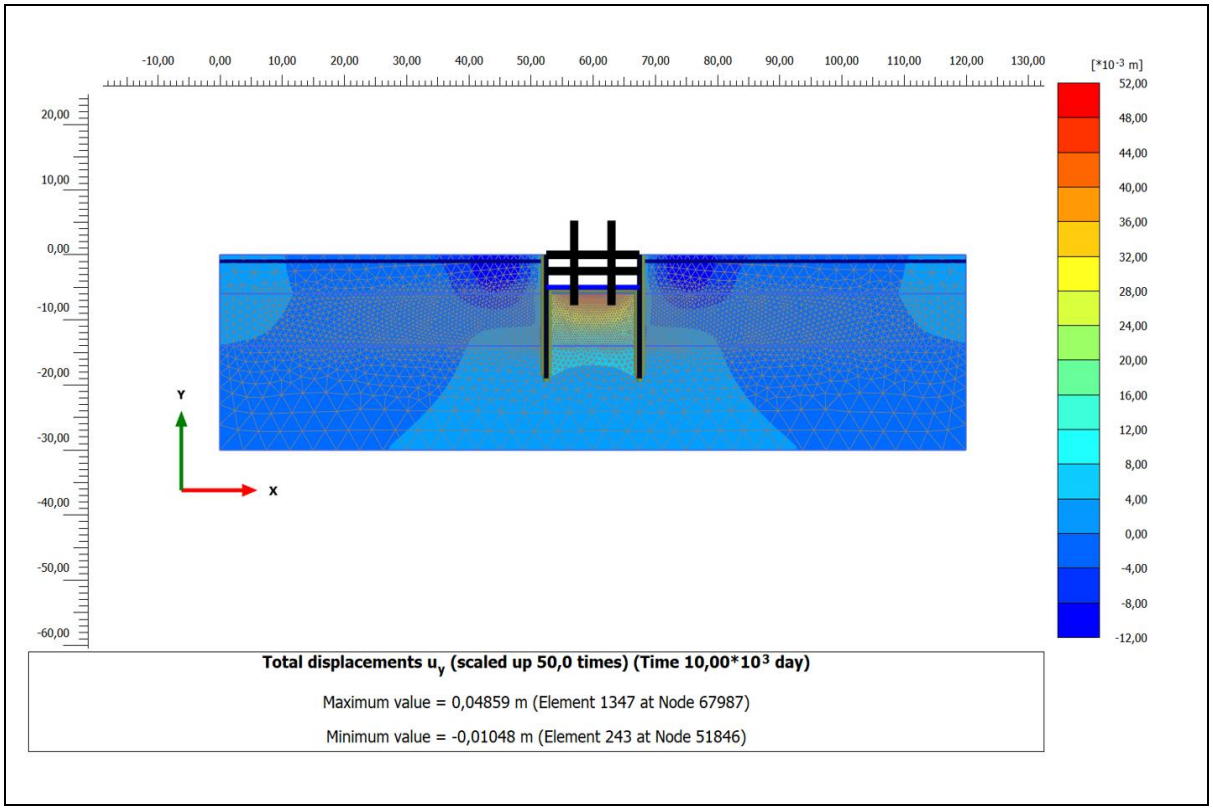

Figure 15: Swelling deformation for case 4 (E3, W=15m).

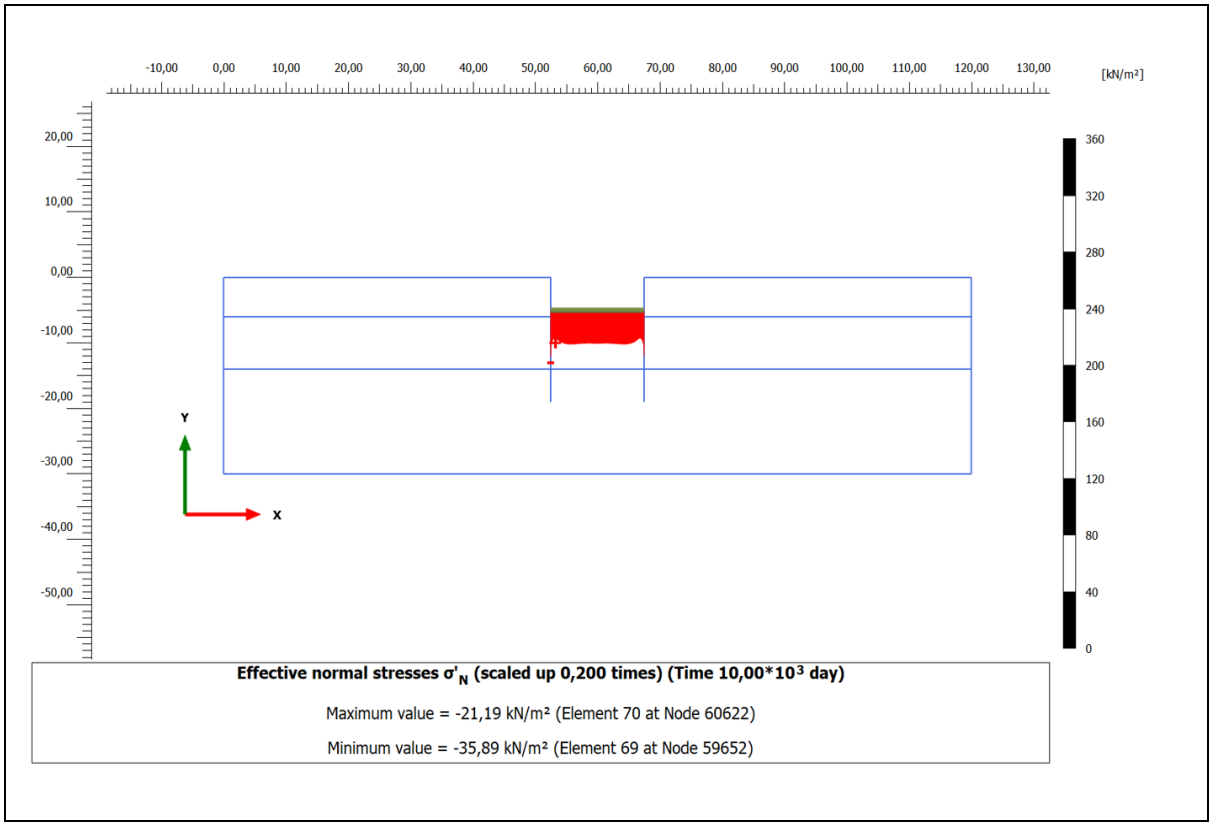

Figure 16: Swelling pressure for case 4 (E3, W=15m).

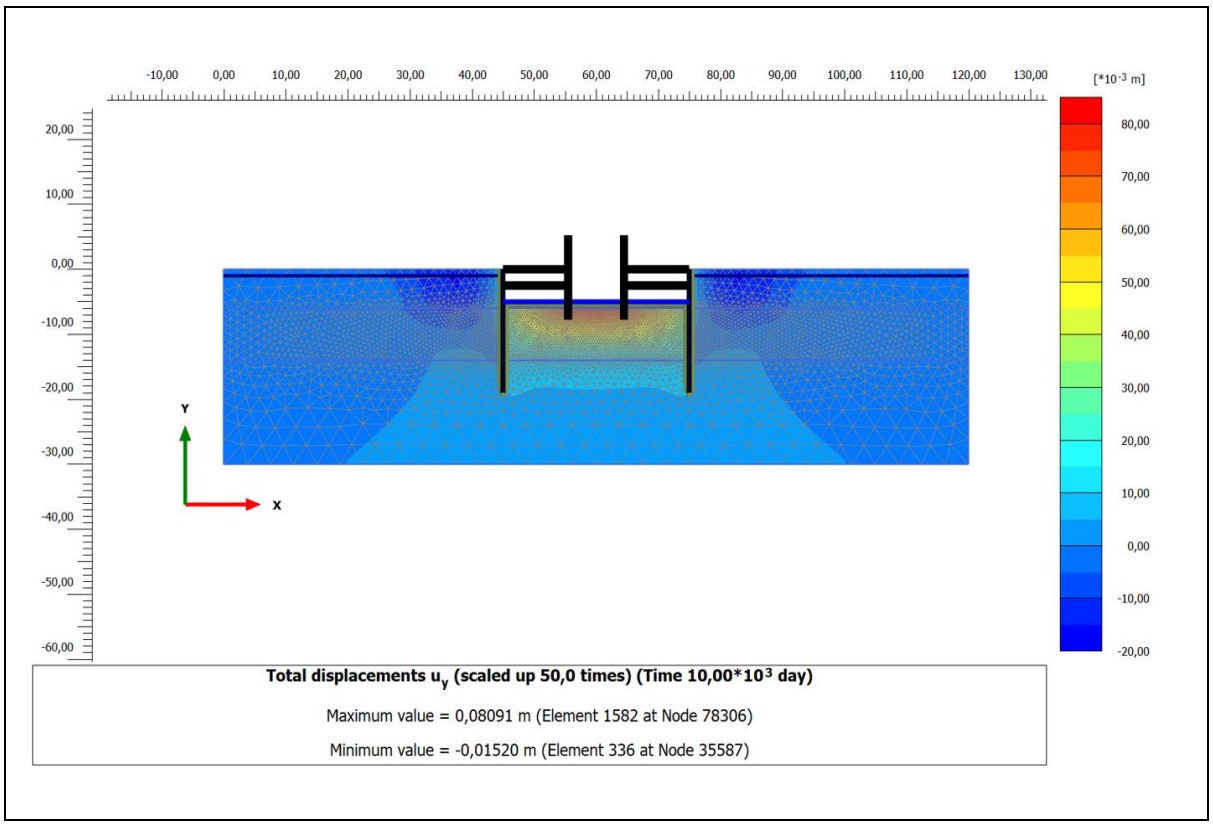

Figure 17: Swelling deformation for case 4 (E3, W=30m).

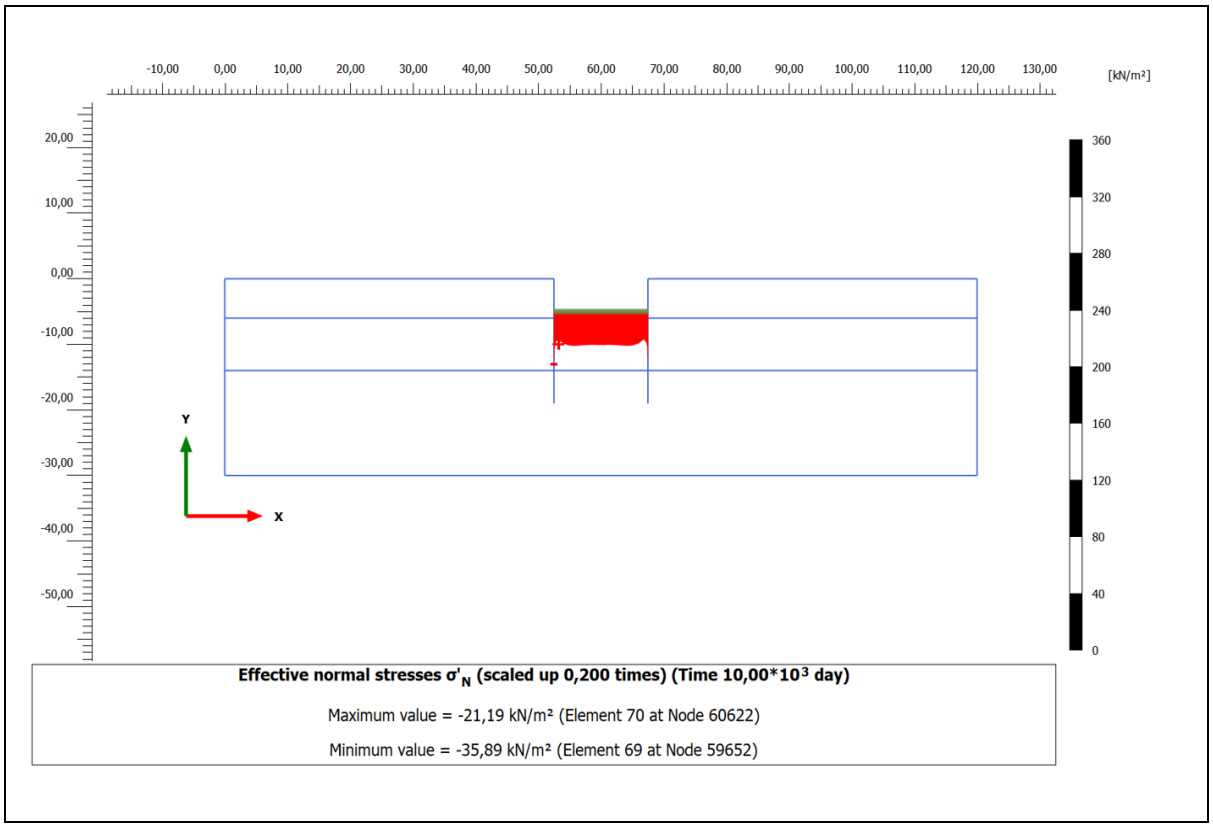

Figure 18: Swelling pressure for case 4 (E3, W=30m).

Case 5: 2D Model- Full Structural System

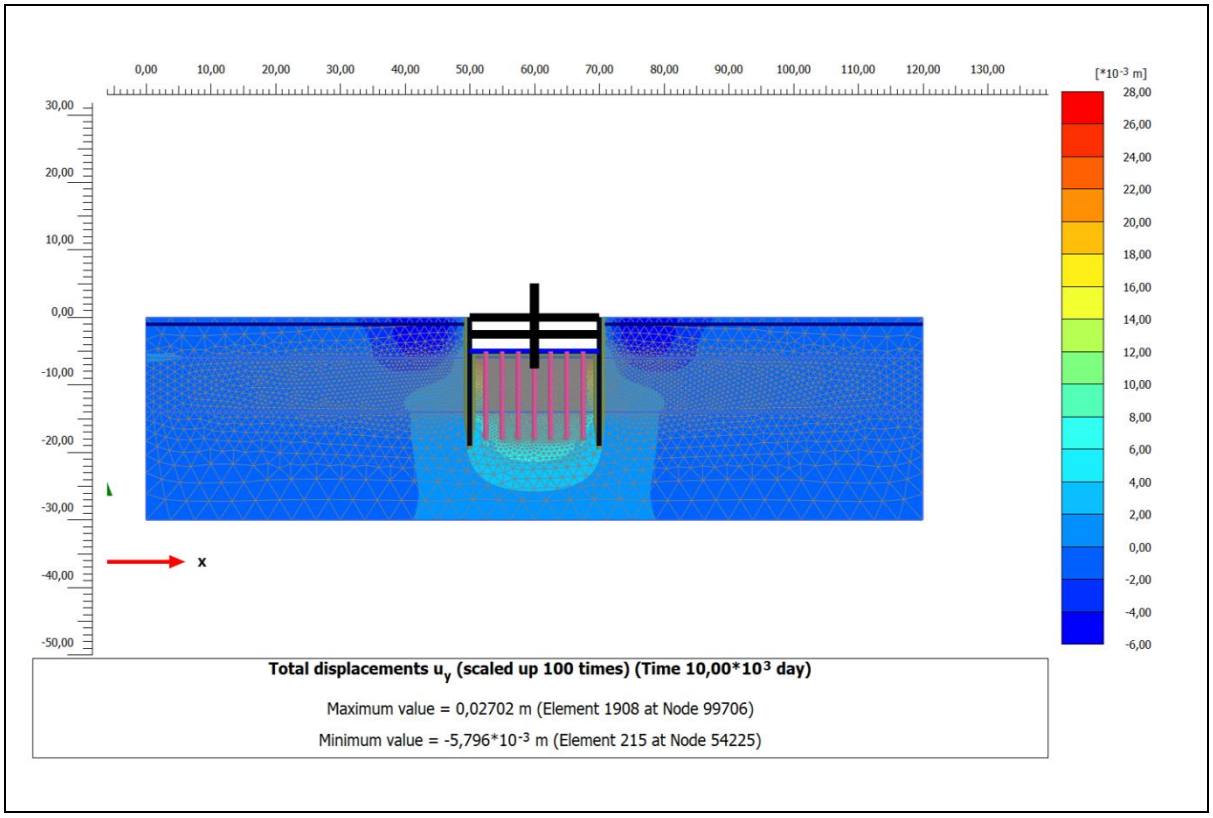

Figure 19: Swelling deformation for case 5 (w=0.25m, and c.t.c=2.5m).

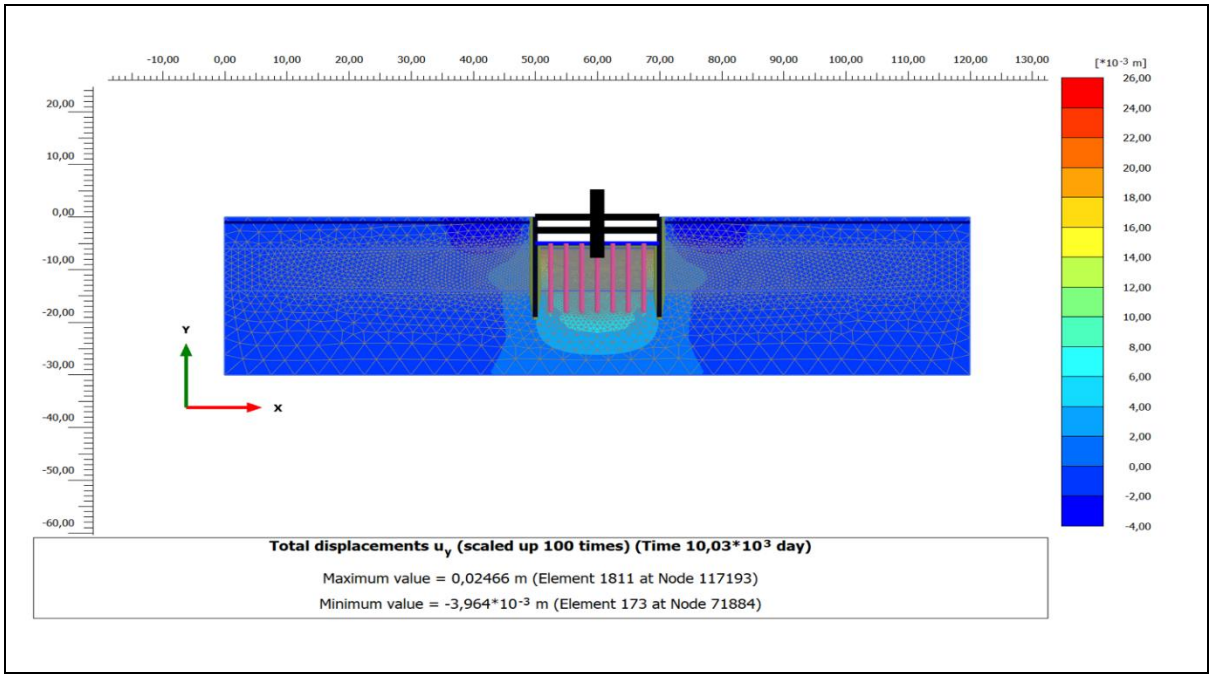

Figure 20: Swelling deformation for case 5 (w=0.3m, and c.t.c=2.5m)

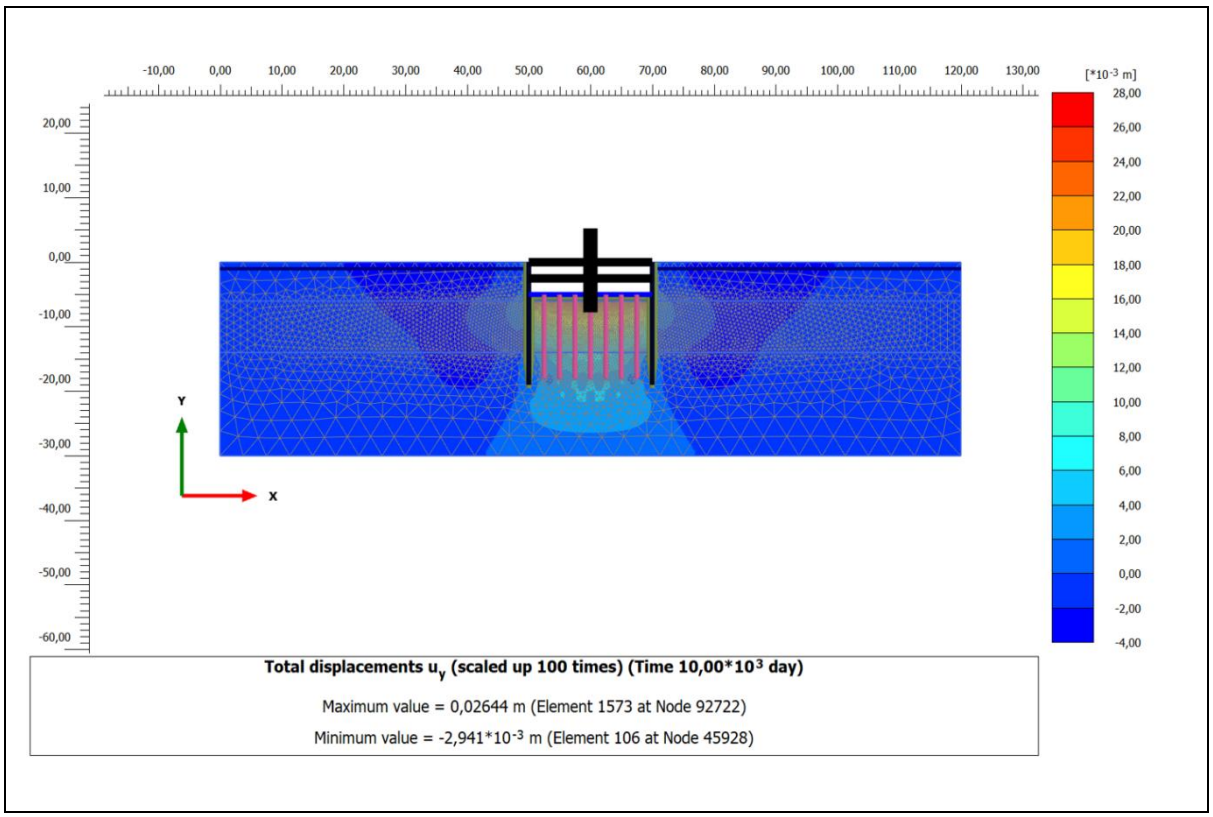

Figure 21: Swelling deformation for case 5 (w=0.4m, and c.t.c=2.5m).

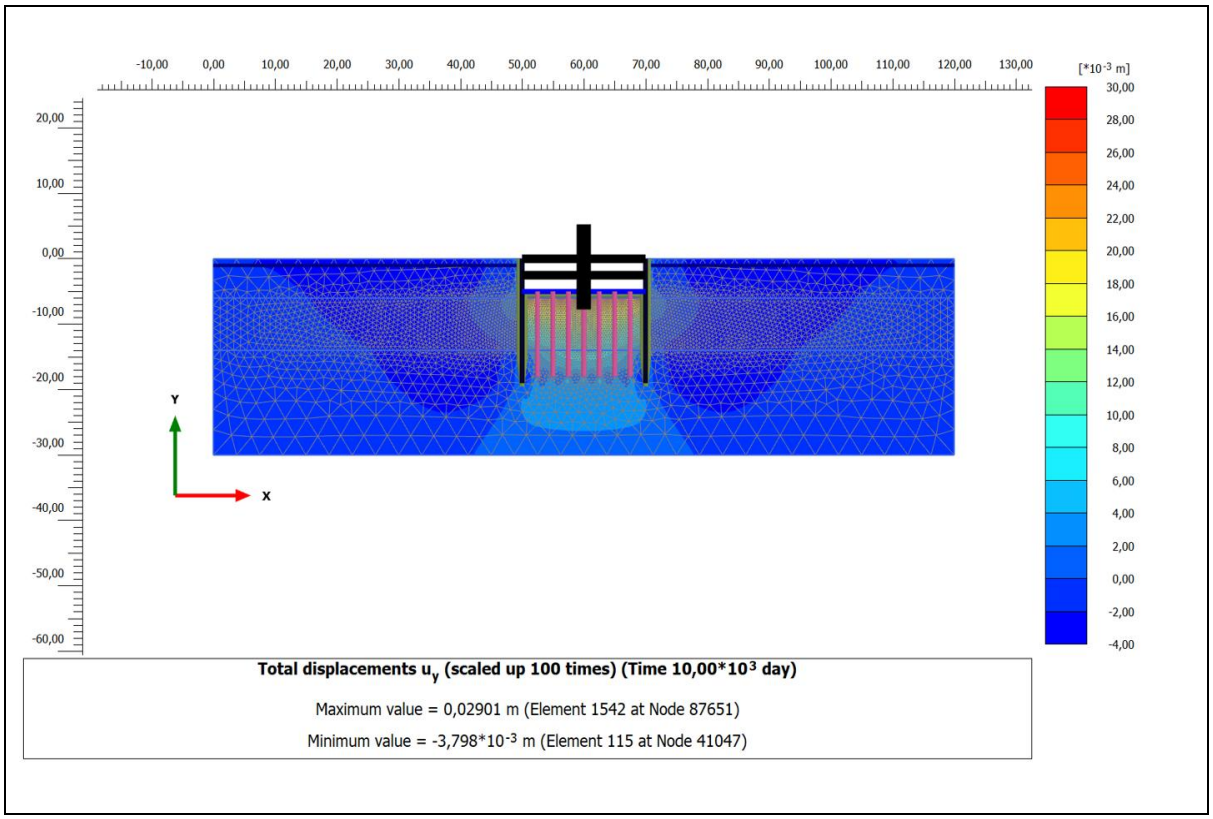

Figure 22: Swelling deformation for case 5 (w=0.45m, and c.t.c=2.5m).

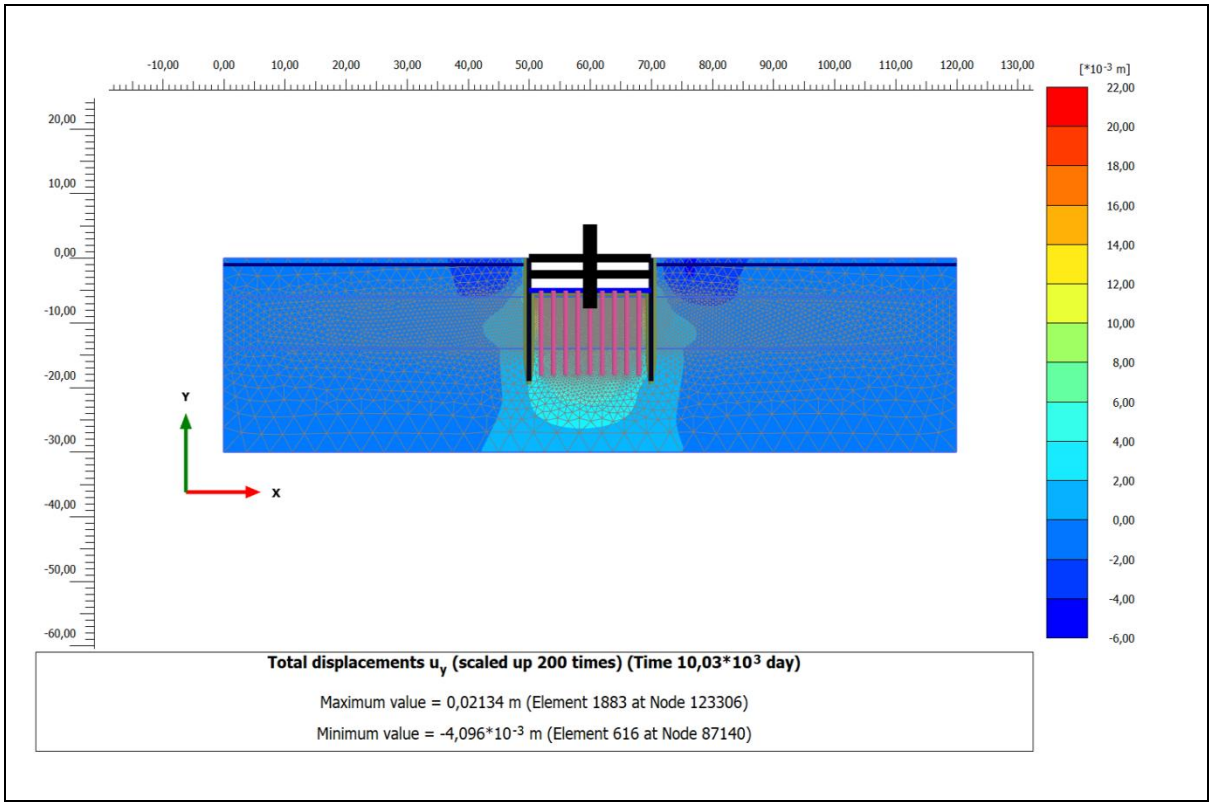

Figure 23: Swelling deformation for case 5 (w=0.25m, and c.t.c=2m).

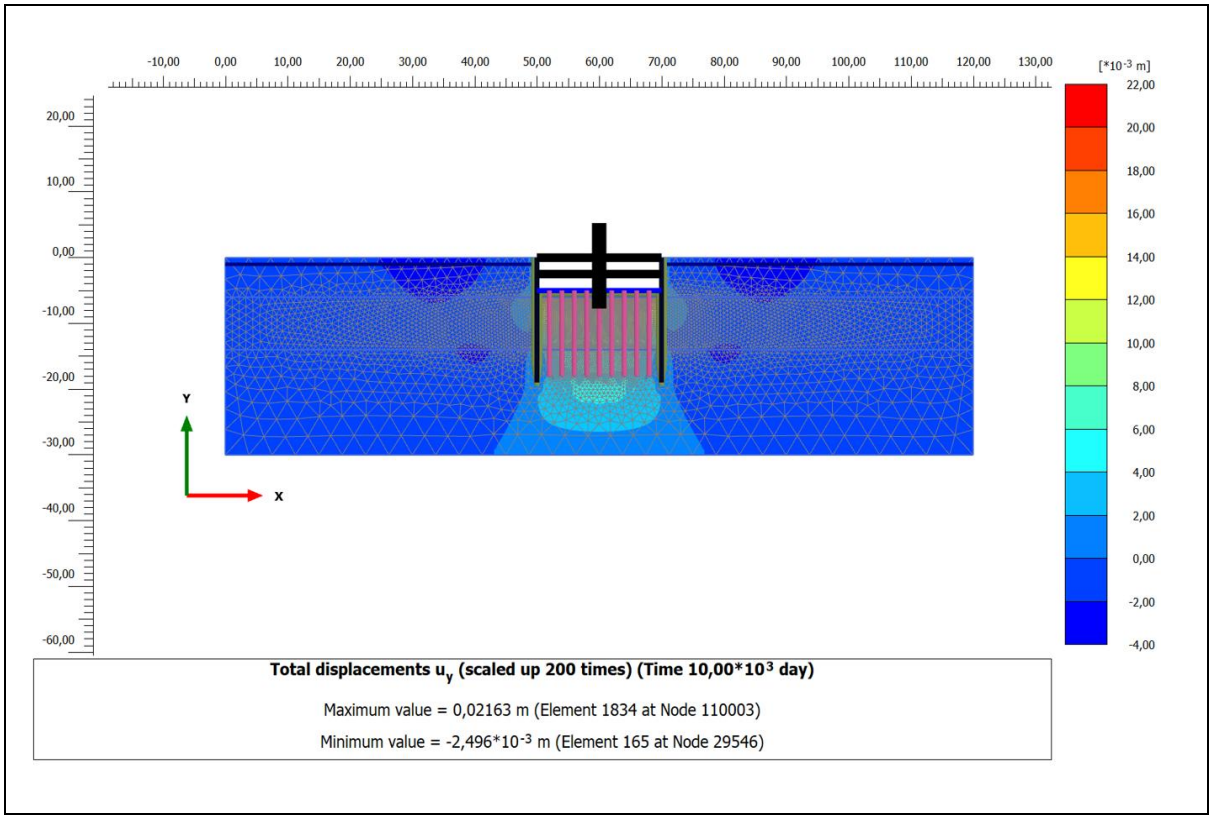

Figure 24: Swelling deformation for case 5 (w=0.3m, and c.t.c=2m).

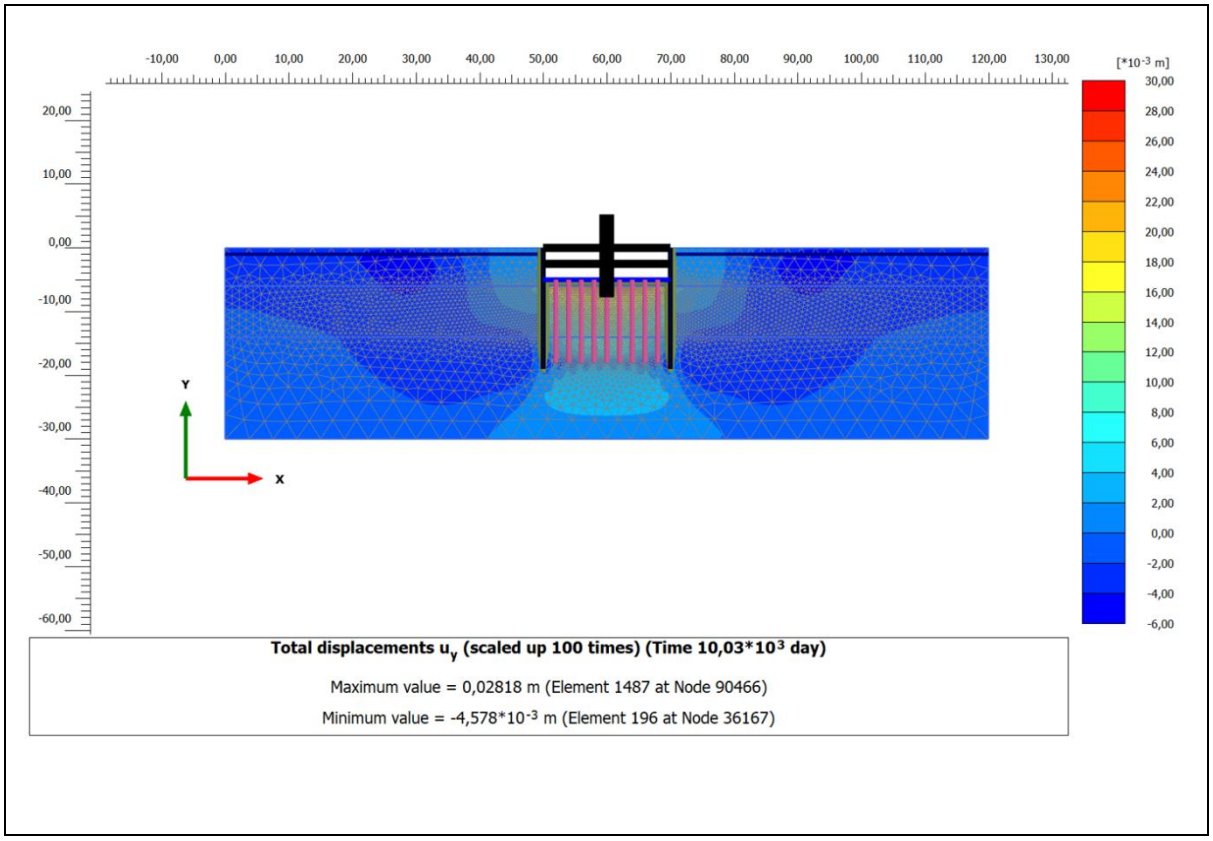

Figure 25: Swelling deformation for case 5 (w=0.4m, and c.t.c=2m).

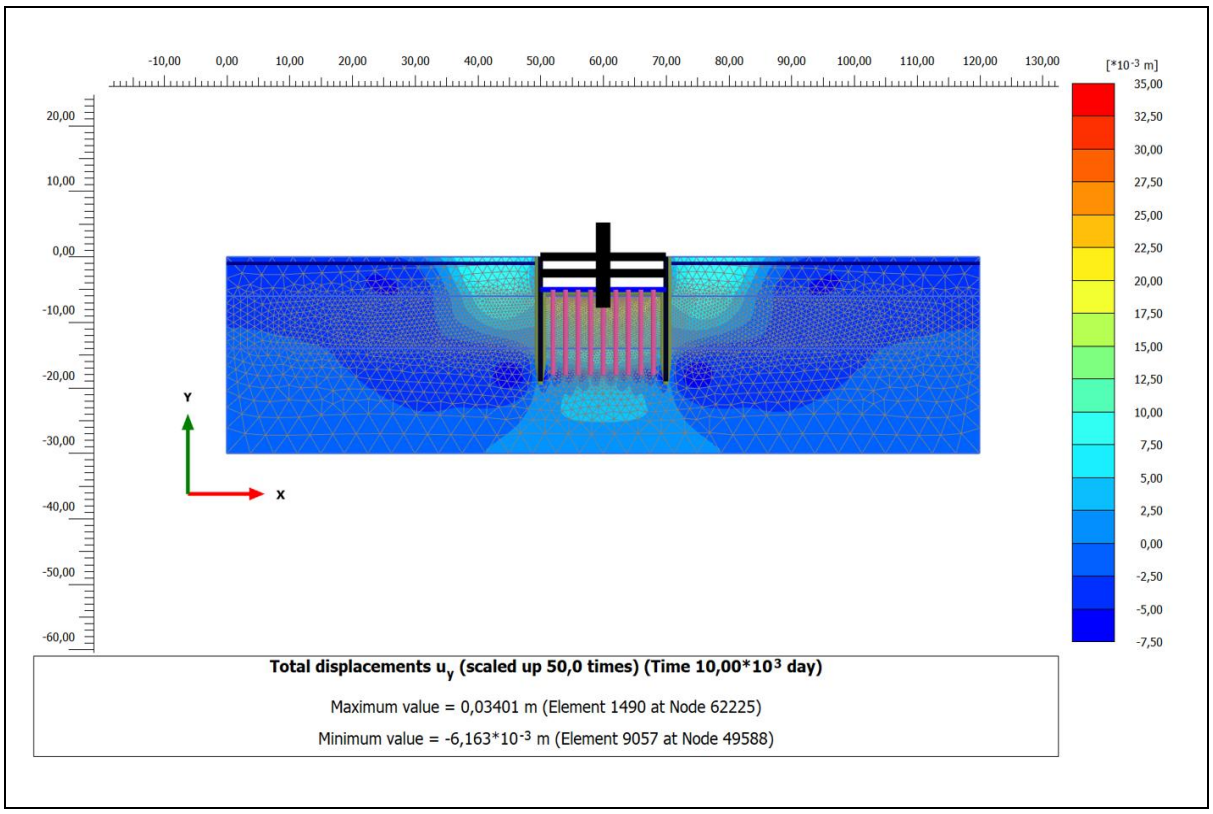

Figure 26: Swelling deformation for case 5 (w=0.45m, and c.t.c=2m).